

# **FFI RAPPORT**

## **BURNING PROPERTIES OF PBXN-5 - Closed Vessel Testing**

NEVSTAD Gunnar Ove, ERIKSEN Svein Walter

**FFI/RAPPORT-2002/04195**



FFIBM/860/130

Approved  
Kjeller 25 october 2002

Bjarne Haugstad  
Director of Research

**BURNING PROPERTIES OF PBXN-5 - Closed  
Vessel Testing**

NEVSTAD Gunnar Ove, ERIKSEN Svein Walter

FFI/RAPPORT-2002/04195

**FORSVARETS FORSKNINGSINSTITUTT**  
**Norwegian Defence Research Establishment**  
P O Box 25, NO-2027 Kjeller, Norway



1) PUBL/REPORT NUMBER FFI/RAPPORT-2002/04195	2) SECURITY CLASSIFICATION UNCLASSIFIED	3) NUMBER OF PAGES 60
1a) PROJECT REFERENCE FFIBM/860/130	2a) DECLASSIFICATION/DOWNGRADING SCHEDULE -	
4) TITLE BURNING PROPERTIES OF PBXN-5 - Closed Vessel Testing		
5) NAMES OF AUTHOR(S) IN FULL (surname first) NEVSTAD Gunnar Ove, ERIKSEN Svein Walter		
6) DISTRIBUTION STATEMENT Approved for public release. Distribution unlimited. (Offentlig tilgjengelig)		
7) INDEXING TERMS IN ENGLISH: IN NORWEGIAN:		
a) <u>PBXN-5</u>	a) <u>PBXN-5</u>	
b) <u>Powder</u>	b) <u>Pulver</u>	
c) <u>Pressed Pellets</u>	c) <u>Presset legemer</u>	
d) <u>Closed Vessel</u>	d) <u>Lukket kammer</u>	
e) <u>Burn Rate</u>	e) <u>Brennhastighet</u>	
THESAURUS REFERENCE:		
8) ABSTRACT <p>PBXN-5, a HMX based explosive composition for press filling has been studied in Closed Vessel for characterisation of burning properties. PBXN-5 has been tested as powder and in form of pressed pellets. Pellets have been pressed and tested with four different densities from 1.59 g/cm<sup>3</sup> to 1.826 g/cm<sup>3</sup>. The purpose with the CV-testing was to see if we were able to observe differences in the burning properties as function of differences in density of the pellets.</p> <p>Pressure-time curves of firings with pellets of different density show clearly that as the density of pellets increase the burn time increase. For the loosely packed pellets the burning start on the surface of the pellets, but as the pressure increase the burning also take place inside the pellets. For the pellets of highest density the burning take place only on the surface of the pellets. For PBXN-5 similar burning rates for powder and pellets of high density is obtained.</p> <p>Experimentally obtained impetuses, co-volumes and maximum pressures are in general lower then theoretically calculated ones by use of the Cheetah code. The differences between experimental and theoretical values increase as the pellet density increase. The explanation for this observation is that when the burn time increase, also the loss of energy to the CV increases.</p>		
9) DATE 25 october 2002	AUTHORIZED BY This page only Bjarne Haugstad	POSITION Director of Research



**CONTENTS**

	<b>Page</b>
1 INTRODUCTION	7
2 EXPERIMENTALLY	7
2.1 Closed Vessel testing	7
2.2 Pellet pressing	9
3 RESULTS	11
3.1 Press Powder	11
3.2 Cylinder pellets pressed with 400 kg	21
3.3 Cylinder pellets pressed with 1340 kg	26
3.4 Cylinder pellets pressed with 5700 kg	30
3.5 Cylinder pellets pressed with 1 GPa	35
3.6 Theoretical calculations	40
3.7 Comparison between experimentally and theoretical calculated properties	42
3.8 Burn rate determination	44
4 SUMMARY	52
APPENDIX	54
A CONTROL REPORT FOR PBXN-5, TYPE II, CLASS 2	54
B CHEETAH CALCULATIONS FOR PBXN-5	55
REFERENCES	59
Distribution list	60





## BURNING PROPERTIES OF PBXN-5 - Closed Vessel Testing

### 1 INTRODUCTION

A Closed Vessel has been used to characterise the burning properties of explosives used in the shell body of MP-ammunitions. The density of pressed fillings can be important for the reaction rate and type of the reaction of explosive fillings. Will the explosive react with a slow reaction as burning or deflagration or will it detonate. The rate of reaction of the explosive filling in warheads as in MP (multipurpose) has influence on the fragmentation pattern. In this report PBXN-5, a HMX based explosive for press filling has been studied. We have for this explosive produced and tested pellets of four different densities to study what effect the density has on the burning rate. In addition to determination of the burn rates for powder and pellets of different densities at different loading densities, the impetuses and the co-volumes have been determined experimentally for all five tests series.

In addition to experimental testing of different forms of the explosives, we have carried out theoretical calculations by use of the thermochemical CHEETAH code. A comparison between experimentally and calculated results has been carried out.

### 2 EXPERIMENTALLY

#### 2.1 Closed Vessel testing

PBXN-5 has been tested under different conditions in a 150 cm<sup>3</sup> Closed Vessel. Figure 2.1 gives a picture of the loaded Closed Vessel. For all experiments ignition has been with 1 g Black Powder and a brown/blue squib. For both powder and pellets the samples were held in a



Figure 2.1 A picture of the 150 cm<sup>3</sup> Closed Vessel used for the experimental testing.

plastic bag. For the powder the ignition unit was placed in the centre of the powder. Figure 3.1 shows how the powder was packed. For pellets the ignition unit was placed at the surface of the stocks of pellets; figure 3.20 gives an example of how they were packed.

To measure the pressure a Kistler 6211, SN 87663 pressure gauge was used. Sampling time for most experiments was 1  $\mu$ s. The exception was for the firings of pellets with high density, where we used sampling times from 1  $\mu$ s and up to 5  $\mu$ s. Table 2.1 gives a summary of the conditions for all firings with PBXN-5. For more details see chapter 3.

CV Firing No.	Material	Form	Date of Firing	Sampling Time ( $\mu$ s)	Sample size (g)	$P_{\max}$ (bars)	Density ( $\text{g}/\text{cm}^3$ )
370	PBXN-5	Powder	19/4-02	1	15.03	1384	
371	PBXN-5	Powder	19/4-02	1	22.49	2197	
372	PBXN-5	Powder	19-4-02	1	22.53	2197	
373*	PBXN-5	Powder	19/4-02	1	30.00	3088	
374	PBXN-5	Powder	19/4-02	1	30.01	3140	
375	PBXN-5	Powder	19/4-02	1	35.00	3750	
376	PBXN-5	Powder	22/4-02	1	25.02	2467	
377	PBXN-5	Powder	22/4-02	1	25.00	2464.5	
382	PBXN-5	Pellets	23/4-02	1	24.92	2373	
383	PBXN-5	Pellets	23/4-02	1	19.96	1774.5	
384	PBXN-5	Pellets	23/4-02	1	14.97	1301	1.71
385	PBXN-5	Pellets	23/4-02	1	29.93	2917	
430	PBXN-5	Pellets	1/6-02	1	20.03	1750	
398	PBXN-5	Pellets	2/5-02	1	20.02	1799	
399	PBXN-5	Pellets	2/5-02	1	15.03	1234	
400	PBXN-5	Pellets	2/5-02	1	25.01	2421.5	1.79
401	PBXN-5	Pellets	2/5-02	1	30.00	3017.5	
402	PBXN-5	Pellets	2/5-02	1	20.04	1843	
403	PBXN-5	Powder	2/5-02	1	20.00	1882	
414	PBXN-5	Pellets	6/5.02	1	22.12	1940.5	1.82
415	PBXN-5	Pellets	6/5.02	5	14.75	1200.5	
418	PBXN-5	Pellets	7/5-02	1	20.06	1882	
419	PBXN-5	Pellets	7/5-02	1	15.00	1340	
420	PBXN-5	Pellets	7/5-02	1	25.01	2375	1.587
421	PBXN-5	Pellets	7/5-02	1	30.06	2937	
422	PBXN-5	Pellets	7/5-02	1	25.00	2272	
426	PBXN-5	Powder	1/6-02	1	19.80	1857.5	
431	PBXN-5	Powder	1/6-02	1	20.03	1699	
433	PBXN-5	Powder	21/8-02	1	20.02	1901.5	
437	PBXN-5	Pellets	21/8-02	4	18.68	1624.5	1.826
438	PBXN-5	Pellets	21/8-02	4	18.68	1623.5	
439	PBXN-5	Powder	29/8-02	1	20.00	1949	
440	PBXN-5	Pellets	29/8-02	2	22.44	2072.5	1.826
444	PBXN-5	Pellets	14/9-02	4	14.96	1250	

\*Leakage

Table 2.1 Overview of the firings performed with PBXN-5.

## 2.2 Pellet pressing

Dyno Nobel ASA delivered the PBXN-5 powder used for pellet pressing. Appendix A gives the producer's control report for the used explosive. The complete name of the used explosive is PBXN-5 type II, class 2. Powder was tested as received. Pellets were pressed to four different pellet densities. The three lowest 1.59, 1.71 and 1.79 g/cm<sup>3</sup> was pressed with the press shown in figure 2.2 and the tool shown in figure 2.3. The diameter of the pellets were 18.60 mm ±, and the weight 5.00 g. Figure 2.4 gives a picture of some pellets obtained with this tool.



Figure 2.2 Picture of the press used to produce pellets with density up to 1.79 g/cm<sup>3</sup>.



Figure 2.3 Picture of press tool used to produce pellets with density up to 1.79 g/cm<sup>3</sup>.



Figure 2.4 Picture of pellets obtained with the tool shown in figure 2.3.



Figure 2.5 Picture of press and tool used to press pellets with high density.

Figure 2.5 shows the press and tool used to produce the pellets with high density. More details about the obtained pellets are given in 3.5.

### 3 RESULTS

#### 3.1 Press Powder

PBXN-5 type II, class 2 consists of grains of different sizes. The control certificate from the producer is given in Appendix A. In figure 3.2 and 3.2 is given SEM (Scanning Electron Microscopy) pictures of some grains from the used charge.

PBXN-5 type II, class 2 powder is produced from a mixture of 75wt.% class 1 and 25wt.% class 5 HMX. Each grain will contain a different number of different crystal sizes.

Through U.S.S. Sieve no.	Sieve opening mm	Class 1(A) %		Class 2 (B) %	Class 3 (C) %	Class 4 (D) %	Class 5 (E) %
8	2.360					100	
12	1.700				99 min.	85 min.	
35	0.500					25 $\pm$ 15	
50	0.300	90 $\pm$ 6	90 $\pm$ 6	100	40 $\pm$ 15		
100	0.150	50 $\pm$ 10	50 $\pm$ 10		20 $\pm$ 10	15 max.	
120	0.125			98 min.			
200	0.075	20 $\pm$ 6	20 $\pm$ 6		10 $\pm$ 10		
325	0.045	13 $\pm$ 5	8 $\pm$ 5	75 min.			98 min.
Note		*	**	*/**	*/**	*/**	*/**

\*Military Specification MIL-H-45444 A (Ord), 24 Apr. 1961, Amendment – 3, 31 July 1962.

\*\*Military Specification MIL-H-45444 B (PA), 27 Feb. 1974, Amendment – 1, 15 July 1975.

Table 3.1 The crystal size distribution for the different classes of HMX.

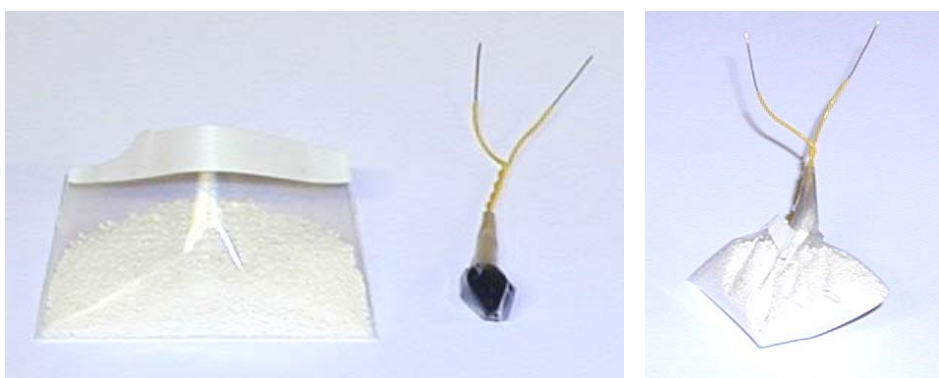
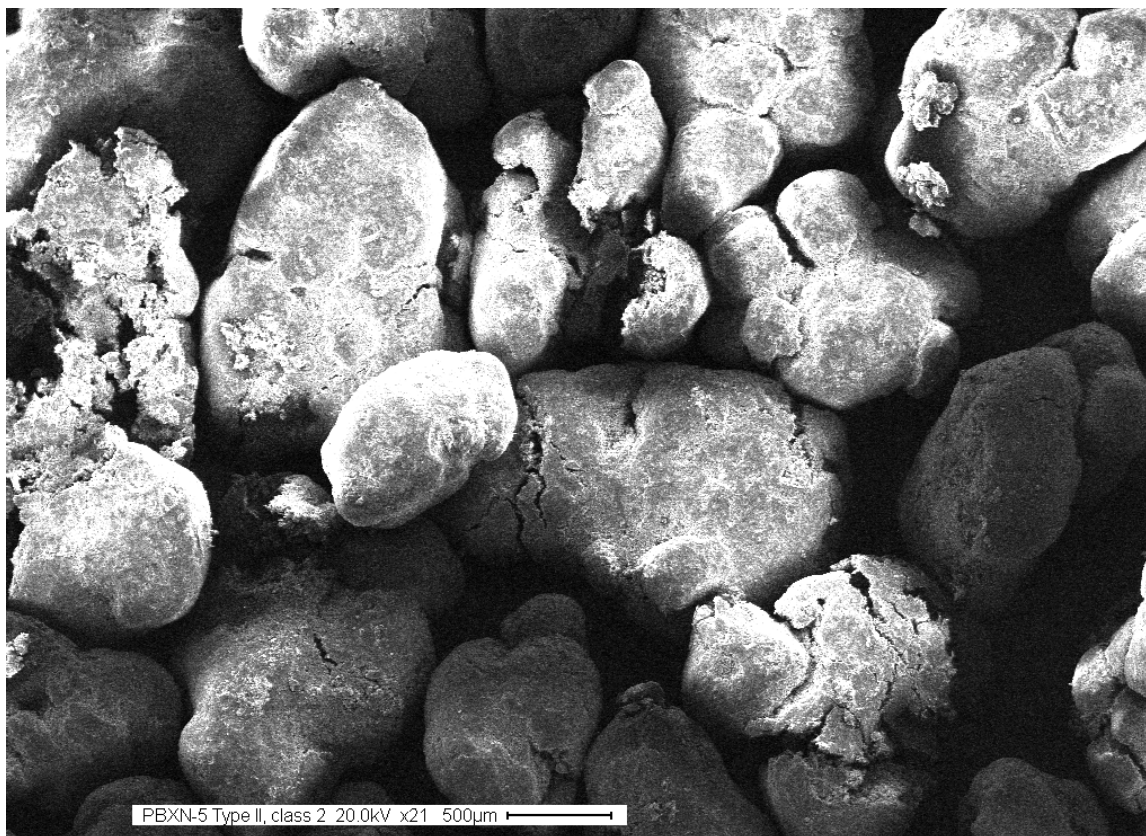
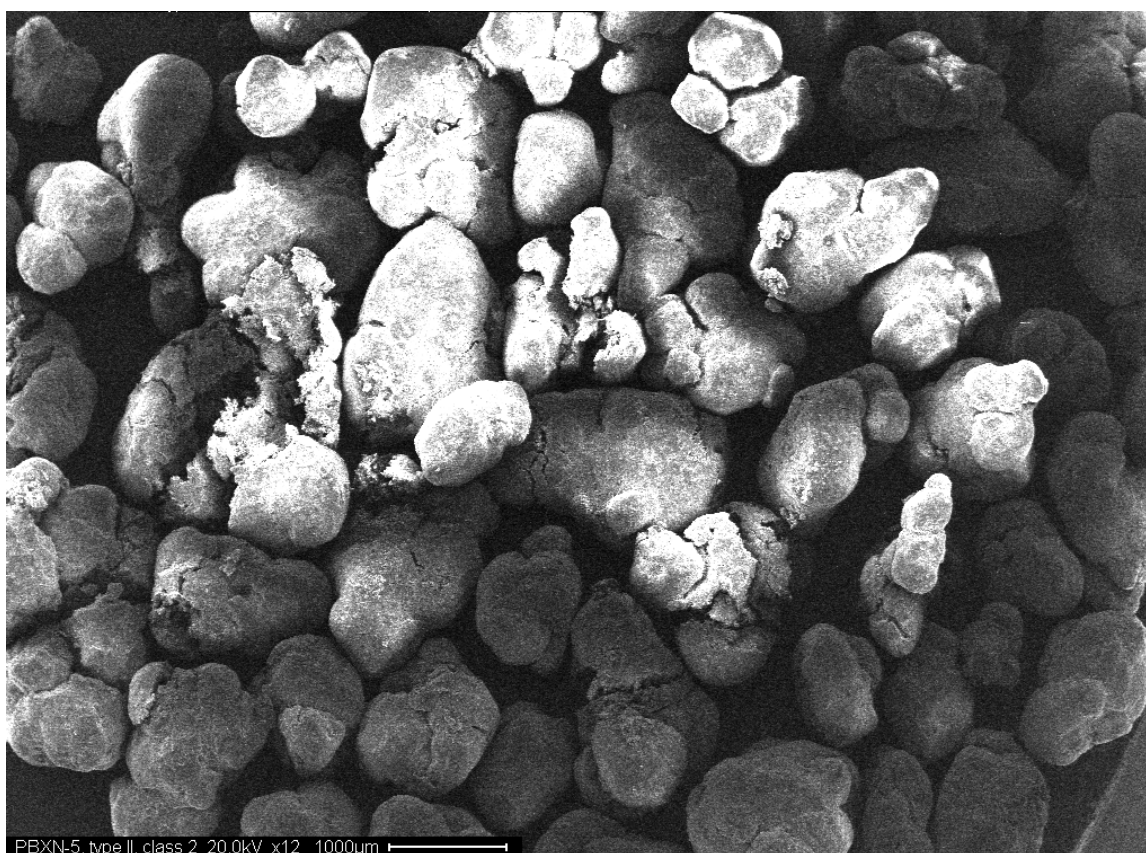


Figure 3.1 Pictures of PBXN-5 powder and the ignition unit (1 g Black Powder + squib).

From table 3.1 above one will see that PBXN-5 will contain a relatively large number of small crystals. The burning of PBXN-5 will be strongly influenced by how the burn front is moving in the grains. The question is: do the grains ignite only on their surface or will most single crystal inside the grains also be ignited? The difference in surface area for these two cases is significant and will give two different pressure-time curves. Figure 3.1 gives a picture of how



*Figure 3.2 SEM picture of PBXN-5 grains, magnification 21x.*



*Figure 3.3 SEM picture of PBXN-5 grains, magnification 12x.*

the powder was packed before testing in the CV. With PBXN-5 powder we have performed 13 firings with 6 different loading densities. The pressure-time curve for each firing is given in figure 3.4 to 3.16. In figure 3.17 has pressure-time curves for all firings with PBXN-5 powder been given in the same plot.

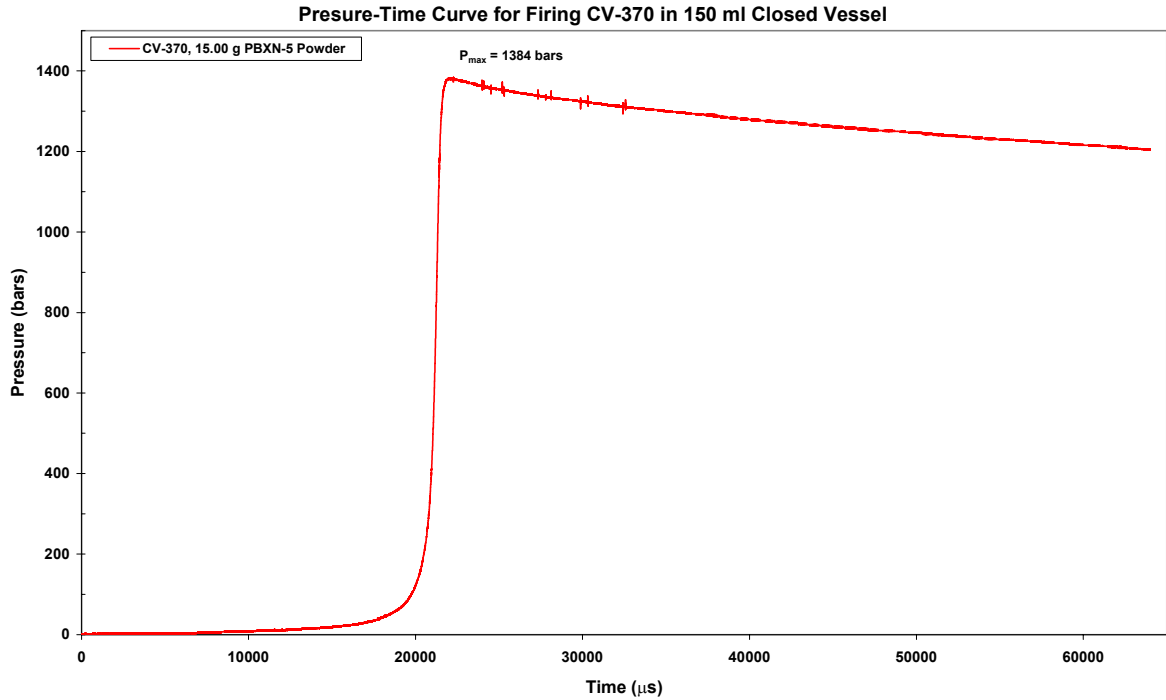


Figure 3.4 Pressure-time curve for firing CV-370 with 15.00 g PBXN-5 powder.

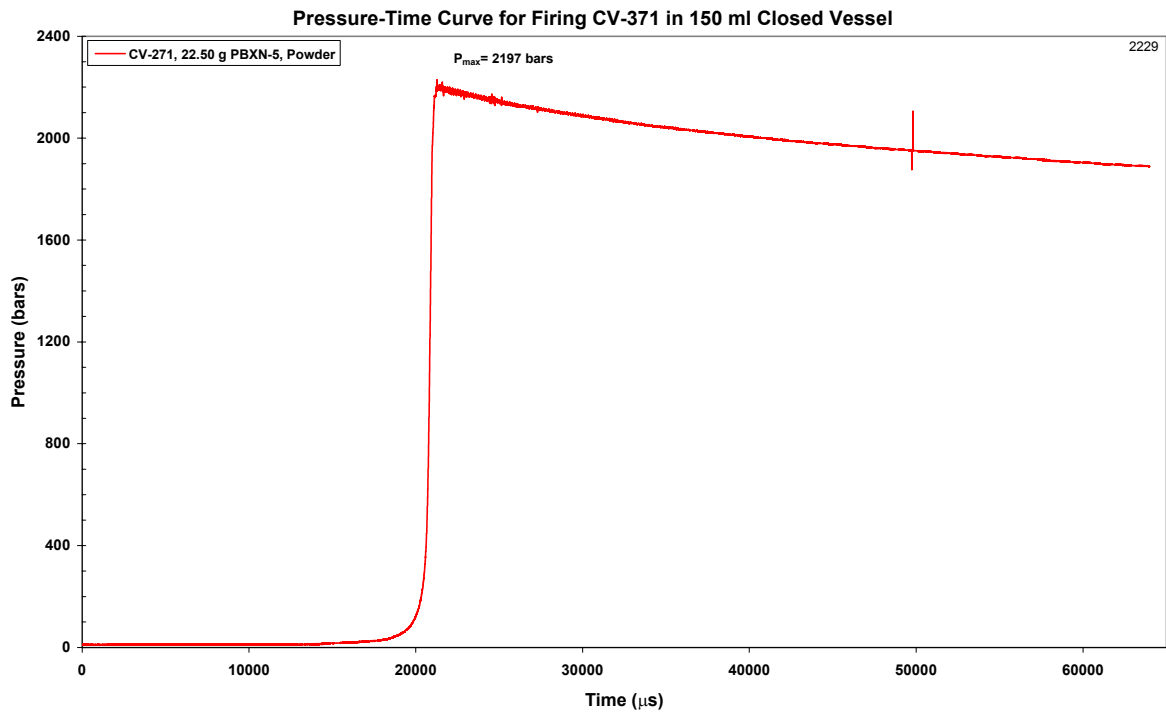


Figure 3.5 Pressure-time curve for firing CV-371 with 22.50 g PBXN-5 powder.

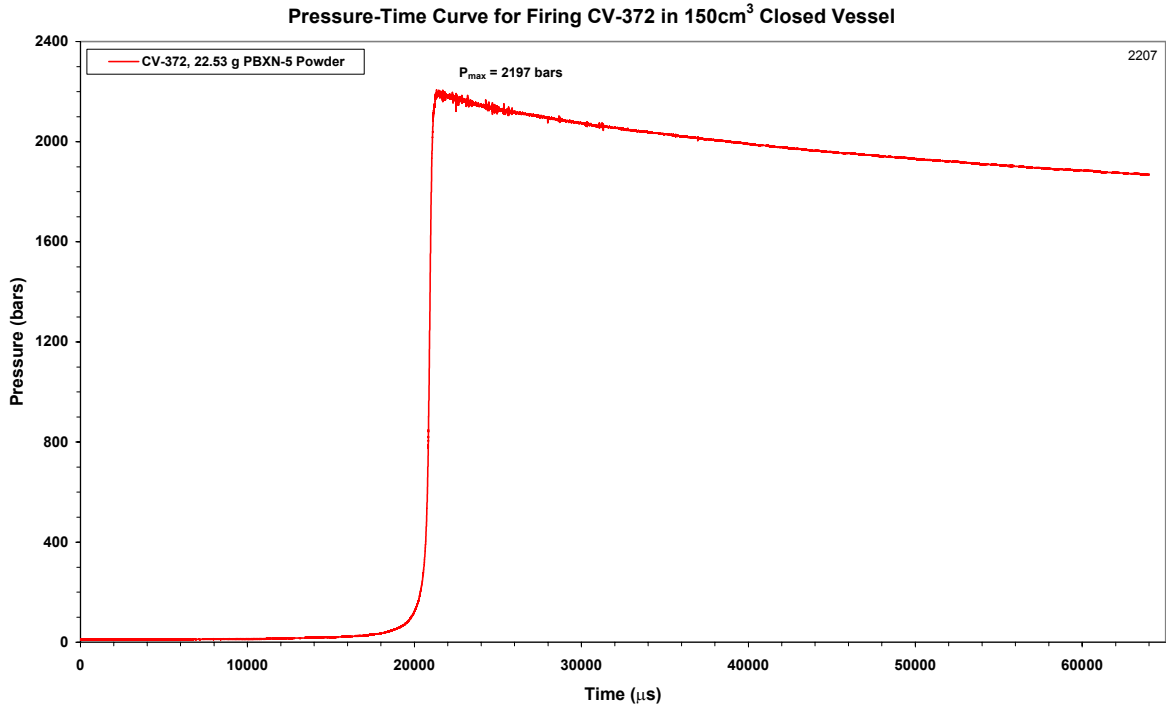


Figure 3.6 Pressure-time curve for firing CV-372 with 22.53 g PBXN-5 powder.

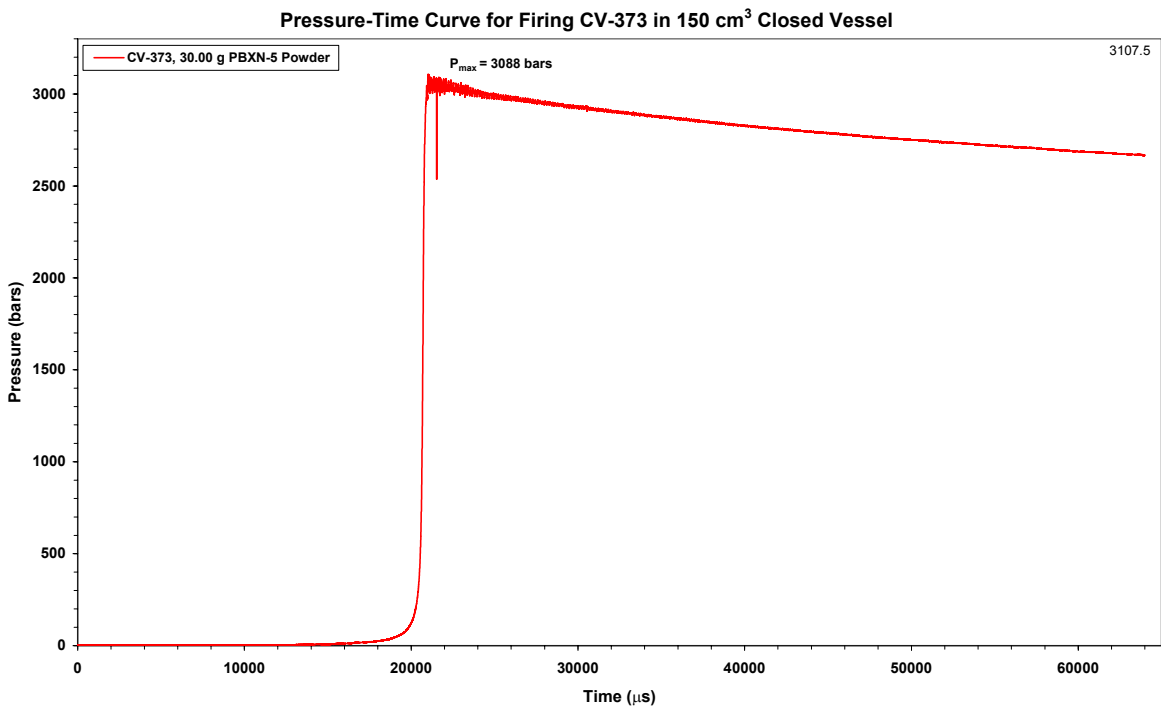


Figure 3.7 Pressure-time curve for firing CV-373 with 30.00 g PBXN-5 powder.



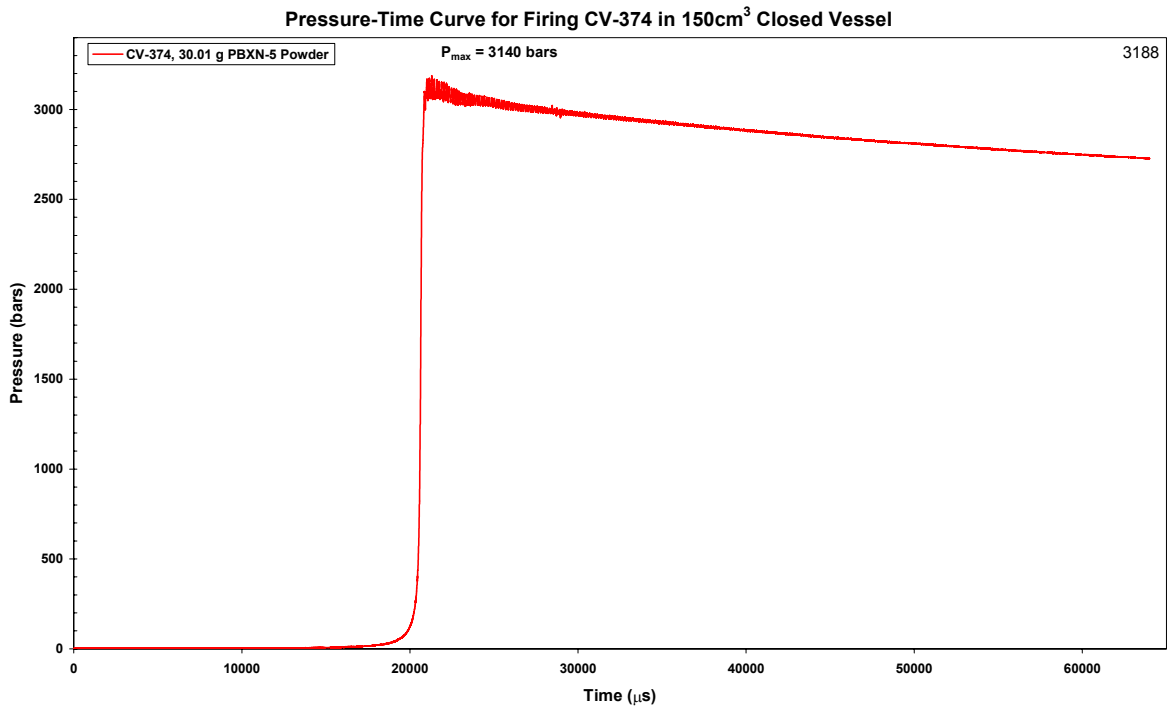


Figure 3.8 Pressure-time curve for firing CV-374 with 30.01 g PBXN-5 powder.

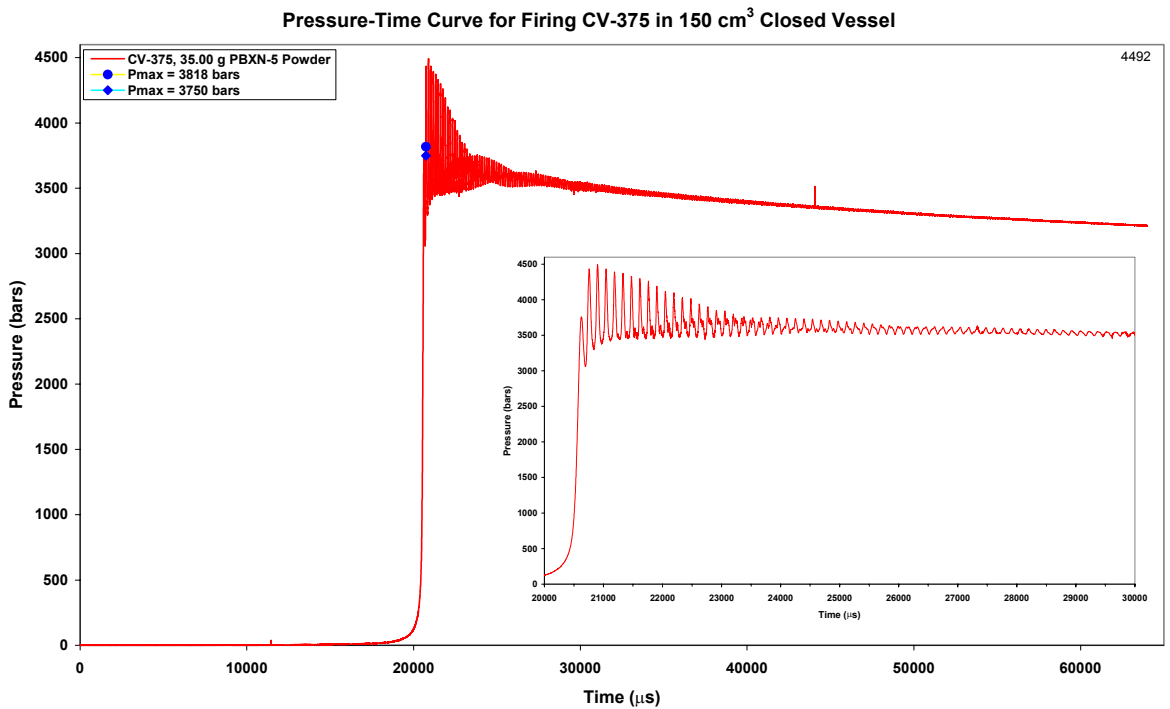


Figure 3.9 Pressure-time curve for firing CV-375 with 35.00 g PBXN-5 powder.

As shown in figure 3.9 the pressure-time curve contains strong disturbances. This makes it difficult to say exactly what is the maximum pressure. We have selected the blue point at 3750 bars as maximum pressure, and used this value for determination of the impetus and co-volume. The choice of maximum pressure at high loading densities has the effect that the

impetus goes down. We did perform only one firing with a loading of 35 g PBXN-5 powder because we were afraid that the closed vessel could collapse.

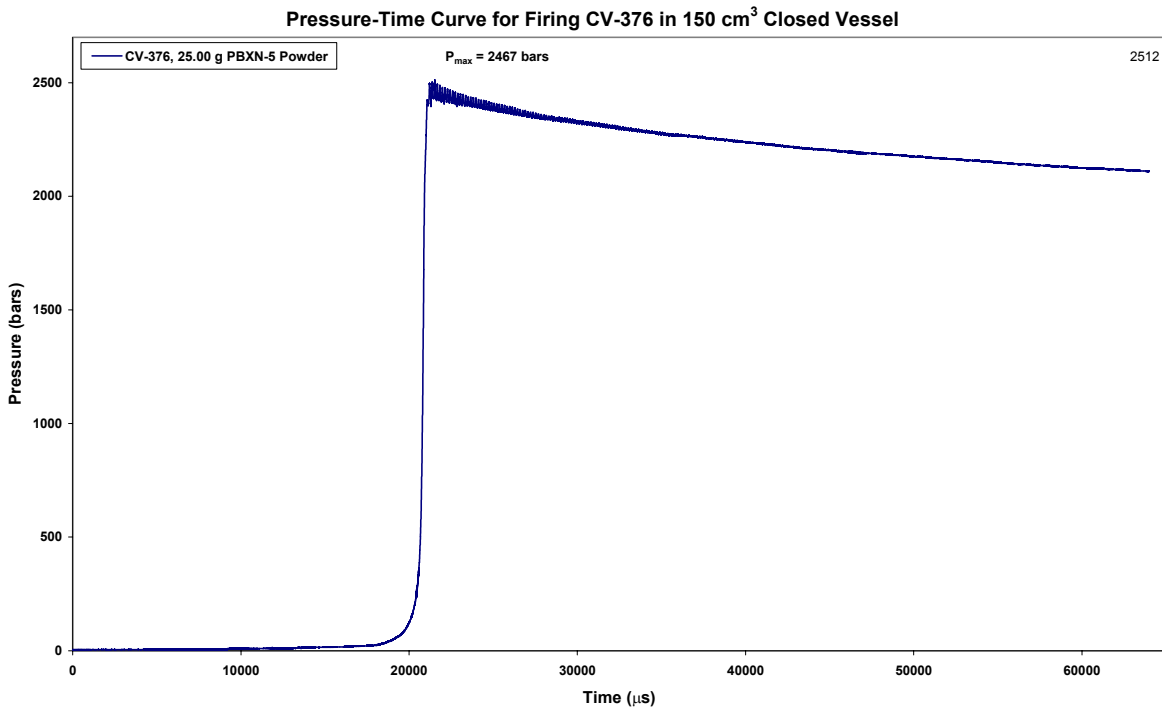


Figure 3.10 Pressure-time curve for firing CV-376 with 25.00 g PBXN-5 powder.

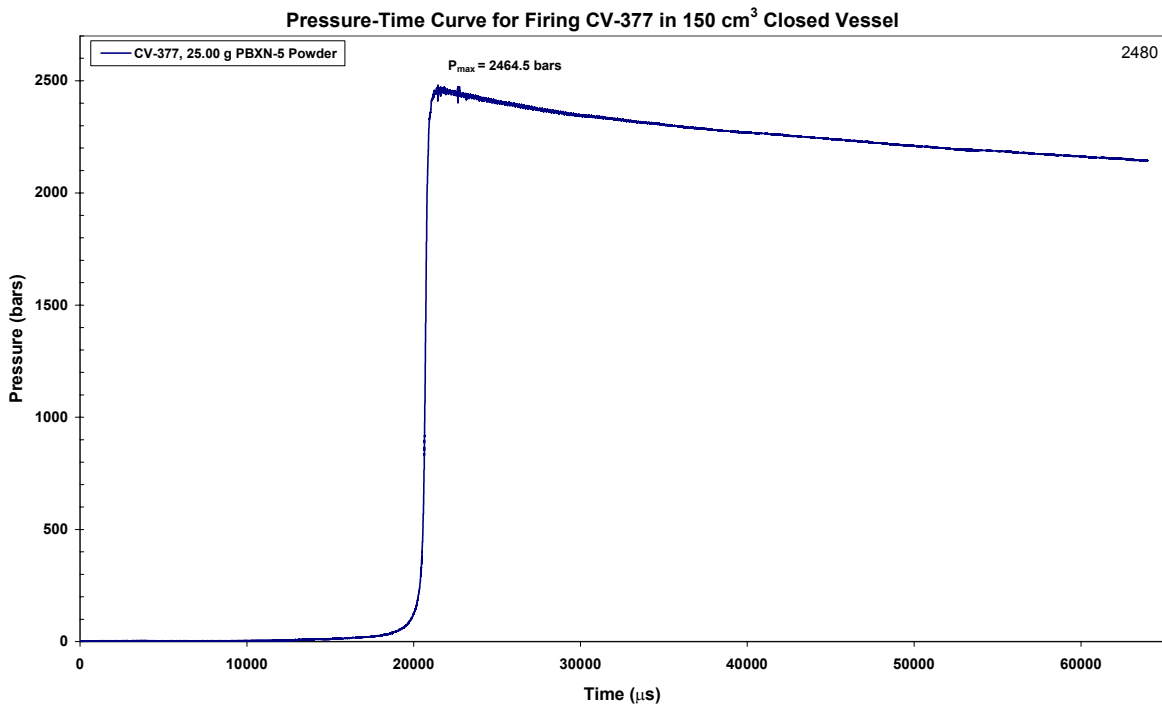


Figure 3.11 Pressure-time curve for firing CV-377 with 25.00 g PBXN-5 powder.

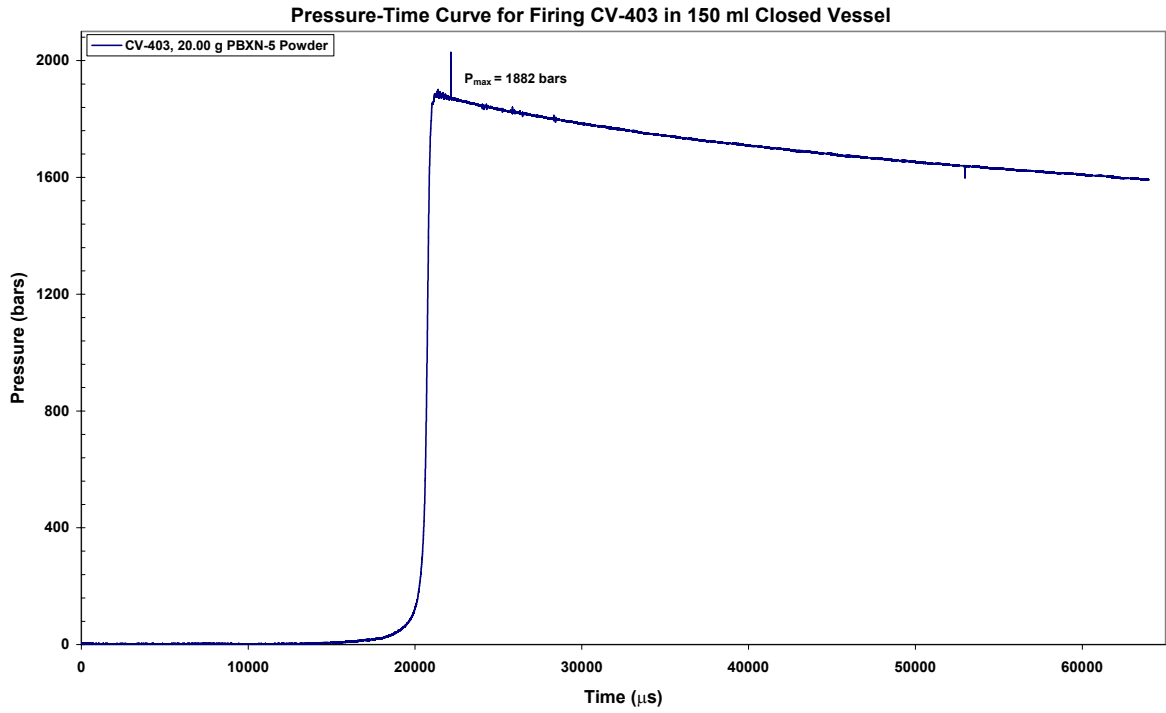


Figure 3.12 Pressure-time curve for firing CV-403 with 20.00 g PBXN-5 powder.

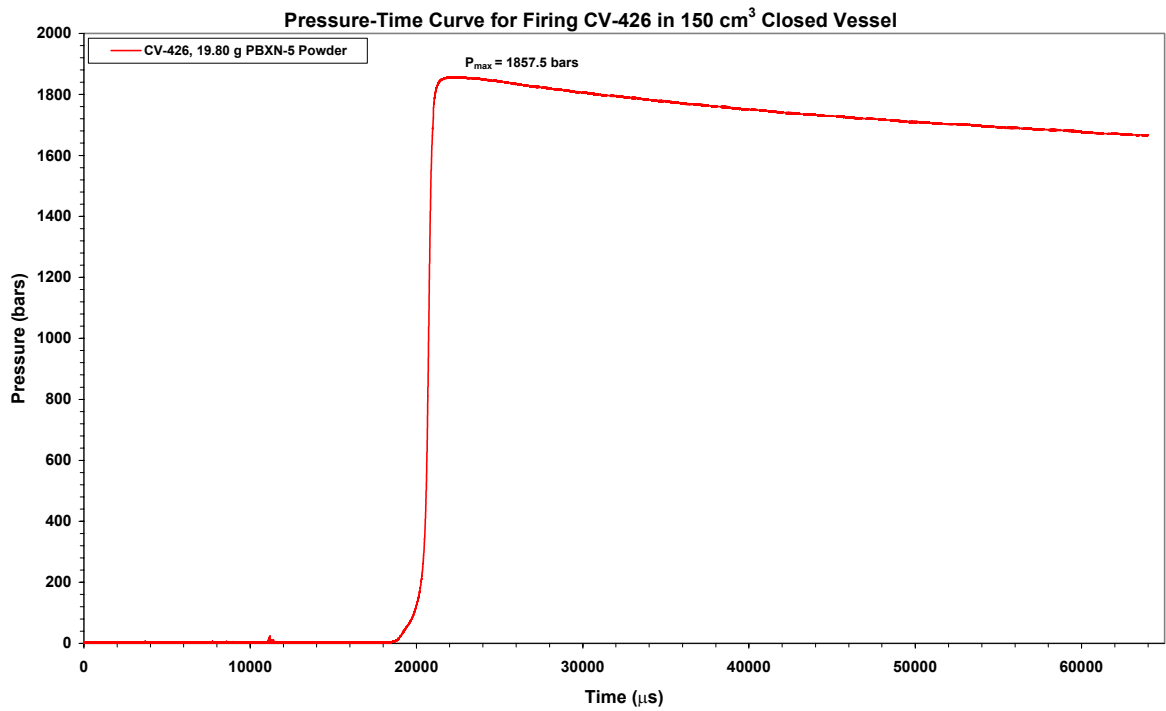


Figure 3.13 Pressure-time curve for firing CV-426 with 19.80 g PBXN-5 powder

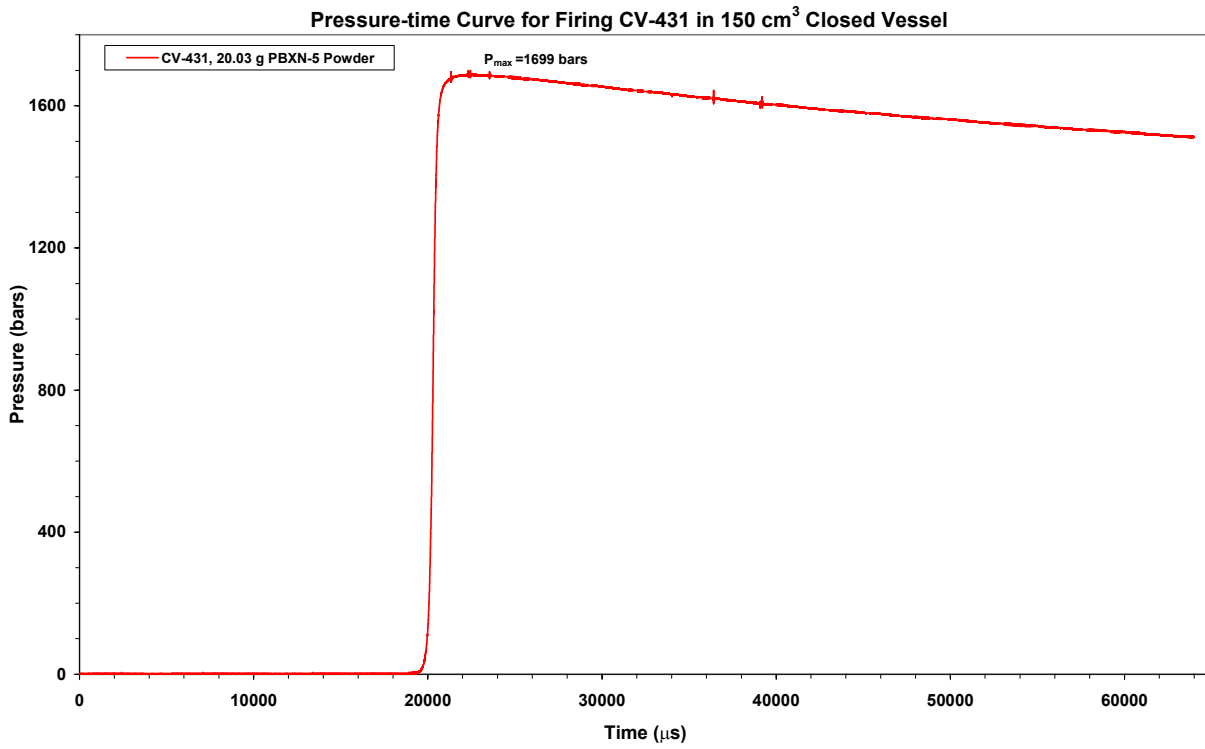


Figure 3.14 Pressure-time curve for firing CV-431 with 20.03 g PBXN-5 powder.

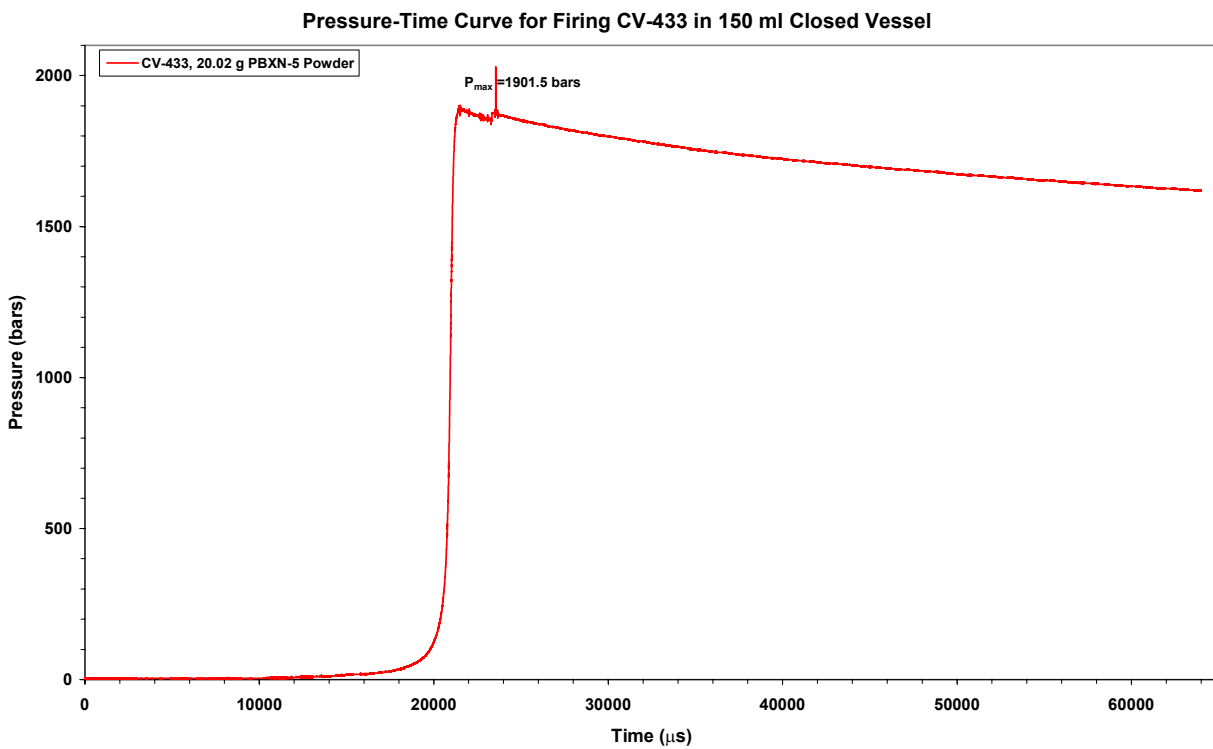


Figure 3.15 Pressure-time curve for firing CV-433 with 20.02 g PBXN-5 powder.

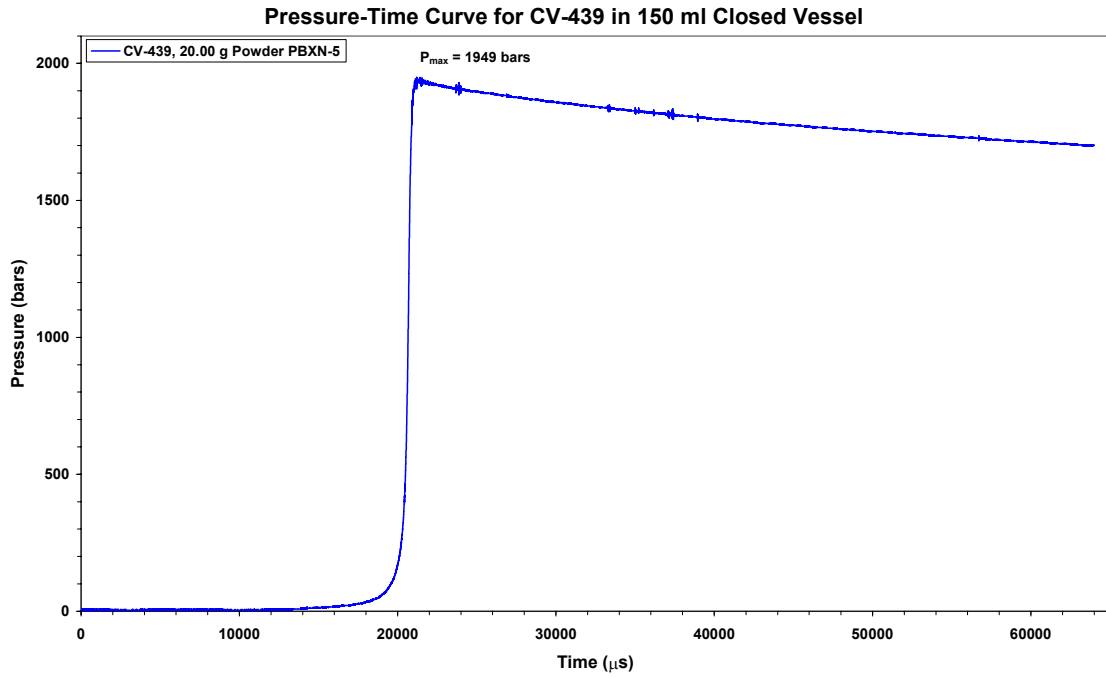


Figure 3.16 Pressure-time curve for firing CV-439 with 20.0 g PBXN-5 powder.

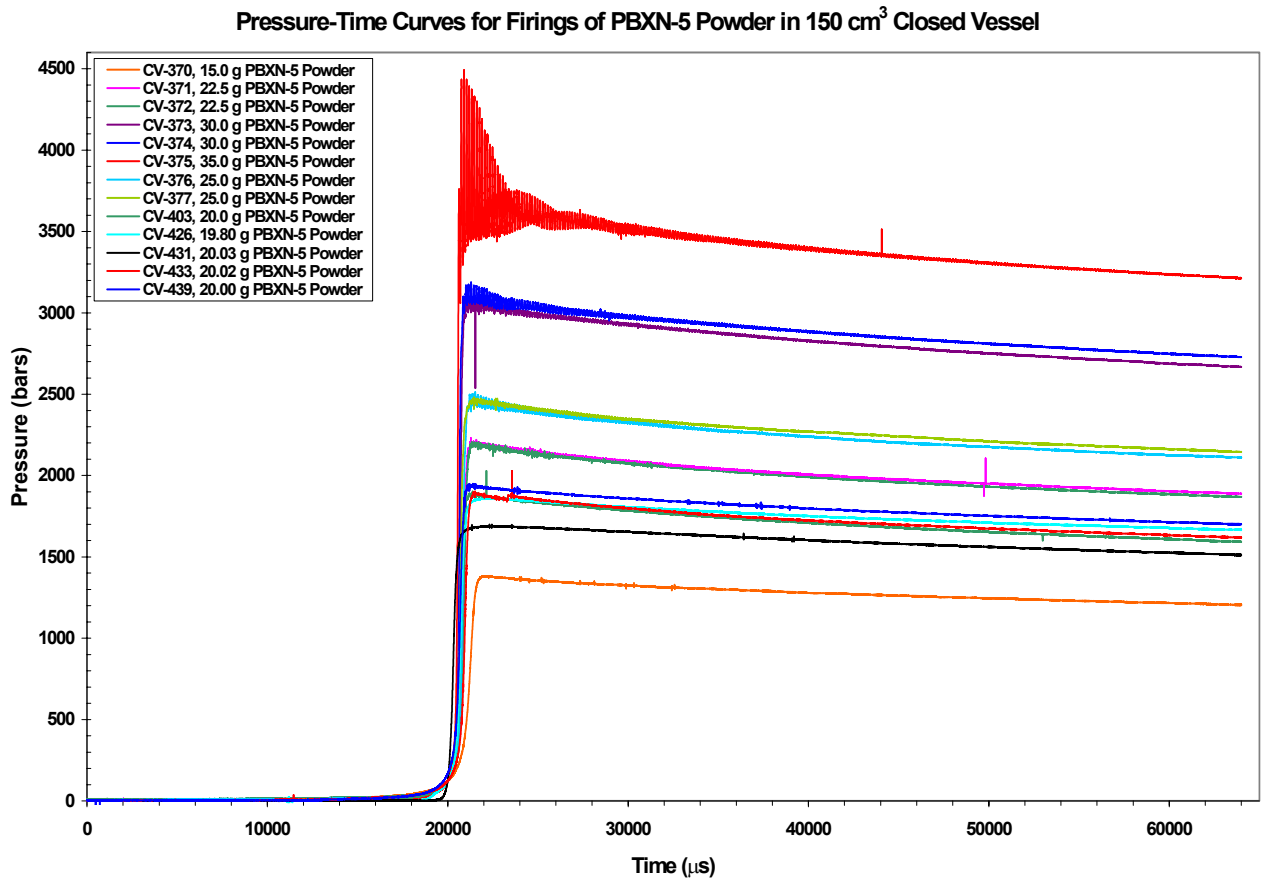


Figure 3.17 Pressure-time curves for all firings with PBXN-5 powder.

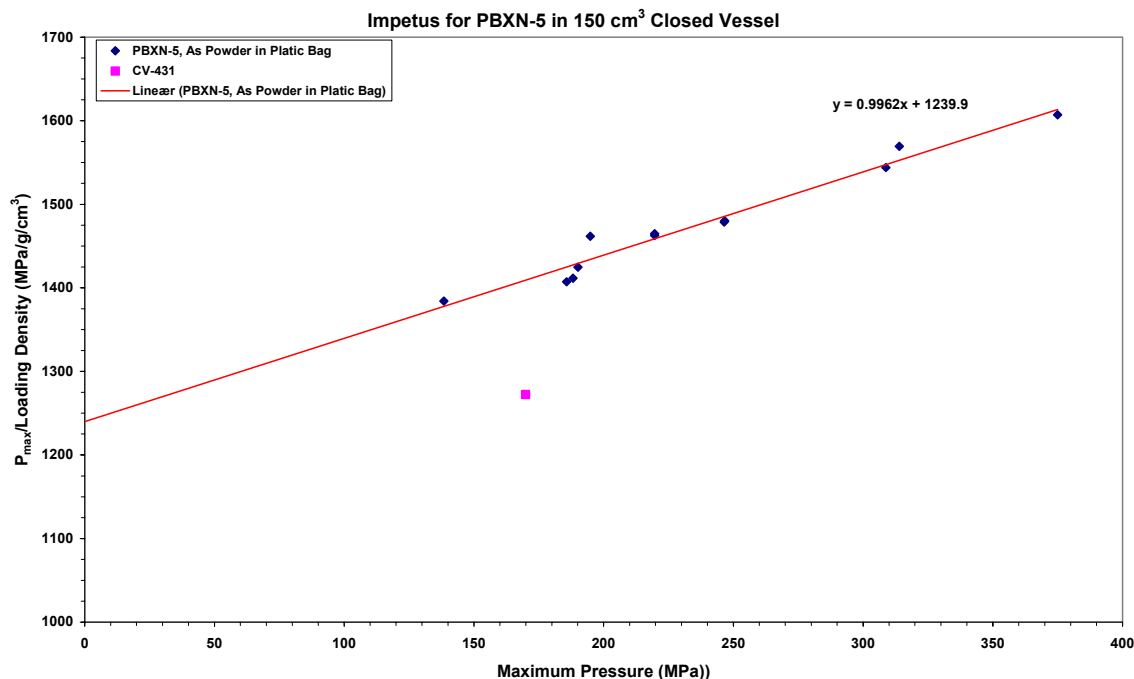


Figure 3.18 Impetus and Co-volume for PBXN-5 powder.

Firing No.	Weight (g)	Load Density (g/cm <sup>3</sup> )	P <sub>max</sub> (MPa)	P <sub>max</sub> /LD (MPa/g/cm <sup>3</sup> )
CV-370	15.00	0.1000	138.40	1384.00
CV-403	20.00	0.1333	188.20	1411.50
CV-371	22.50	0.1500	219.70	1464.67
CV-372	22.53	0.1502	219.70	1462.72
CV-376	25.00	0.1667	246.70	1480.20
CV-377	25.00	0.1667	246.45	1478.70
CV-373	30.00	0.2000	308.80	1544.00
CV-374	30.01	0.2067	314.00	1569.48
CV-375	35.00	0.2333	375.00	1607.14
CV-426	19.80	0.1320	185.75	1407.20
CV-431	20.03	0.1335	169.90	1272.34
CV-433	20.02	0.1335	190.15	1424.70
CV-439	20.00	0.1333	194.90	1461.75

Table 3.2 Properties of the CV-firings with PBXN-5 Powder.

Table 3.2 gives a summary of all firings performed with powder PBXN-5. In figure 3.18 has P<sub>max</sub>/LD (maximum pressure/loading density) been plotted as function of maximum pressure, this gives, when firing CV-431 is excluded, an impetus of 1240 J/g and a co-volume of 0.9962 cm<sup>3</sup>/g. The obtained impetus is lower than the theoretical calculation by Cheetah given in 3.6. For the firings with powder PBXN-5 the obtained pressure-time curves have disturbances in the maximum pressure that make it difficult to set the right value. Therefore by choosing lower maximum pressures for some of the firings with the highest loading densities will give a higher impetus.

### 3.2 Cylinder pellets pressed with 400 kg

Pellets of different densities were produced by use of different compaction pressures on different press tools and presses. To obtain a density of the PBXN-5 pellets of approximately  $1.6 \text{ g/cm}^3$ , we used a pressure of 400 kg on a tool with internal diameter of 18.60 mm. Figure 3.19 gives a picture of some of the pellets obtained with the tool and press shown in figure 2.2 and 2.3. Table 3.3 gives the obtained density of the 23 pellets produced with a press pressure of 400kg.



Figure 3.19 Pressed PBXN-5 pellets for testing in Closed Vessel.

Pellet No.	Weight (g)	Height (mm)	Volume (mm <sup>3</sup> )	Density (g/cm <sup>3</sup> )	Firing No. Weight (g)
1	4.98	11.54	3144.13	1.5839	CV-419 15.00 g
2	5.02	11.59	3157.76	1.5897	
3	4.99	11.55	3146.86	1.5857	
4	5.01	11.62	3165.93	1.5825	CV-418 20.06 g
5	5.01	11.62	3165.93	1.5825	
6	5.00	11.60	3160.48	1.5820	
7	5.03	11.62	3165.93	1.5888	
8	5.02	11.62	3165.93	1.5856	CV-420 25.01 g
9	5.00	11.62	3165.93	1.5793	
10	5.00	11.59	3157.76	1.5834	
11	5.00	11.62	3165.93	1.5793	
12	4.99	11.56	3149.58	1.5843	
13	5.02	11.54	3144.13	1.5966	CV-421 30.06 g
14	5.01	11.62	3165.93	1.5825	
15	5.01	11.63	3168.66	1.5811	
16	5.02	11.60	3160.48	1.5884	
17	5.01	11.53	3141.41	1.5948	
18	5.00	11.54	3144.13	1.5903	
19	5.01	11.56	3149.58	1.5907	CV-422 25.00 g
20	5.00	11.54	3144.13	1.5907	
21	5.01	11.56	3149.58	1.5907	
22	4.99	11.52	3138.69	1.5898	
23	5.00	11.48	3127.79	1.5986	
<b>*Diameter 18.63 mm</b>		<b>Average Density</b>		<b>1.5870</b>	

Table 3.3 Weight and dimensions for PBXN-5 pellets pressed to a density of  $1.59 \text{ g/cm}^3$ .

Figure 3.20 shows how the pellets were packed together with the ignition unit we used. Figure 3.21 to 3.25 gives all single pressure-time curves performed with pellets with average density of  $1.59 \text{ g/cm}^3$ . Figure 3.26 gives all pressure-time curves obtained with pellets having a density

of  $1.59 \text{ g/cm}^3$ . Table 3.4 gives a summary of measured pressures and properties needed to experimentally determine the impetus and co-volume.



Figure 3.20 Picture of the orientation of the pellets and ignition device before firing.

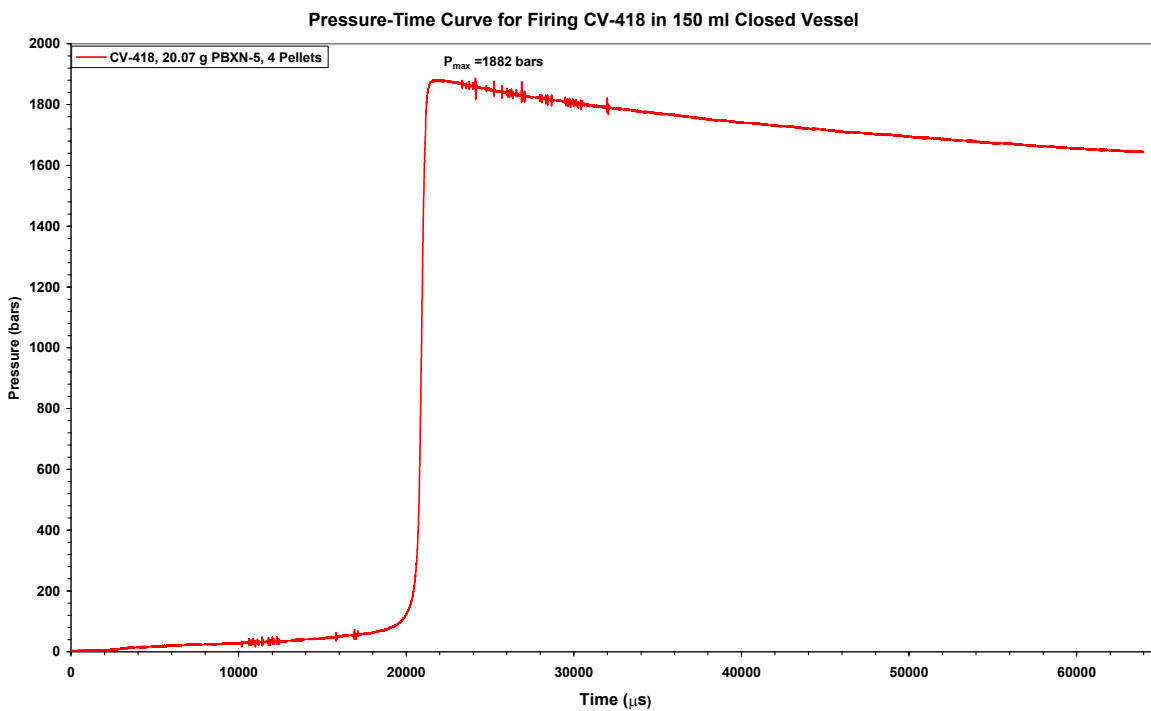


Figure 3.21 The Pressure-Time curve for firing CV-418 with 4 pellets.



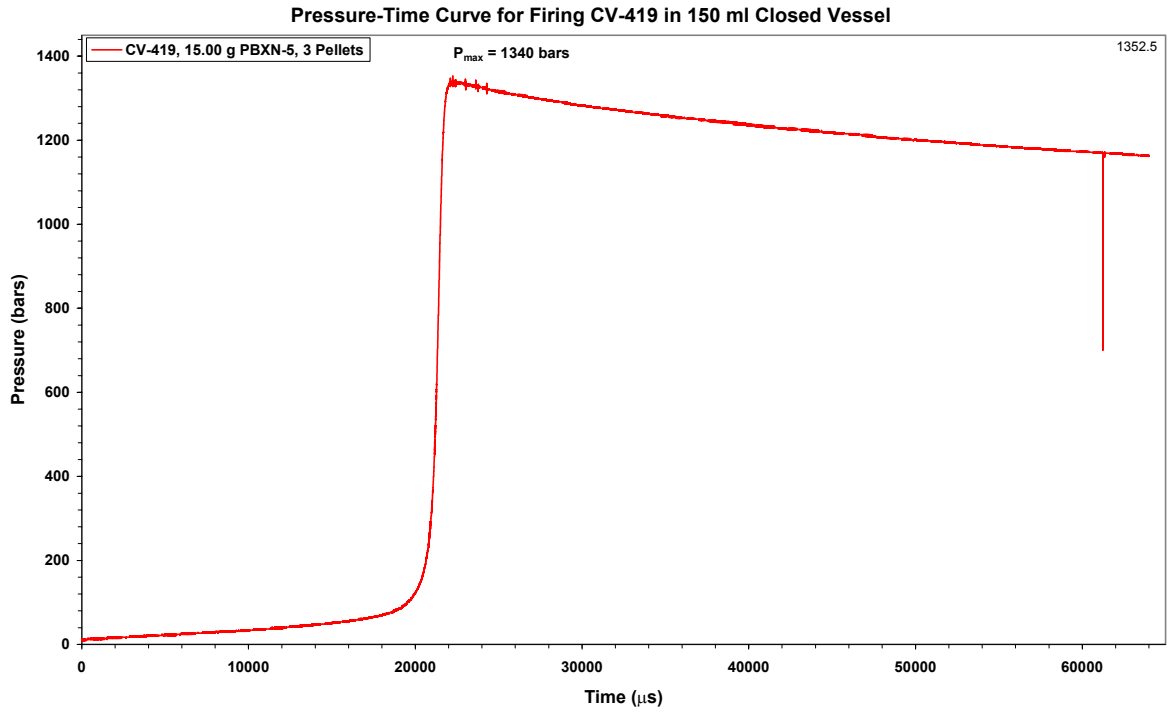


Figure 3.22 The Pressure-Time curve for firing CV-419 with 5 pellets.

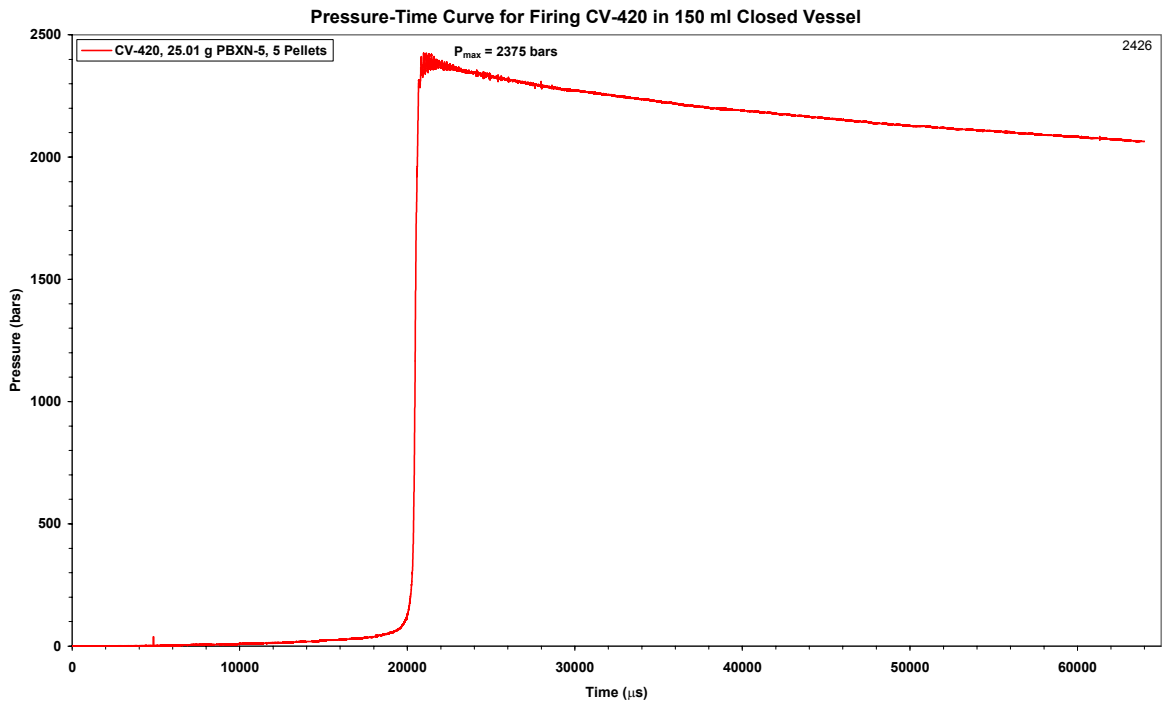


Figure 3.23 The Pressure-Time curve for firing CV-420 with 6 pellets.

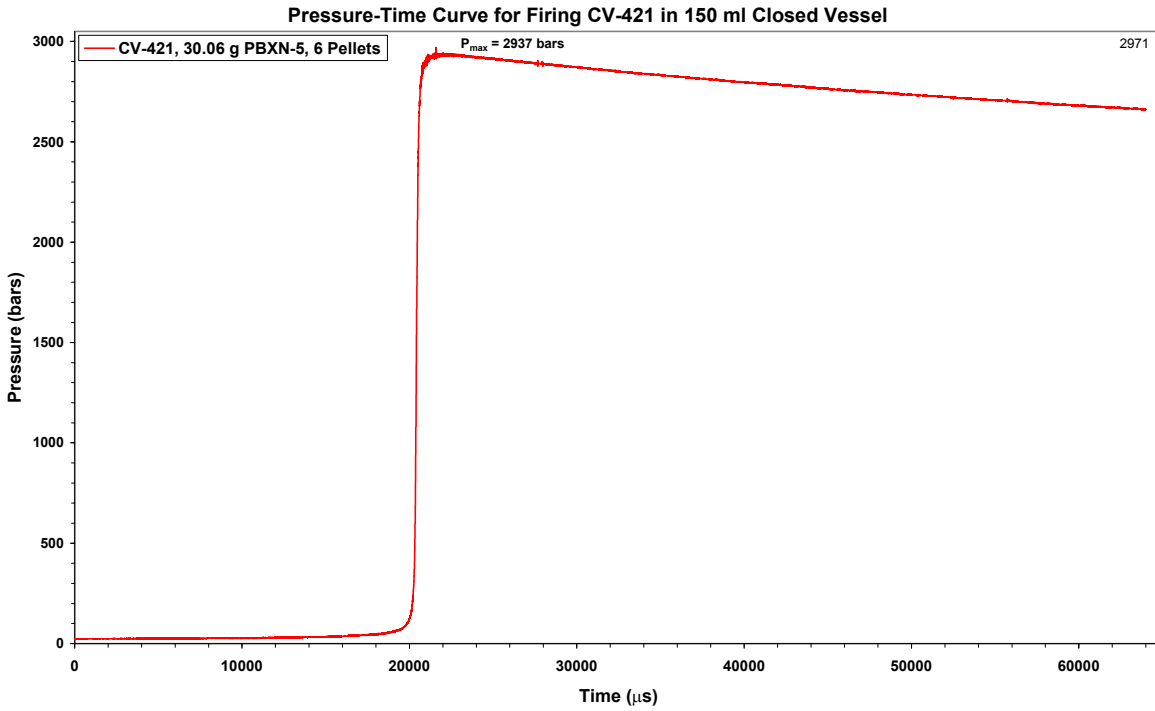


Figure 3.24 The Pressure-Time curve for firing CV-421 with 6 pellets.

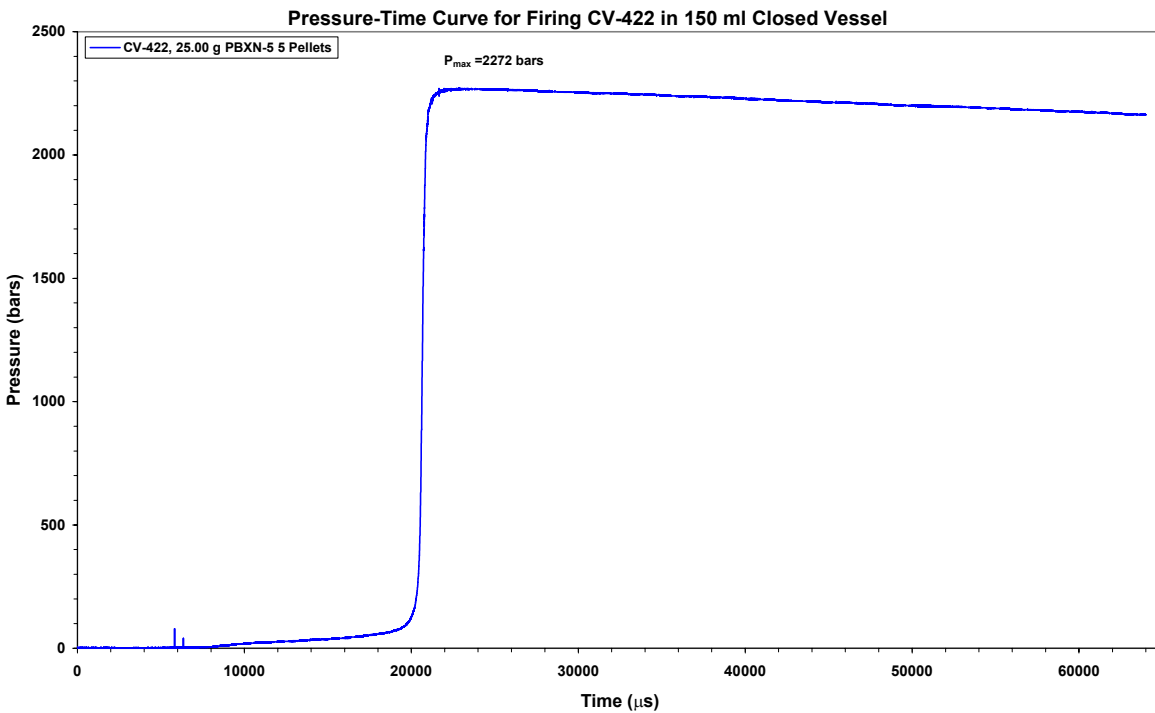


Figure 3.25 The Pressure-Time curve for firing CV-422 with 5 pellets.

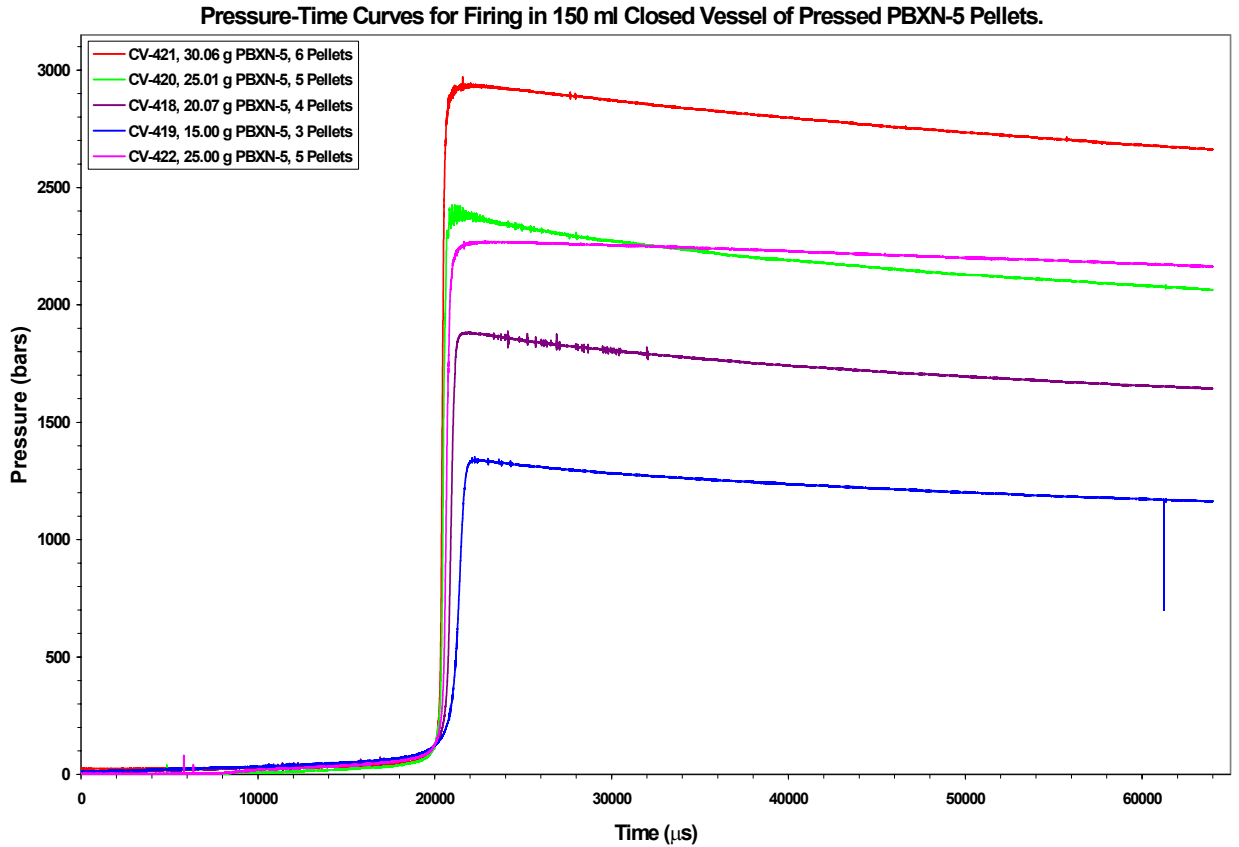


Figure 3.26 Pressure-time curves for all firings with pellets pressed with 400 kg.

Firing No.	PBXN-5 weight (g)	Loading Density (g/cm <sup>3</sup> )	Maximum Pressure (MPa)	Pmax/LD (MPa/g/cm <sup>3</sup> )
CV-419	15.00	0.1000	134.0	1340.00
CV-418	20.07	0.1338	188.2	1406.58
CV-422	25.00	0.1667	227.2	1363.20
CV-420	25.01	0.1667	237.5	1424.43
CV-421	30.06	0.2004	293.7	1465.57

Table 3.4 Properties for CV-firings with PBXN-5 pellets with density of 1.59 g/cm<sup>3</sup>.

In figure 3.27 has the properties in table 3.4 been plotted. This gives an experimental impetus of 1248 J/g or 1250 J/g if we do not include firing CV-422. From figure 4.26 we can see that the pressure-time curve for firing CV-422 has an abnormal form different from the other pressure-time curves. For CV-422 the pressure increases or at least stays more or less constant long after the material should have burned up. In ref. 2 we tried to explain this observation by changes in the properties of the grease in the channel in front of the pressure gauge. For the co-volume figure 3.27 gives a result of 0.7484 cm<sup>3</sup>/g, a result below the theoretical calculated value obtained in 3.6.

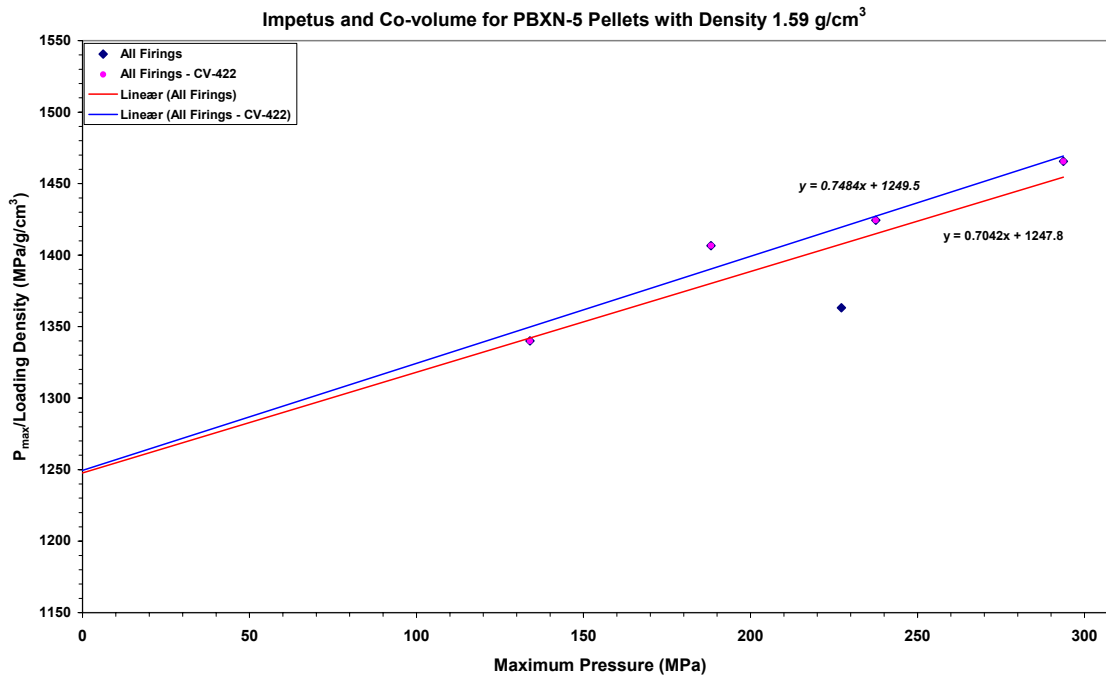


Figure 3.27 Experimentally impetus and co-volume for PBXN-5 pellets with density 1.59 g/cm<sup>3</sup>.

### 3.3 Cylinder pellets pressed with 1340 kg

The next density of PBXN-5 pellets we planned to test was 1.70 g/cm<sup>3</sup>. To produce these pellets we used the same press and tool as we used to produce the pellets tested in 3.2.

Pellet No.	Weight (g)	Height (mm)	Volume (cm <sup>3</sup> )	Density (g/cm <sup>3</sup> )	Firing No. Weight (g)
1	4.97	10.77	2.9249	1.6992	CV-384, 14.97 g
2	5.00	10.79	2.9303	1.7063	
3	4.99	10.79	2.9303	1.7029	
4	4.98	10.75	2.9195	1.7058	CV-383, 19.96 g
5	4.98	10.68	2.9005	1.7170	
6	4.99	10.79	2.9303	1.7029	
7	4.98	10.79	2.9303	1.6995	
8	4.99	10.78	2.9276	1.7045	CV-382, 24.92 g
9	5.00	10.76	2.9222	1.7110	
10	4.98	10.78	2.9276	1.7010	
11	5.00	10.77	2.9249	1.7095	
12	4.97	10.75	2.9195	1.7024	
13	4.99	10.74	2.9168	1.7108	CV-385, 29.93 g
14	5.01	10.79	2.9303	1.7097	
15	5.00	10.74	2.9168	1.7142	
16	4.97	10.62	2.8842	1.7232	
17	4.99	10.65	2.8923	1.7253	
18	5.02	10.70	2.9059	1.7275	
19	5.01	10.67	2.8977	1.7289	CV-430, 20.03 g
20	5.02	10.67	2.8977	1.7324	
21	5.00	10.67	2.8977	1.7255	
22	5.03	10.72	2.9113	1.7277	
<b>*Diameter 18.60 mm</b>		<b>Average Density</b>		<b>1.7131</b>	

Table 3.5 Weight and dimensions of PBXN-5 pellets pressed to a density of 1.713 g/cm<sup>3</sup>.

Table 3.5 gives the weight and dimensions of the pellets used in the five firings we did perform with these pellets. Figure 3.28 to 3.32 gives the pressure-time curves for all firings, while figure 3.33 gives all firings with PBXN-5 pellets with density of  $1.713 \text{ g/cm}^3$ .

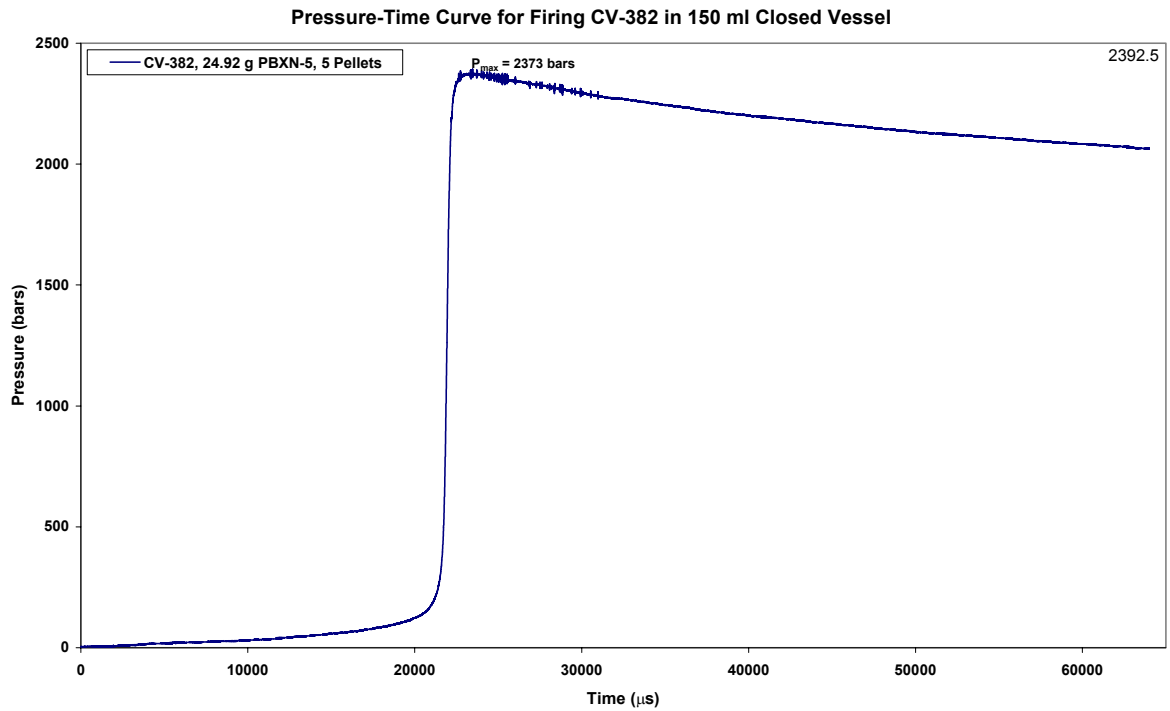


Figure 3.28 Pressure-time curve for firing CV-382.

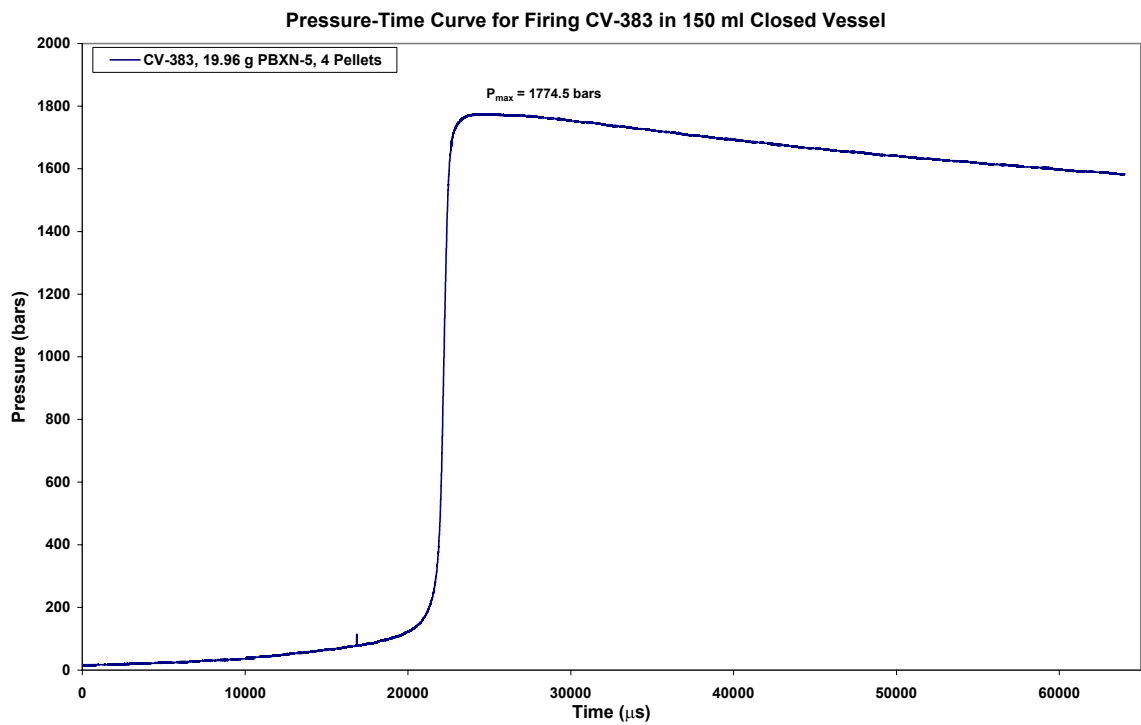


Figure 3.29 Pressure-time curve for firing CV-383.

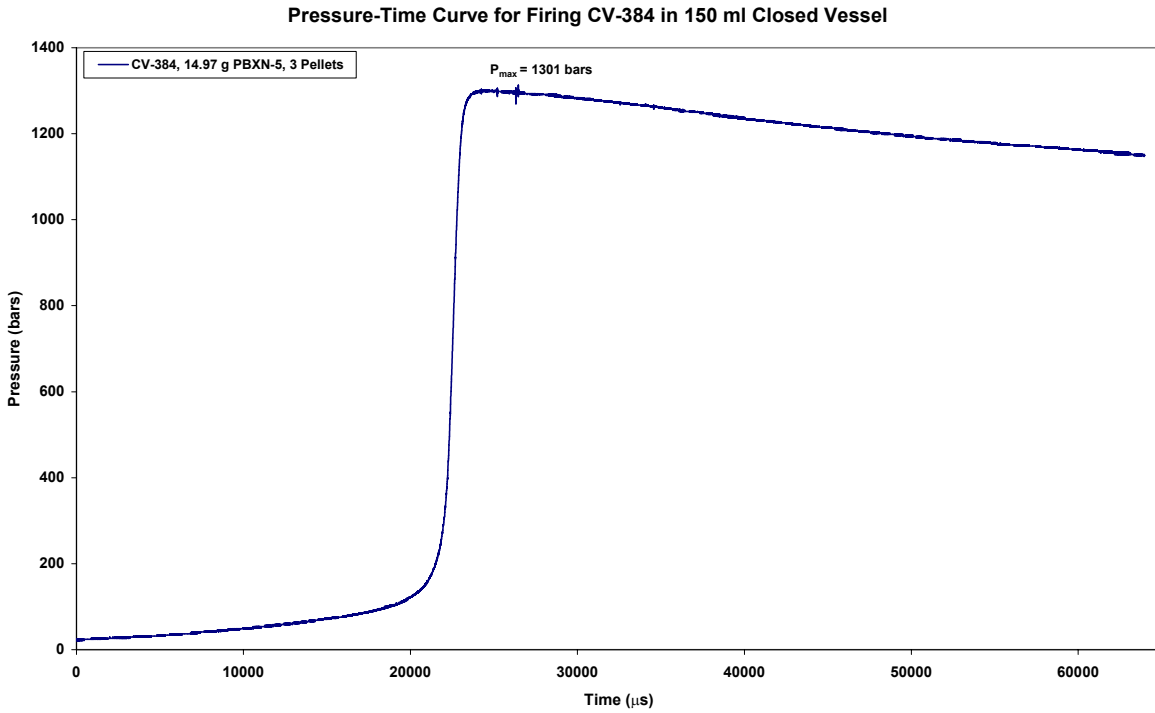


Figure 3.30 Pressure-time curve for firing CV-384.

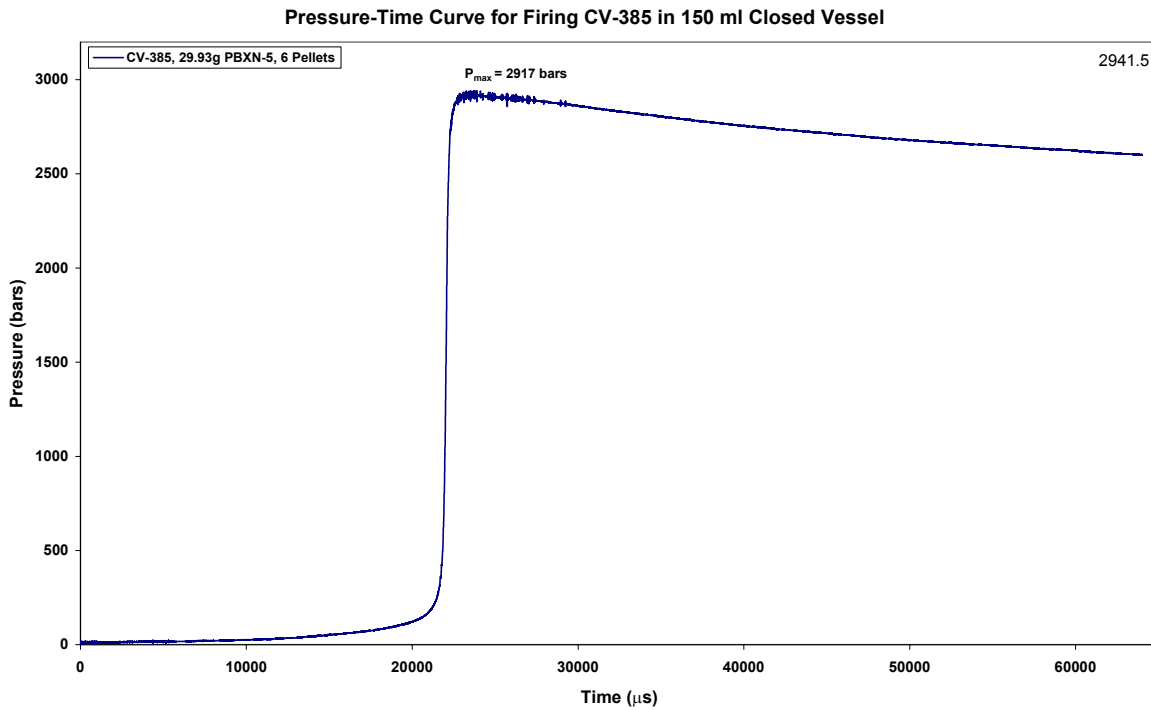


Figure 3.31 Pressure-time curve for firing CV-385, 6 PBXN-5 pellets.

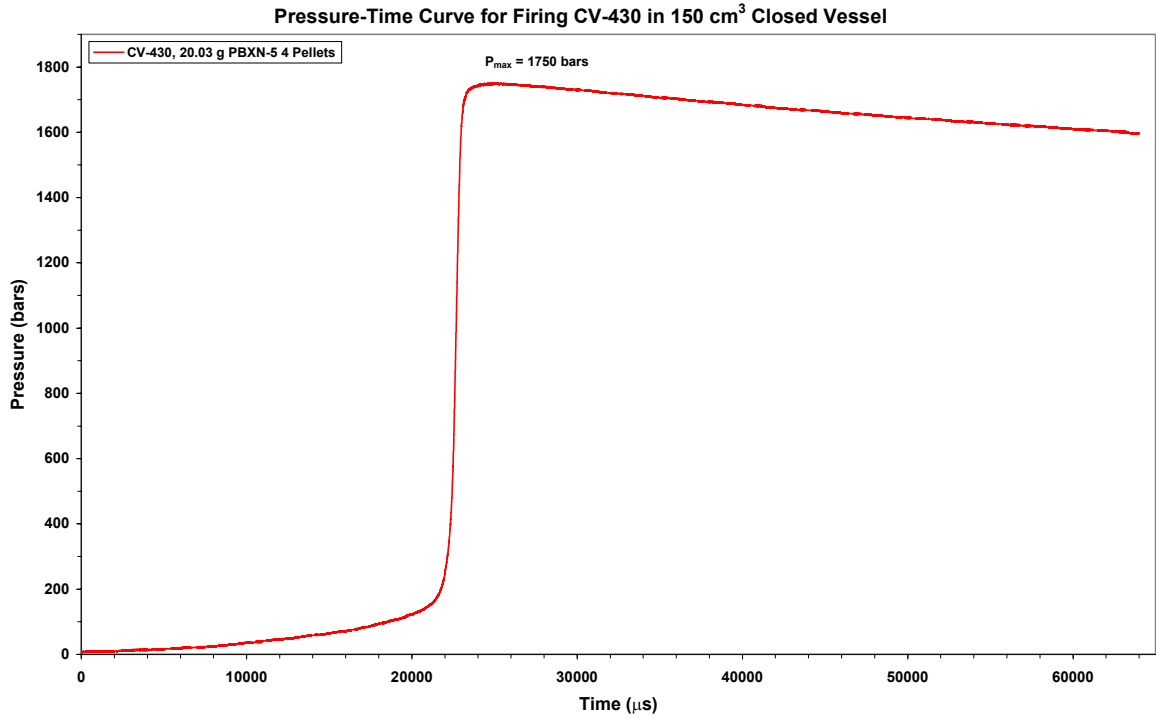


Figure 3.32 Pressure-time curve for firing CV-430, 4 PBXN-5 pellets.

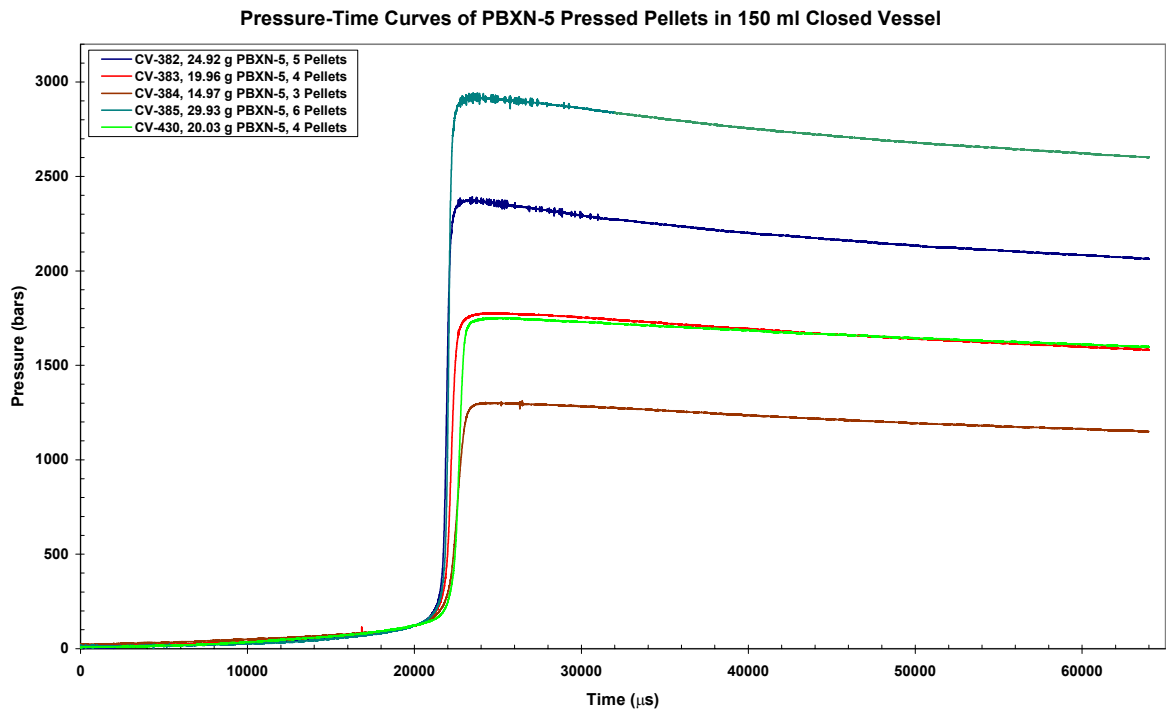


Figure 3.33 All pressure-time curves for PBXN-5 pellets pressed with 1340 kg.

Firing No.	Weight (g)	Pressure (MPa)	Load Density (g/cm <sup>3</sup> )	P <sub>max</sub> /LD (MPa/g/cm <sup>3</sup> )
CV-384	14.97	130.1	0.0998	1303.61
CV-383	19.96	177.45	0.1331	1333.54
CV-382	24.92	237.3	0.1661	1428.37
CV-385	29.93	291.7	0.1995	1461.91
CV-430	20.03	175.0	0.1335	1310.53

Table 3.6 Properties of firings with PBXN-5 pellets with density 1.71 g/cm<sup>3</sup>.

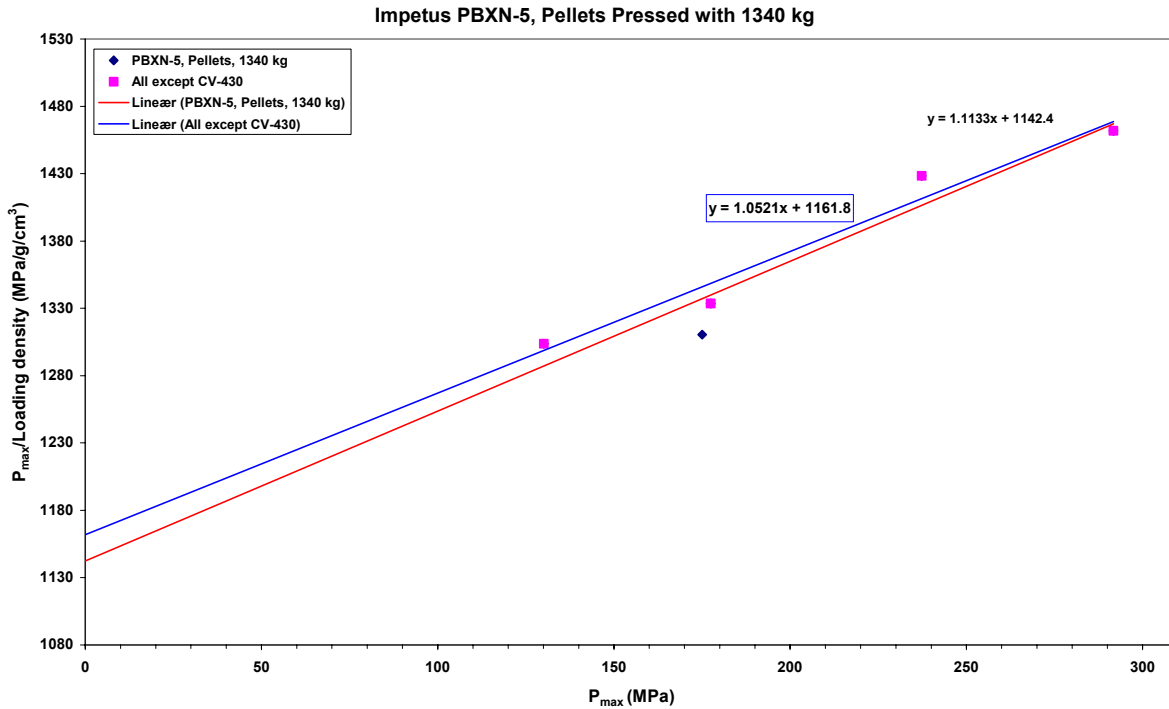


Figure 3.34 Impetus for PBXN-5 pellets pressed with 1340 kg.

Table 3.6 gives a summary of the properties for all firings performed with pellets of PBXN-5 with density 1.713 g/cm<sup>3</sup>. In figure 3.34 P<sub>max</sub>/LD (maximum pressure/loading density) has been plotted as function of maximum pressure, this gives, when firing CV-430 is excluded, an impetus of 1162 J/g and a co-volume of 1.0521 cm<sup>3</sup>/g. By using all firings we obtain for impetus and co-volume respectively 1142.4 J/g and 1.1133 cm<sup>3</sup>/g.

### 3.4 Cylinder pellets pressed with 5700 kg

The next pellet density we tried to obtain was 1.80 g/cm<sup>3</sup>. To press these pellets we used the press and tool given respectively in figure 2.2 and 2.3 and a pressing pressure of 5700 kg. The weight of powder used in each pellet was 5.00 g. Results obtained with respect to dimensions and density of each of the 22 pellets we produced is given in table 3.7. The average pellet density for these pellets was 1.79 g/cm<sup>3</sup>.



Pellet No.	Weight (g)	Height (mm)	Volume (cm <sup>3</sup> )	Density (g/cm <sup>3</sup> )	Firing No. Weight (g)
1	5.02	10.31	2.8000	1.7929	CV-399 15.03 g
2	5.01	10.28	2.7918	1.7945	
3	5.00	10.30	2.7973	1.7875	
4	5.02	10.33	2.8054	1.7894	CV-402 20.04 g
5	4.99	10.25	2.7837	1.7926	
6	5.01	10.30	2.7973	1.7910	
7	5.02	10.33	2.8054	1.7894	
8	5.00	10.27	2.7891	1.7927	CV-400 25.01 g
9	5.01	10.30	2.7973	1.7910	
10	5.01	10.30	2.7973	1.7910	
11	4.99	10.27	2.7891	1.7891	
12	5.01	10.29	2.7945	1.7928	
13	5.03	10.35	2.8108	1.7895	CV-401 30.00 g
14	5.00	10.28	2.7918	1.7909	
15	5.00	10.30	2.7973	1.7875	
16	4.98	10.25	2.7837	1.7890	
17	5.00	10.28	2.7918	1.7909	
18	4.99	10.29	2.7945	1.7856	
19	5.03	10.32	2.8027	1.7947	CV-398 20.02 g
20	5.00	10.30	2.7973	1.7875	
21	5.00	10.30	2.7973	1.7875	
22	5.00	10.31	2.8000	1.7857	
<b>Diameter 18.60 mm</b>		<b>Average Density</b>		<b>1.7901</b>	

Table 3.7 Dimensions and weights of pressed pellets.

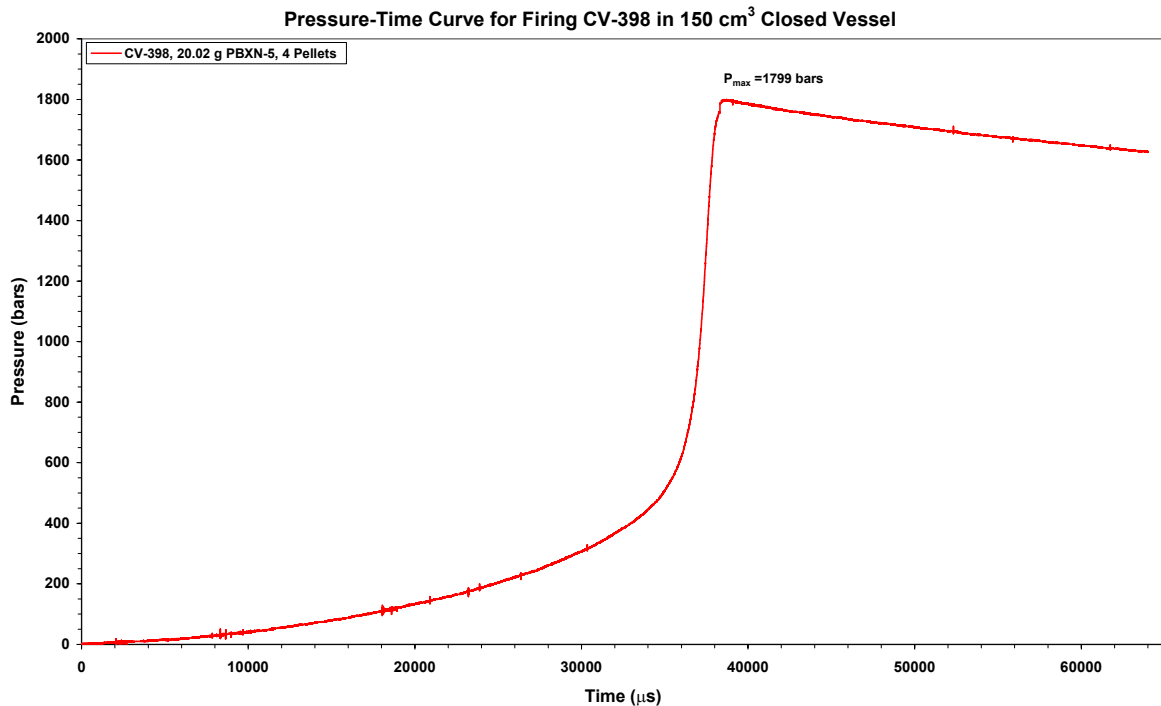


Figure 3.35 Pressure-time curve for firing CV-398, 4 PBXN-5 pellets, density 1.79 g/cm<sup>3</sup>.

With these pellets we performed five firings at four different loading densities. Figure 3.35 to 3.39 gives each single pressure-time curves, while figure 3.40 gives all pressure-time curves for pellets with density  $1.7091 \text{ g/cm}^3$ .

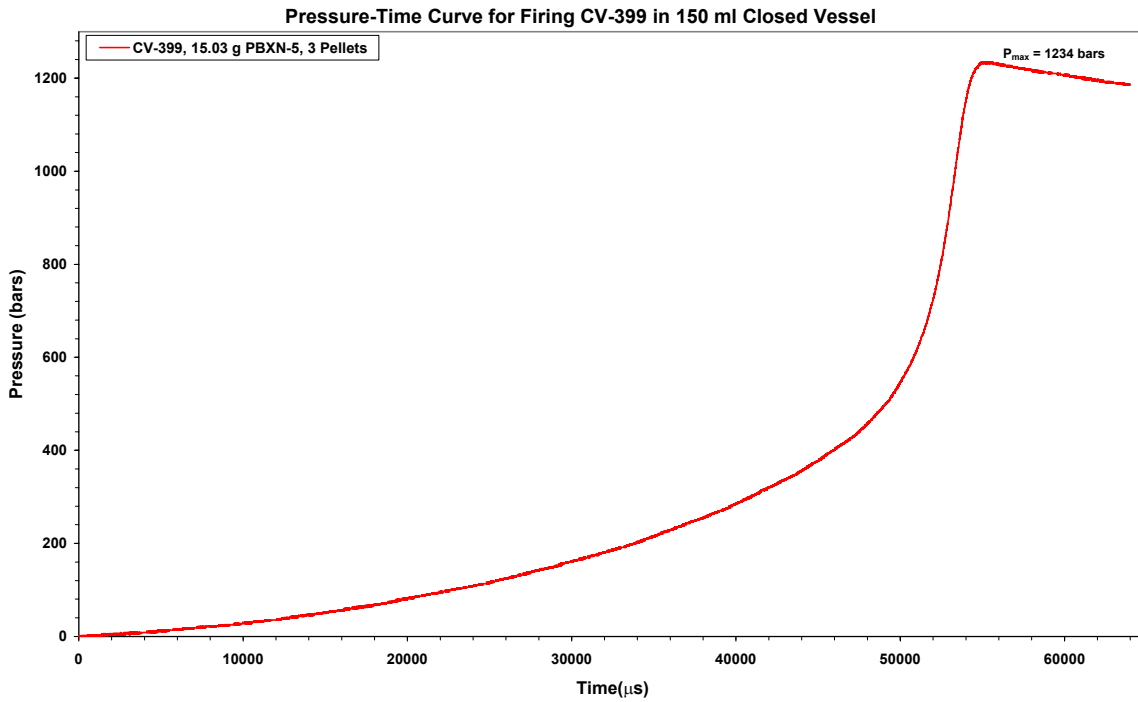


Figure 3.36 Pressure-time curve for firing CV-399, 3 PBXN-5 pellets pressed with 5.7 tons.

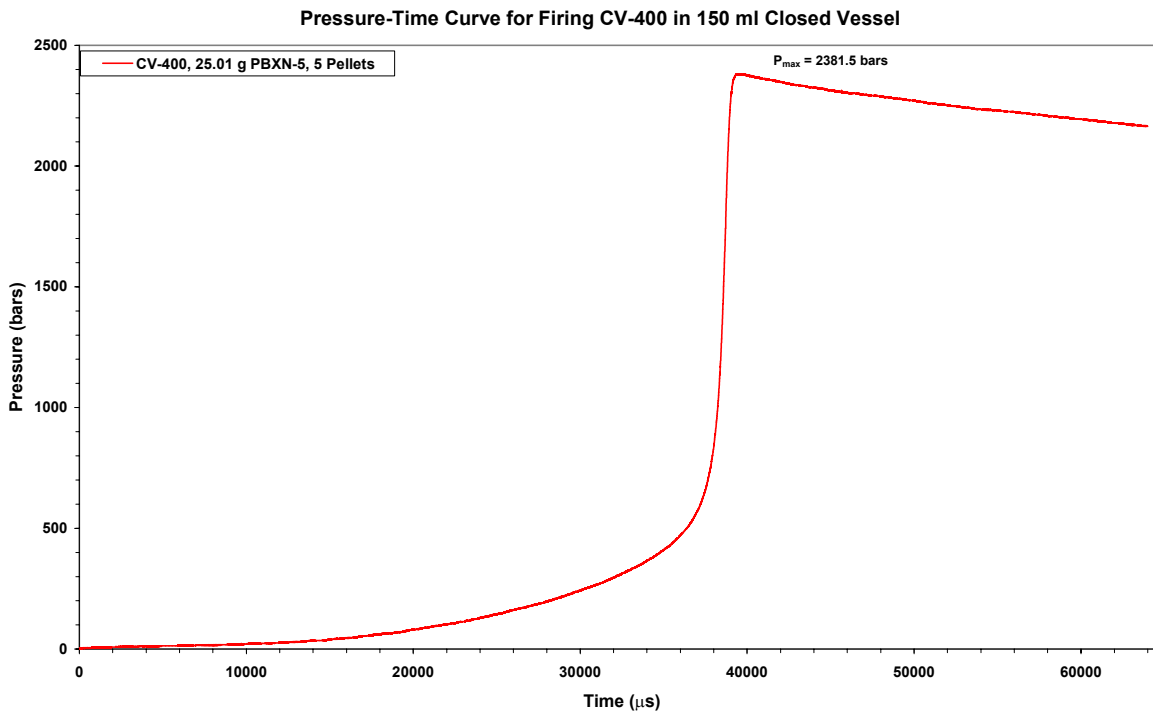


Figure 3.37 Pressure-time curve for firing CV-400, 5 pellets PBXN-5 pressed with 5.7 tons.

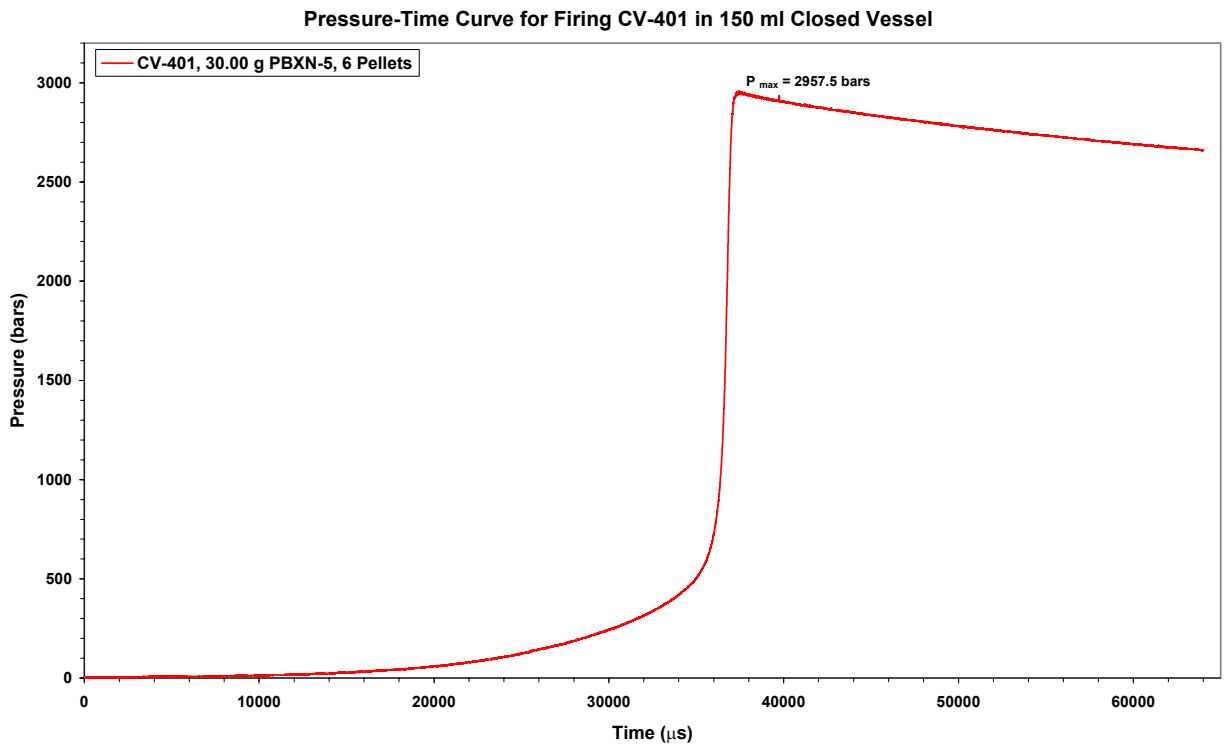


Figure 3.38 Pressure-time curve for firing CV-401, 6 pellets PBXN-5 pressed with 5.7 tons.

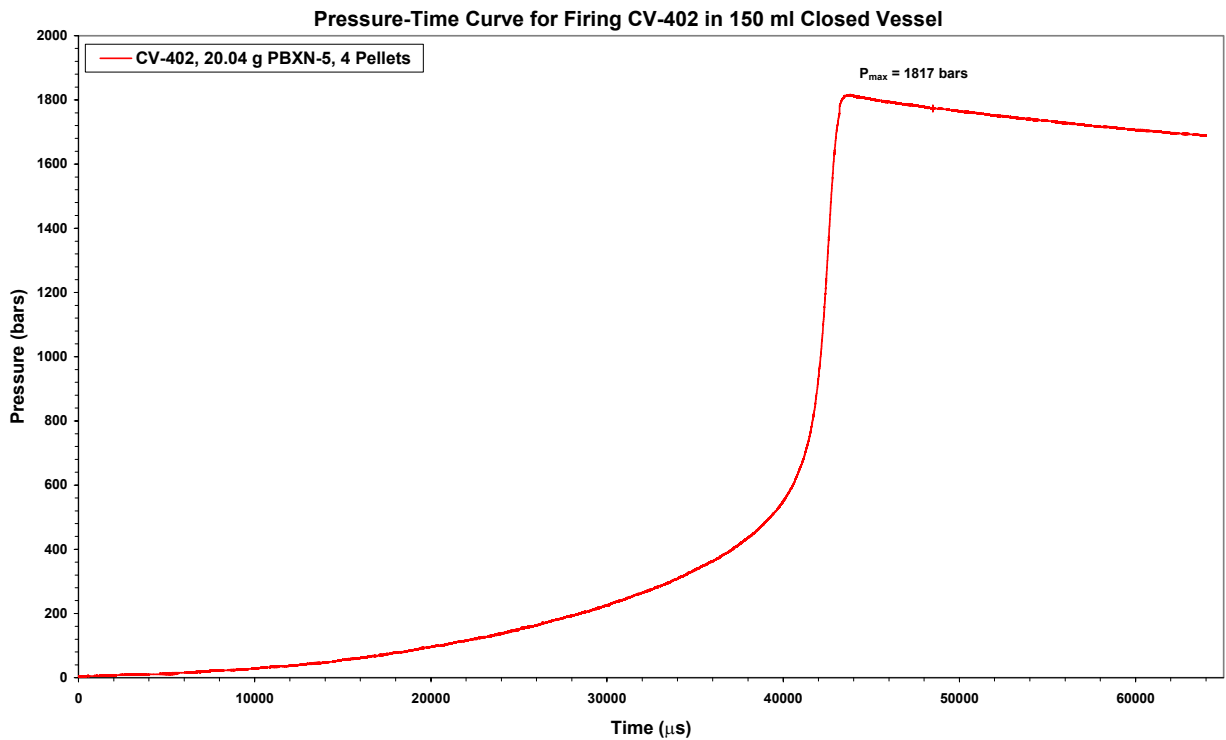


Figure 3.39 Pressure-time curve for firing CV-402, 4 pellets PBXN-5 pressed with 5.7 tons.

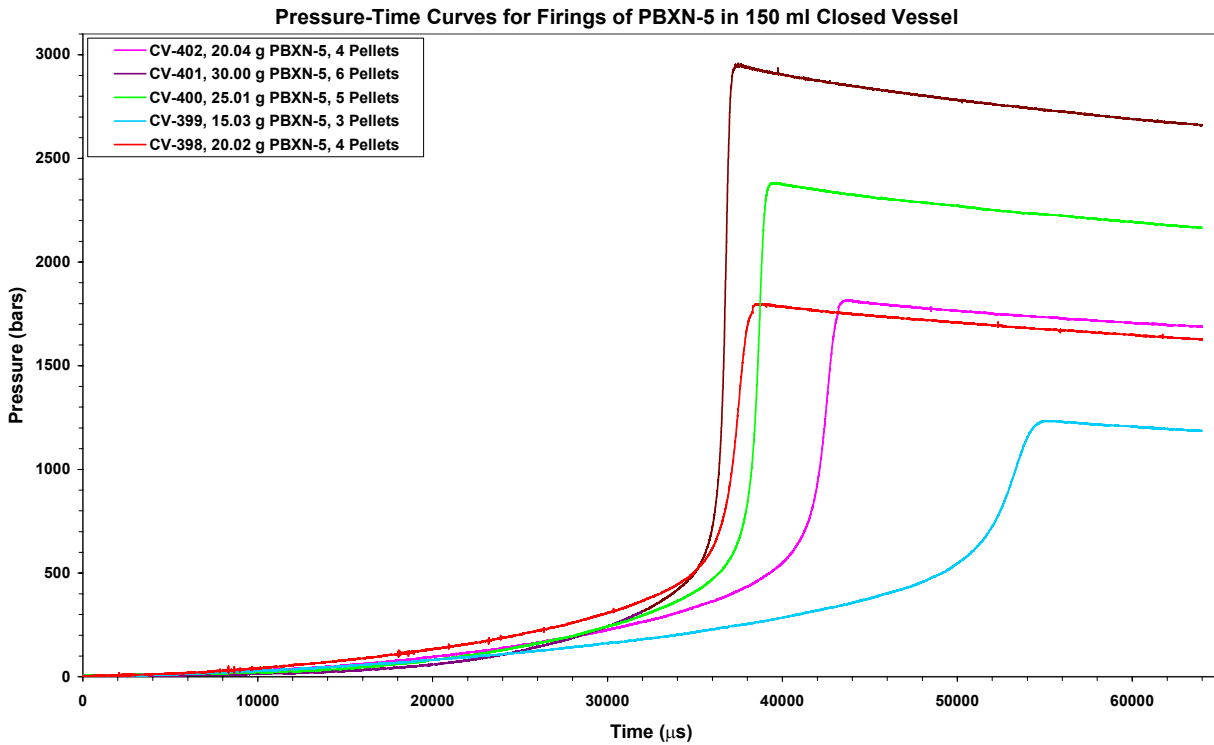


Figure 3.40 Pressure-time curves for all firings of PBXN-5 pellets pressed with 5.7 tons.

From the above figure it starts to be clear that the burn time increases significantly especially at low loading densities. There is only one explanation for this observation and that is that the surface area taking part in the burning has been reduced compared to what is available when we burn loosely packed powder or pellets with moderate density. We did see some tendency to slower pressure build up also for the pellets with a density of  $1.71 \text{ g/cm}^3$  but it was much smaller.

Firing No.	Weight (g)	Load Density ( $\text{g/cm}^3$ )	Maximum Pressure (MPa)	$P_{\text{max}}/\text{LD}$ ( $\text{MPa/g/cm}^3$ )
CV-399	15.03	0.1002	123.40	1231.54
CV-398	20.02	0.1335	179.90	1347.90
CV-402	20.04	0.1336	181.70	1360.03
CV-400	25.01	0.1667	238.15	1428.33
CV-401	30.00	0.2000	295.75	1478.75

Table 3.8 Properties of performed firings with pellets pressed with 5.7 tons pressure.

Table 3.8 summaries the properties needed to determine the impetus and co-volume experimentally. In figure 3.41 has these properties for the different firings been plotted. By using the firings for the three highest loading densities we obtain an impetus of  $1156.2 \text{ J/g}$  with the corresponding co-volume of  $1.1056 \text{ cm}^3/\text{g}$ . By using all four loading densities we obtain an impetus of  $1085.7 \text{ J/g}$  and a co-volume of  $1.392 \text{ cm}^3/\text{g}$ . The maximum pressure for the lowest loading density is most influenced by the long burning time and thereby loss of energy to the CV.

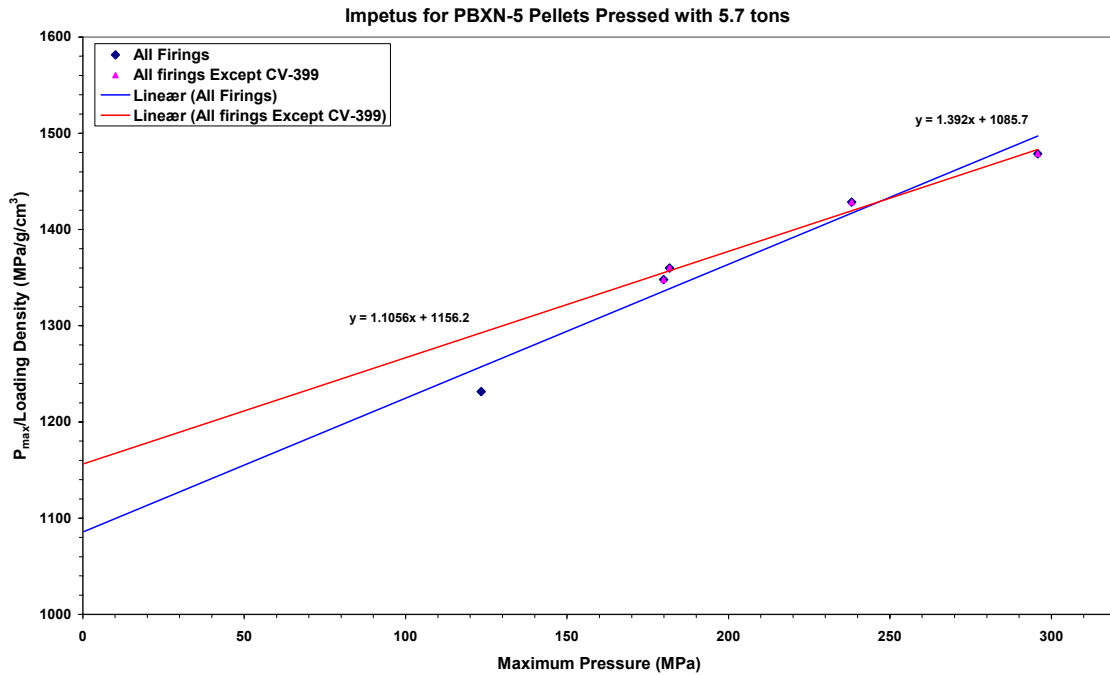


Figure 3.41 Impetus and co-volume for PBXN-5 pellets pressed with 5.7 tons press pressure.

### 3.5 Cylinder pellets pressed with 1 GPa

The pellets with the highest density we were able to produce were pressed with the press and tool shown in figure 2.5. Pellets were pressed in two series. For the first series we obtained a density of 1.8215 g/cm<sup>3</sup>. Table 3.9 gives all relevant information for dimensions and weight for these pellets. These pellets were used in two firings: CV-414 and CV-415. The pressure time curves for these two firings are given in figure 3.42 and 3.43.

Pellet No.	Weight (g)	Height (mm)	Volume (cm <sup>3</sup> )	Density (g/cm <sup>3</sup> )	Firing No. Weight (g)
1	3.6887	8.74	2.0203	1.8258	CV-415, 14.75 g
2	3.684	8.74	2.0203	1.8235	
3	3.6836	8.75	2.0226	1.8212	
4	3.6943	8.78	2.0295	1.8203	
5	3.6898	8.75	2.0226	1.8243	CV-414, 22.12 g
6	3.6867	8.75	2.0226	1.8227	
7	3.6819	8.75	2.0226	1.8204	
8	3.6876	8.78	2.0295	1.8170	
9	3.6899	8.77	2.0272	1.8202	
10	3.6896	8.77	2.0272	1.8200	
<b>Diameter 17.16mm</b>		<b>Average Density</b>		<b>1.8215</b>	

Table 3.9 Properties of the PBXN-5 pellets pressed with 1 GPa pressure.

From figure 3.42 one can see that the burn time of the explosive did increase significantly so we nearly missed the maximum pressure. For this firing the sampling time was 1  $\mu$ s. For firing CV-415 with lower loading density we therefore changed the sampling time to 5  $\mu$ s to be sure that we were able to collect the complete burning process.

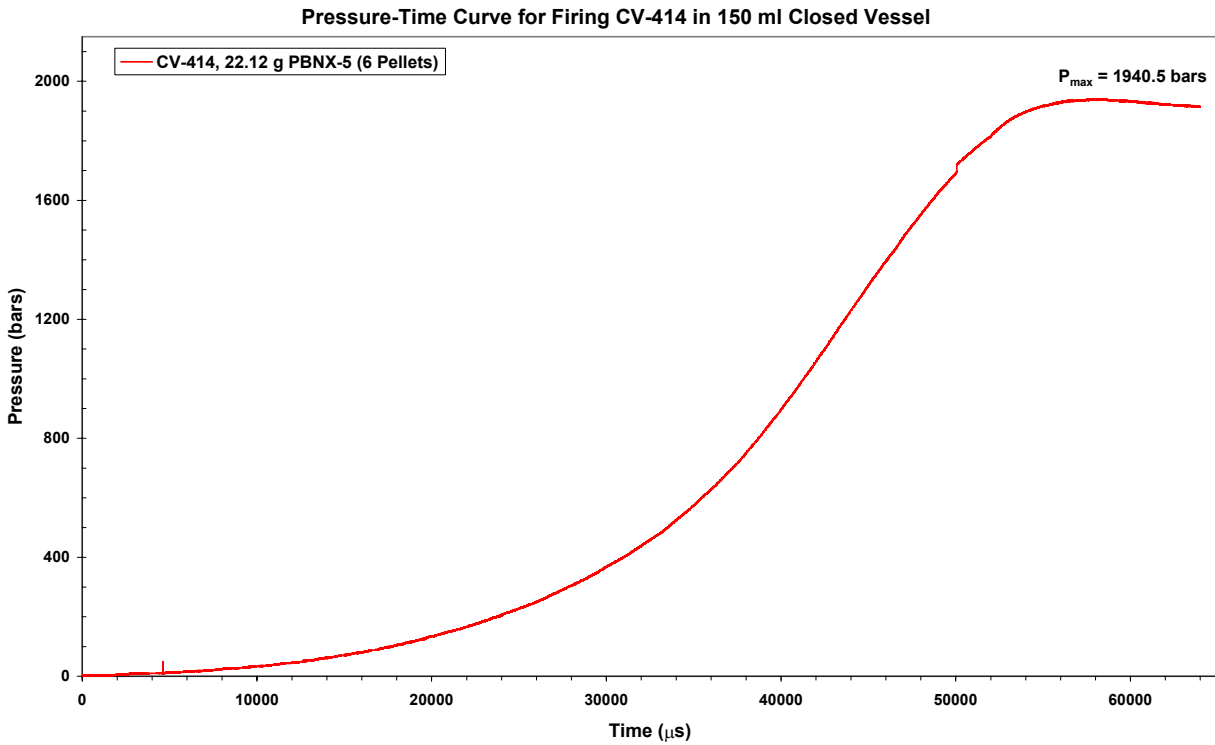


Figure 3.42 Pressure-time curve for CV-414 pressed PBXN-5 pellets with  $\rho=1.82$  g/cm<sup>3</sup>.

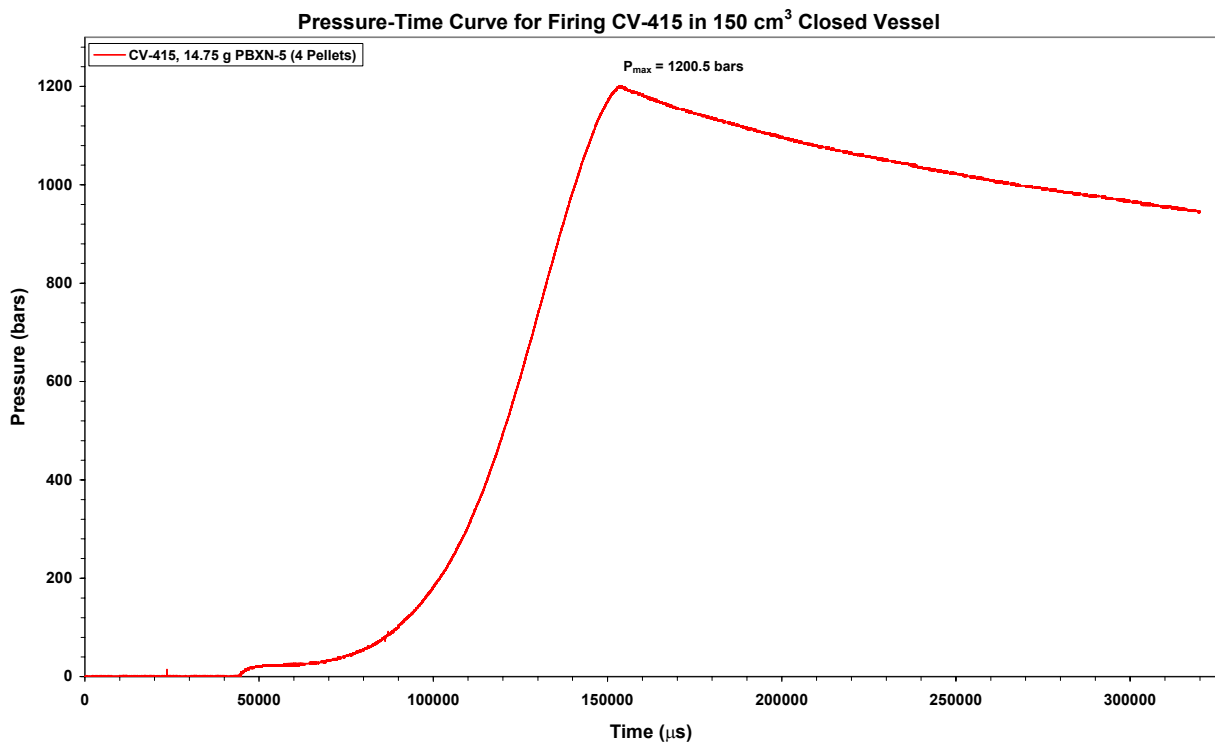


Figure 3.43 Pressure-time curve for CV-415 pressed PBXN-5 pellets with  $\rho=1.82$  g/cm<sup>3</sup>.

For the second series of pellets we obtained a density of the pellets of 1.826 g/cm<sup>3</sup>. All the properties of the pellets are given in table 3.10. The pellets were used to perform four firings of

three different loading densities. Pressure-time curves for these firings are given in figure 3.44 to 3.47. Figure 3.48 gives all pressure-time curves obtained for pellets pressed with 1 GPa.

Pellet No.	Weight (g)	Height (mm)	Volume (cm <sup>3</sup> )	Density (g/cm <sup>3</sup> )	Firing No. Weight (g)
1	3.73	8.840	2.0434	1.8254	CV-437 18.68 g (1-5)
2	3.72	8.835	2.0423	1.8215	
3	3.75	8.855	2.0469	1.8321	
4	3.73	8.855	2.0469	1.8223	
5	3.74	8.850	2.0457	1.8282	
6	3.74	8.870	2.0503	1.8241	CV-438 18.68 g (6-10)
7	3.73	8.830	2.0411	1.8274	
8	3.74	8.845	2.0446	1.8292	
9	3.73	8.840	2.0434	1.8254	
10	3.74	8.845	2.0446	1.8292	
11	3.7398	8.880	2.0527	1.8219	CV-440 22.44 g (11-16)
12	3.7380	8.850	2.0457	1.8272	
13	3.7368	8.860	2.0480	1.8246	
14	3.7393	8.870	2.0503	1.8237	
15	3.7328	8.850	2.0457	1.8247	
16	3.7377	8.840	2.0434	1.8291	
17	3.7353	8.840	2.0434	1.8280	CV-444, 14.96 g
18	3.7361	8.840	2.0434	1.8284	
19	3.7387	8.860	2.0480	1.8255	
20	3.7360	8.850	2.0457	1.8262	
<b>*Diameter 17.16mm</b>		<b>Average density</b>		<b>1.8262</b>	

Table 3.10 Weight and dimensions for tested PBXN-5 pellets.

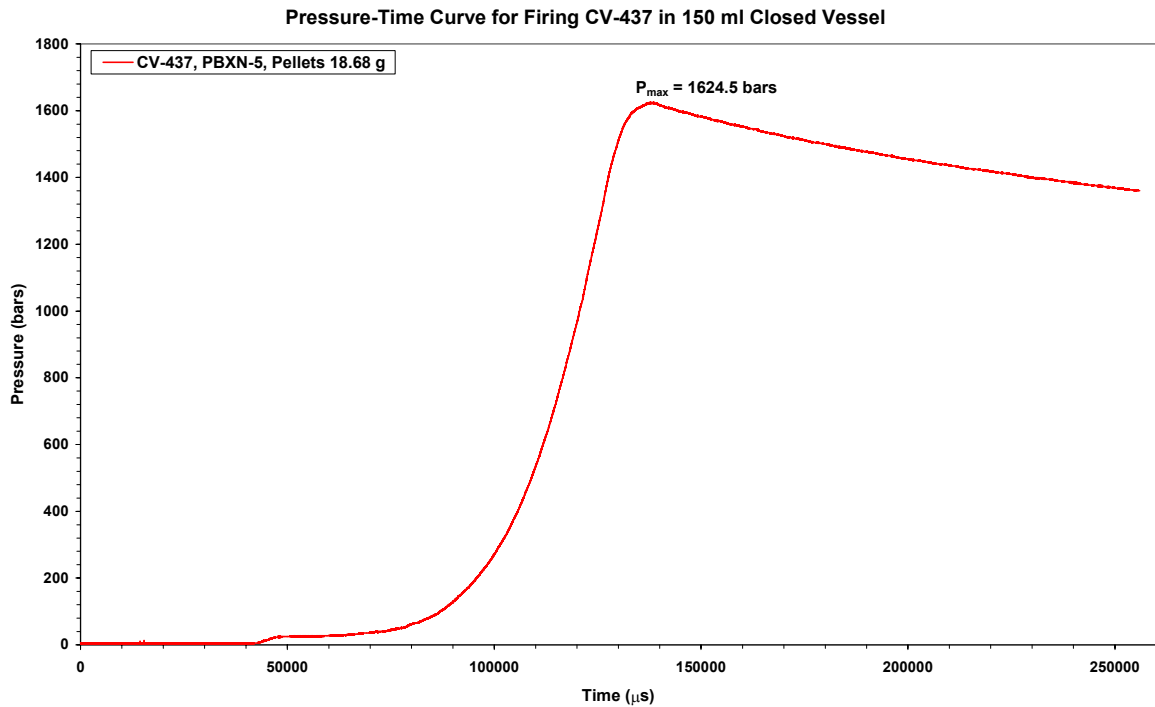


Figure 3.44 Pressure-time for firing CV-437.

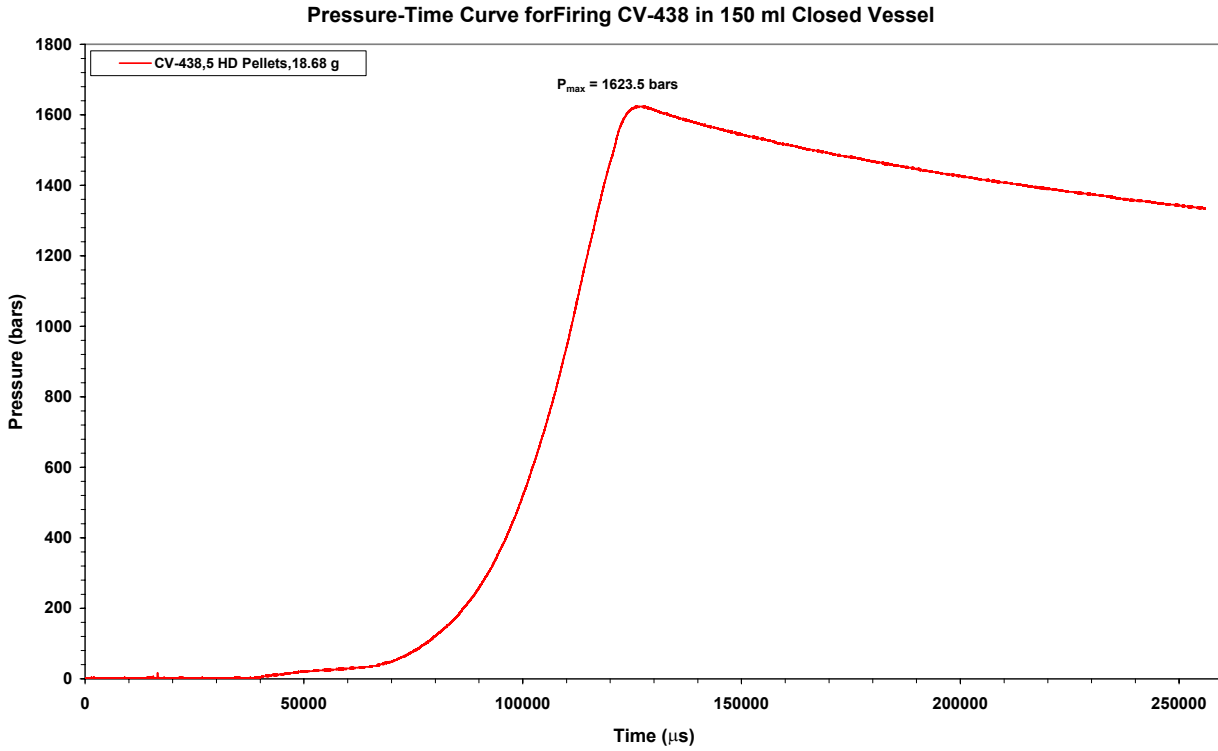


Figure 3.45 Pressure-time curve for firing CV-438.

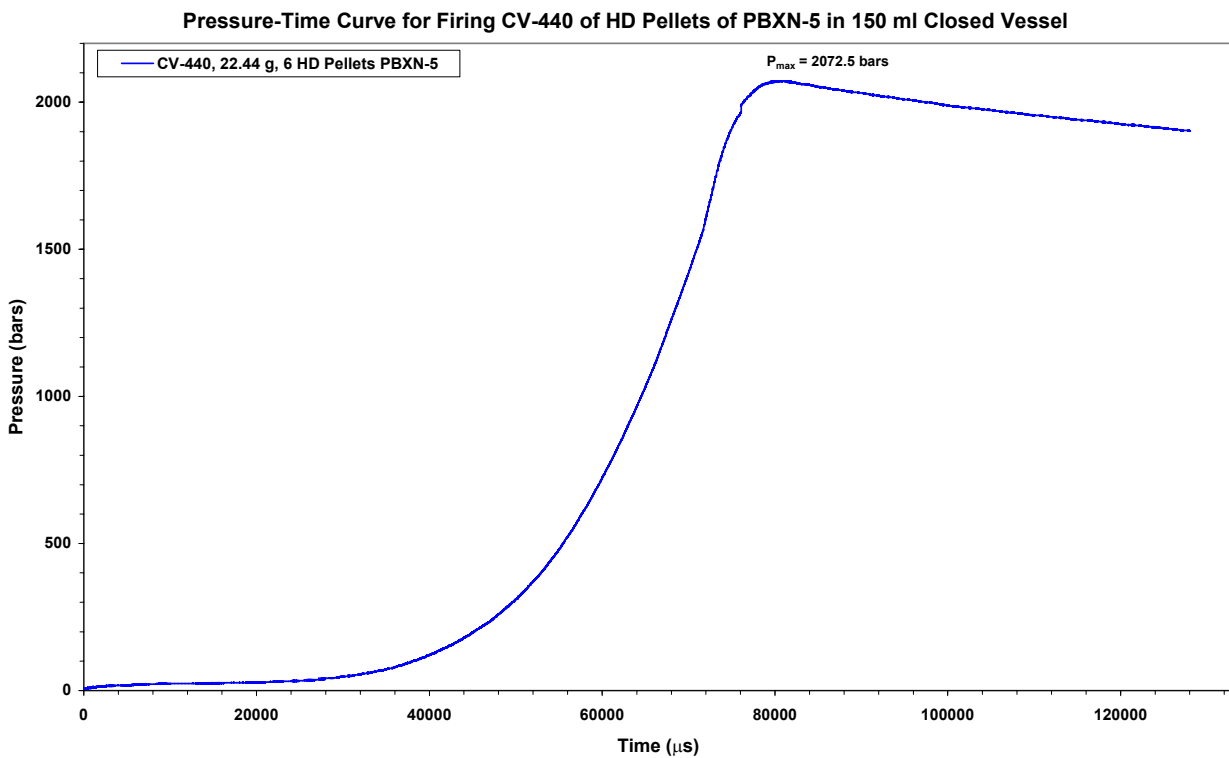


Figure 3.46 Pressure-time curve for CV-440, PBXN-5 pellets with high density.



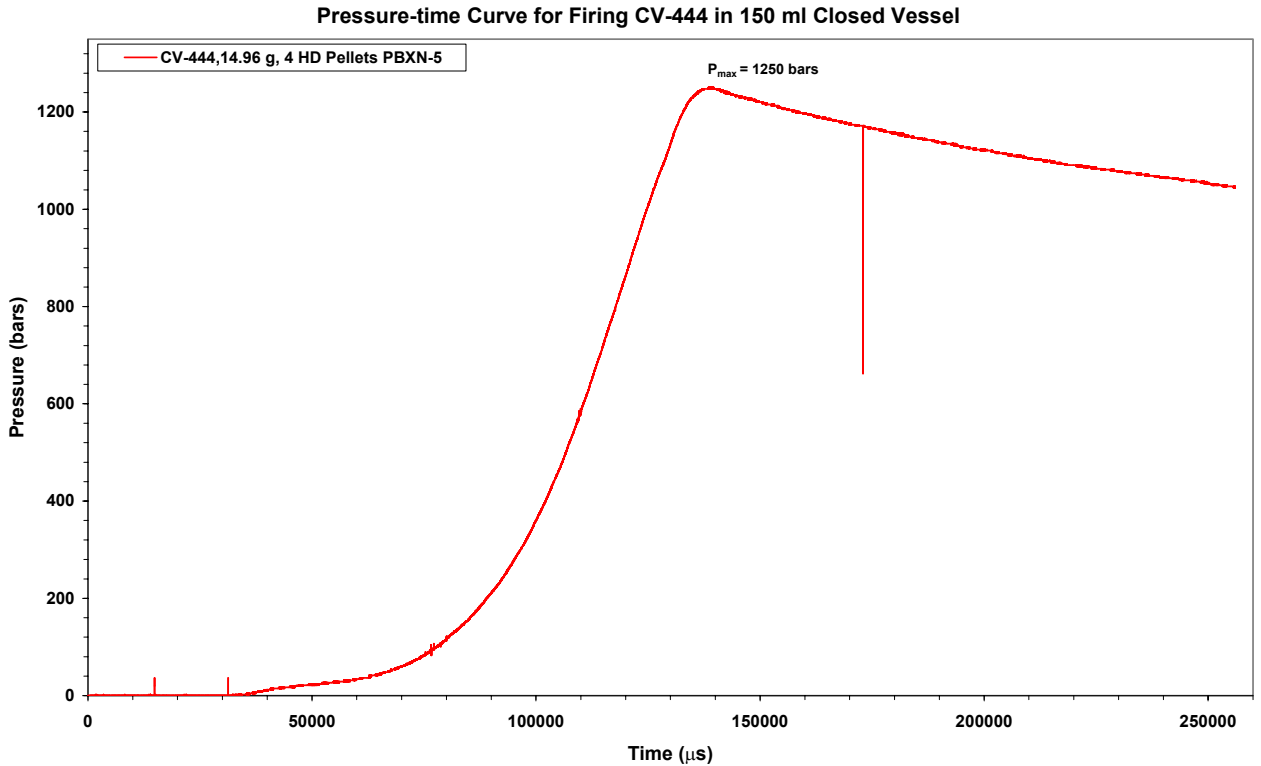


Figure 3.47 Pressure-time curve for firing CV-444 with HD pellets of PBXN-5.

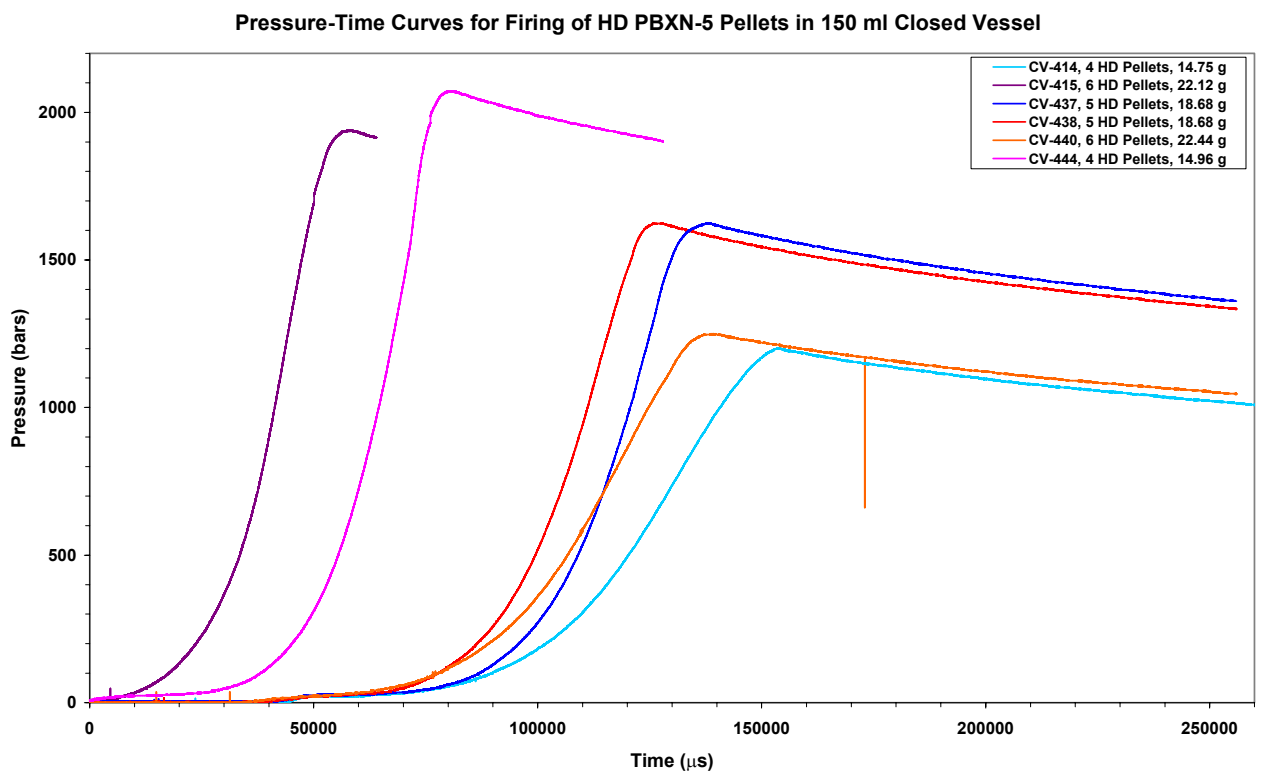


Figure 3.48 Pressure-time curve for the firings with HD pellets of PBXN-5.

In figure 3.48 all curves have the same form. For CV-414 however we can't observe the ignition pressure from the ignition unit that for the other firings have a contribution of

approximately 20 kbar. An increase in pressure of lets say 20 kbar for firing CV-414 vil reduce the impetus by 20 J/g.

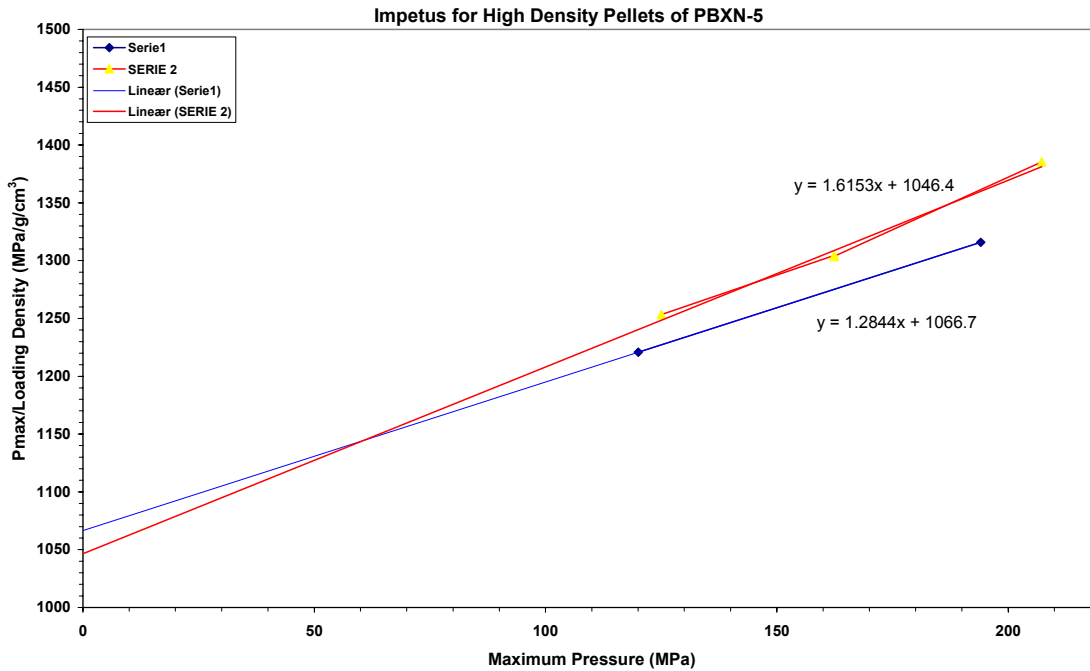


Figure 3.49 Experimental impetus and co-volume for PBXN-5 pellets of high density.

Firing No.	Weight (g)	Pressure (MPa)	Load Density (g/cm <sup>3</sup> )	P <sub>max</sub> /LD (MPa/g/cm <sup>3</sup> )
CV-444	14.96	125.00	0.0997	1253.34
CV-414	14.75	120.05	0.0983	1220.85
CV-438	18.68	162.45	0.1245	1304.47
CV-437	18.68	162.35	0.1245	1303.67
CV-415	22.12	194.05	0.1475	1315.89
CV-440	22.44	207.25	0.1496	1385.36

Table 3.11 Properties of CV-firings performed with pellets pressed with 1 GPa pressure.

In figure 3.49 are the properties from the two series of firings with pellets pressed with 1 GPa potted. We prefer to look on the firings as two series since the density is slightly different. For the first we obtain an impetus of 1066.7 J/g and a co-volume of 1.2844 cm<sup>3</sup>/g. For the second we get 1046.4 J/g and 1.6153 cm<sup>3</sup>/g for respectively the impetus and the co-volume.

### 3.6 Theoretical calculations

To calculate some thermochemical properties theoretically we have used the Cheetah 2.0 code (1). Appendix B gives a complete listing of the print-out from the program for the performed calculations. In figure 3.50 the major properties for PBNX-5 has been plotted as function of loading density. In figure 3.51 the major combustion products have been plotted as function of the loading density. Of the major products the most striking changes is observed in the concentrations of CO, H<sub>2</sub>O and N<sub>2</sub>, which decrease, and CO<sub>2</sub> and HCN, which increase, as the loading density, increases.

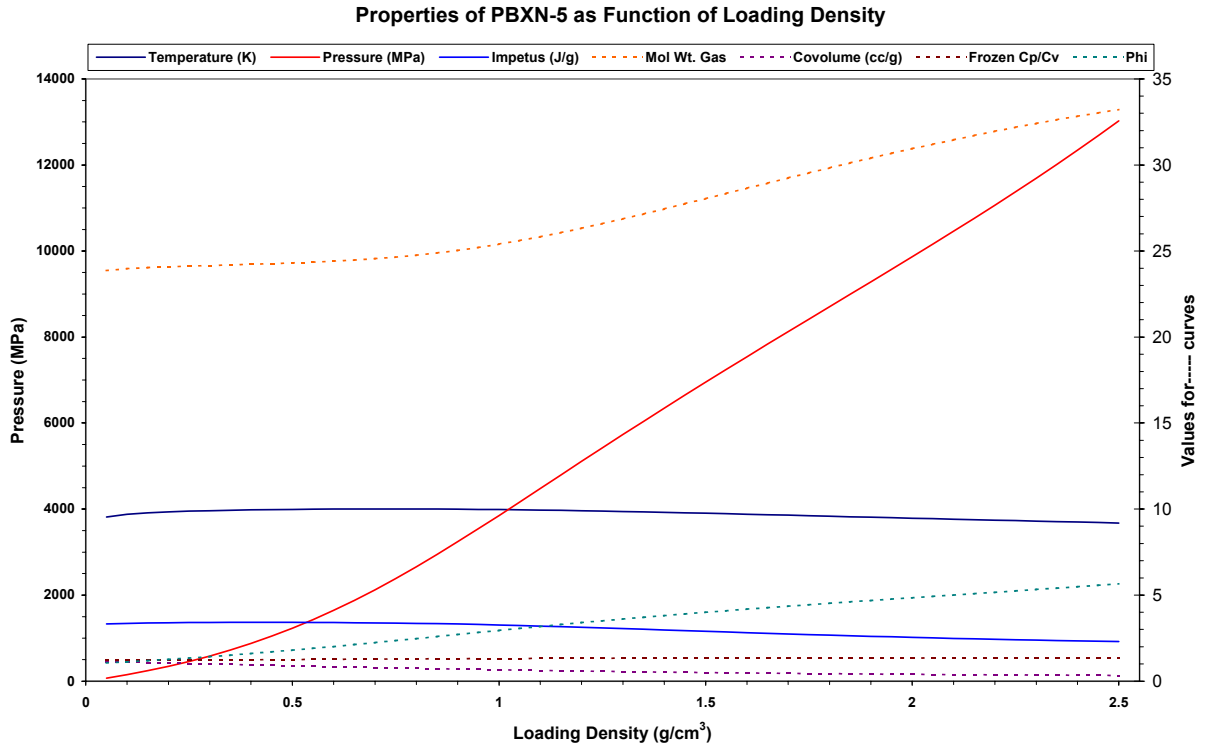


Figure 3.50 Theoretical calculated properties of PBXN-5.

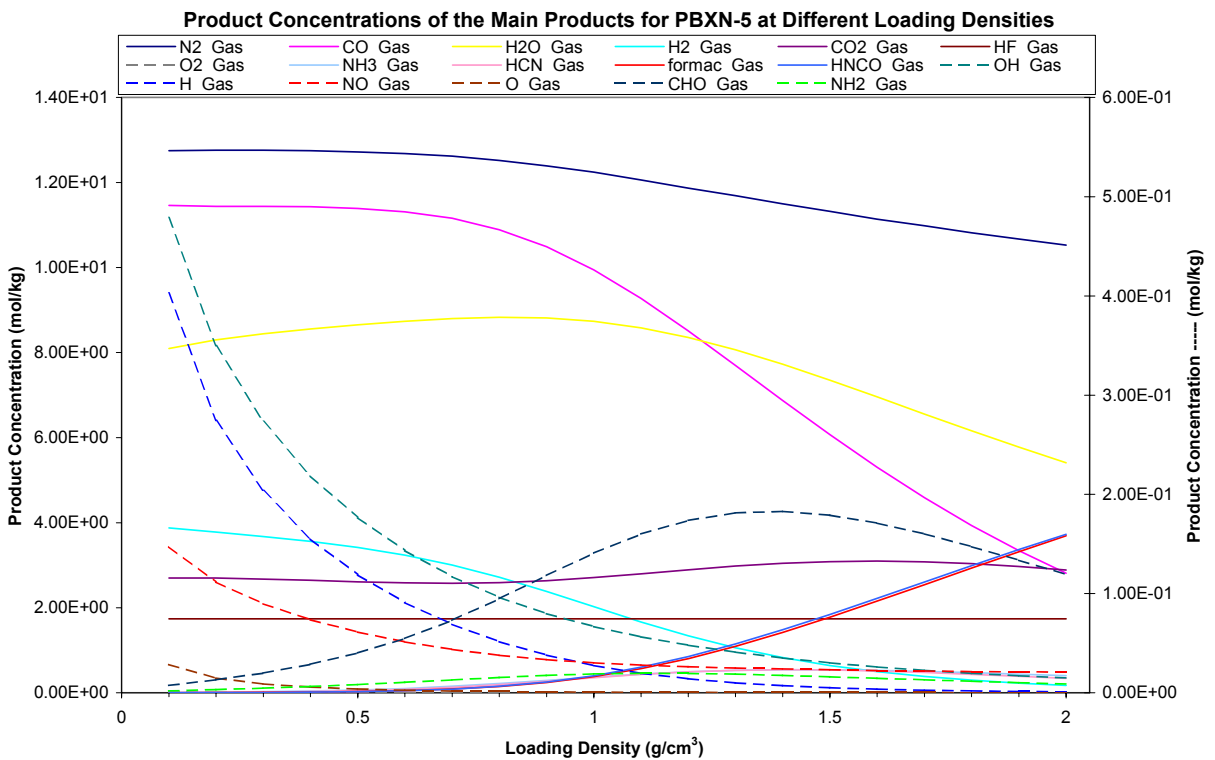


Figure 3.51 Product concentration of the main products as function of loading density.

### 3.7 Comparison between experimentally and theoretical calculated properties

Table 3.12 gives a summary of the results of the firings we have performed with PBXN-5 powder and pellets. The general trend is that the experimentally obtained impetus decreases as the density of pellets increase. For the co-volume an opposite trend is observed with increase as the pellet density increase. Compared with the theoretical impetus, all experimental test series are lower, while the experimentally found co-volumes in general are higher than the theoretically calculated. The theoretically calculated impetus and co-volume is given in table 3.13.

CV Firing No.	Form	Sample size (g)	Loading Density (g/cm <sup>3</sup> )	P <sub>max</sub> (bars)	Density (g/cm <sup>3</sup> )	Impetus (J/g)	Co-volume (cm <sup>3</sup> /g)
370	Powder	15.03	0.1000	1384			
371	Powder	22.49	0.1500	2197			
372	Powder	22.53	0.1502	2197			
373*	Powder	30.00	0.2000	3088			
374	Powder	30.01	0.2067	3140			
375	Powder	35.00	0.2333	3750		1239.9	0.9962
376	Powder	25.02	0.1667	2467			
377	Powder	25.00	0.1667	2464.5			
403	Powder	20.00	0.1333	1882			
426	Powder	19.80	0.1320	1857.5			
431	Powder	20.00	0.1333	1699			
433	Powder	20.02	0.1335	1901.5			
439	Powder	20.00	0.1333	1949			
382	Pellets	24.92	0.1661	2373			
383	Pellets	19.96	0.1331	1774.5			
384	Pellets	14.97	0.0998	1301	1.71	1161.8	1.0521
385	Pellets	29.93	0.1995	2917		1142.4	1.1133
430	Pellets	20.03	0.1335	1750			
398	Pellets	20.02	0.1335	1799			
399	Pellets	15.03	0.1002	1234			
400	Pellets	25.01	0.1667	2421.5	1.79	1156.2	1.1056
401	Pellets	30.00	0.2000	3017.5		1085.7	1.3692
402	Pellets	20.04	0.1336	1843			
414	Pellets	22.12	0.0983	1940.5	1.8215	1066.7	1.2844
415	Pellets	14.75	0.1475	1200.5			
418	Pellets	20.06	0.1338	1882			
419	Pellets	15.00	0.1000	1340		1249.5	0.7484
420	Pellets	25.01	0.1667	2375	1.587	1247.8	0.7042
421	Pellets	30.06	0.1667	2937			
422	Pellets	25.00	0.2004	2272			
437	Pellets	18.68	0.1245	1624.5			
438	Pellets	18.68	0.1245	1623.5	1.826	1046.4	1.6153
440	Pellets	22.44	0.1496	2072.5			
444	Pellets	14.96	0.0997	1250			

\*Leakage

Table 3.12 Experimental determined properties of PBXN-5.

Rho g/cc	Temperature (K)	Pressure (MPa)	Impetus (J/g)	Mol Wt. Gas	Co-volume (cc/g)	Frozen Cp/Cv	Phi
0.05	3818.3	70.5	1330.48	23.862	1.116	1.239	1.059
0.1	3880.0	151.1	1345.79	23.972	1.094	1.237	1.123
0.15	3913.2	241.9	1353.66	24.036	1.070	1.237	1.191
0.2	3935.3	343.6	1358.63	24.084	1.046	1.237	1.264
0.25	3951.5	457.1	1362.00	24.123	1.020	1.238	1.342
0.3	3964.0	583.2	1364.31	24.159	0.994	1.240	1.425
0.35	3974.0	722.9	1365.78	24.193	0.968	1.243	1.512
0.4	3982.0	876.8	1366.55	24.228	0.941	1.247	1.604
0.45	3988.5	1045.7	1366.65	24.266	0.915	1.251	1.700
0.5	3993.6	1229.9	1366.06	24.308	0.889	1.256	1.801
0.55	3997.6	1430.0	1364.75	24.355	0.864	1.261	1.905

Table 3.13 Theoretical calculated properties of PBXN-5.

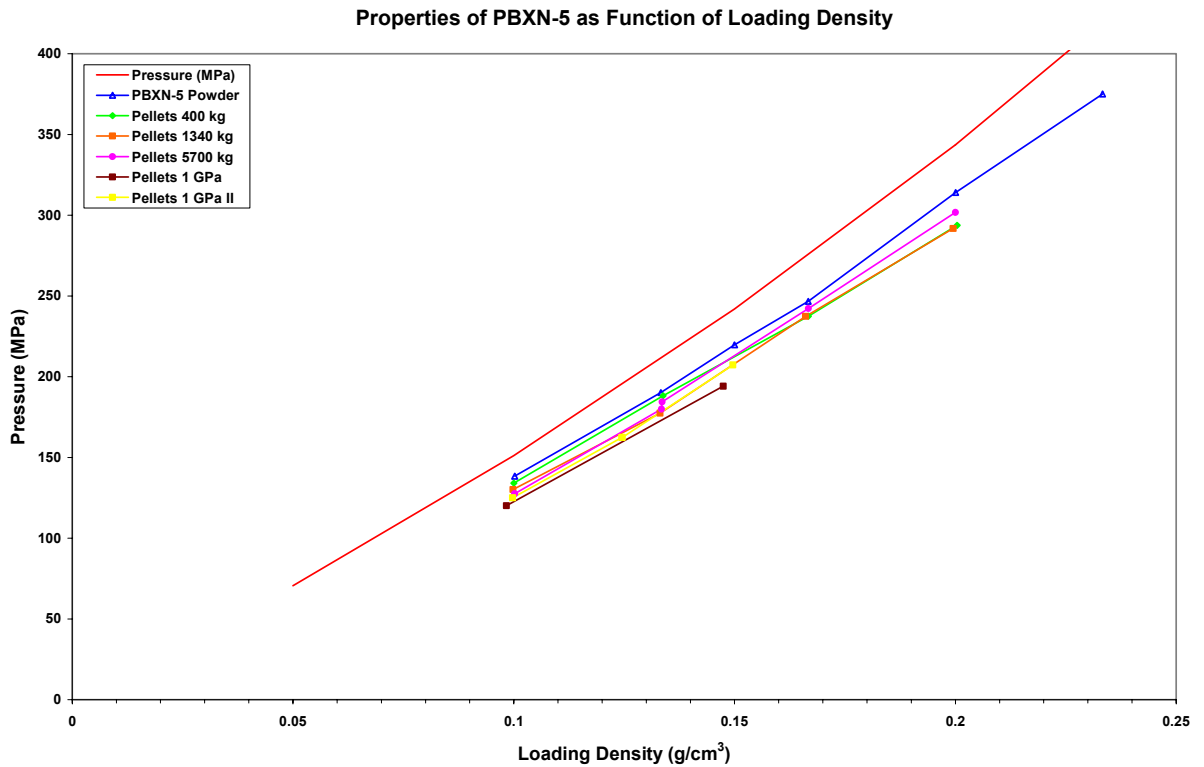


Figure 3.52 The figure shown a comparison between theoretical and experimentally determined pressures.

In figure 3.52 has maximum pressures as function of loading density been plotted for powder and pellets of different density. Compared with the theoretical calculated pressure, all experimentally measured maximum pressures show lower values, and the difference increase as the density of pellets increase. That the difference in pressure between experimentally measured and theoretically calculated values increase as the pellet density increase, can be explained by the longer burn time for pellets of high density and thereby increased loss of energy to the CV.

### 3.8 Burn rate determination

We have tested PBXN-5 in closed vessel for five different conditions, four with pellets of different densities and powder as received from the producer. Table 3.14 and 3.15 gives the properties under the different conditions tested. In table 3.16 is the distribution of the particle and form factors given for the powder.

Property	CV-403	CV-418	CV-383	CV-398	CV-414	CV-415
Test date	2/5-02	7/5-02	23/4-02	7/5-02	6/5-02	6/5-02
Test temperature (°C)	20	20	20	20	20	20
PBXN-5, Press pressure	Powder	400 kg	1340 kg	5700 kg	1 GPa	1 GPa
Loading density (g/cm <sup>3</sup> )	0.1333	0.1337	0.1331	0.1335	0.1477	0.0983
Igniters	1 g BP	1 g BP	1 g BP	1 g BP	1 g BP	1 g BP
Density (g/cm <sup>3</sup> )	1.90	1.580	1.710	1.790	1.825	1.825
Co volume (cm <sup>3</sup> /g)	1.00	1.00	1.00	1.00	1.00	1.00
Geometry	Powder	Cylinder	Cylinder	Cylinder	Cylinder	Cylinder
Diameter (mm)	*	18.63	18.60	18.60	17.16	17.16
Length (mm)		11.60	10.75	10.30	8.76	8.76
Calibration factor	500	500	500	500	500	500
Sampling time (μs)	1	1	1	1	1	5
Averaging time (μs)	4	4	4	4	20	20
P <sub>max</sub> (bars)	1913	1882	1775	1787	1940	1200

\*See table below

Table 3.14 Properties of CV-firings of different PBXN-5 pellets and powder used in calculation of the burn rate.

Property	CV-415	CV-437	CV-438	CV-440	CV-444
Test date	6/5-02	21/8-02	21/8-02	29/8-02	14/9-02
Test temperature (°C)	20	25	25	25	25
PBXN-5, Press pressure	1 GPa	1GPa	1 GPa	1 GPa	1 GPa
Loading density (g/cm <sup>3</sup> )	0.0983	0.1245	0.1245	0.1496	0.0997
Igniters	1 g BK	1 g BP	1 g BP	1 g BP	1 g BP
Density (g/cm <sup>3</sup> )	1.825	1.826	1.826	1.826	1.826
Co-volume (cm <sup>3</sup> /g)	1.00	1.00	1.00	1.00	1.00
Geometry	Cylinder	Cylinder	Cylinder	Cylinder	Cylinder
Diameter (mm)	17.16	17.16	17.16	17.16	17.16
Length/web (mm)	8.76	8.85	8.85	8.85	8.85
Calibration factor	500	500	500	500	500
Sampling time (μs)	5	4	4	2	4
Averaging time (μs)	20	80	80	80	80
P <sub>max</sub> (bars)	1200	1622	1622	2063	1250
a <sub>1</sub>	4.614	4.591	4.591	4.591	4.591
a <sub>2</sub>	-6.680	-6.626	-6.626	-6.626	-6.626
a <sub>3</sub>	3.101	3.070	3.070	3.070	3.070

Table 3.15 Properties of CV-firings of different PBXN-5 pellets and powder used in calculation of the burn rate.

Diameter ( $\mu\text{m}$ )	Weight %	Form factor		
		$a_1$	$a_2$	$a_3$
400	7.5	150	-7500	125000
180	30	333.333	-337037.04	1371742
130	30	461.539	-71005.91	3641329
45	7.5	1333.333	-592592.60	87791500
10	25.0	6005.842	-12005358.24	7999289307

Table 3.16 Particle distribution and form factors used to calculate burn rate for PBXN-5 powder.

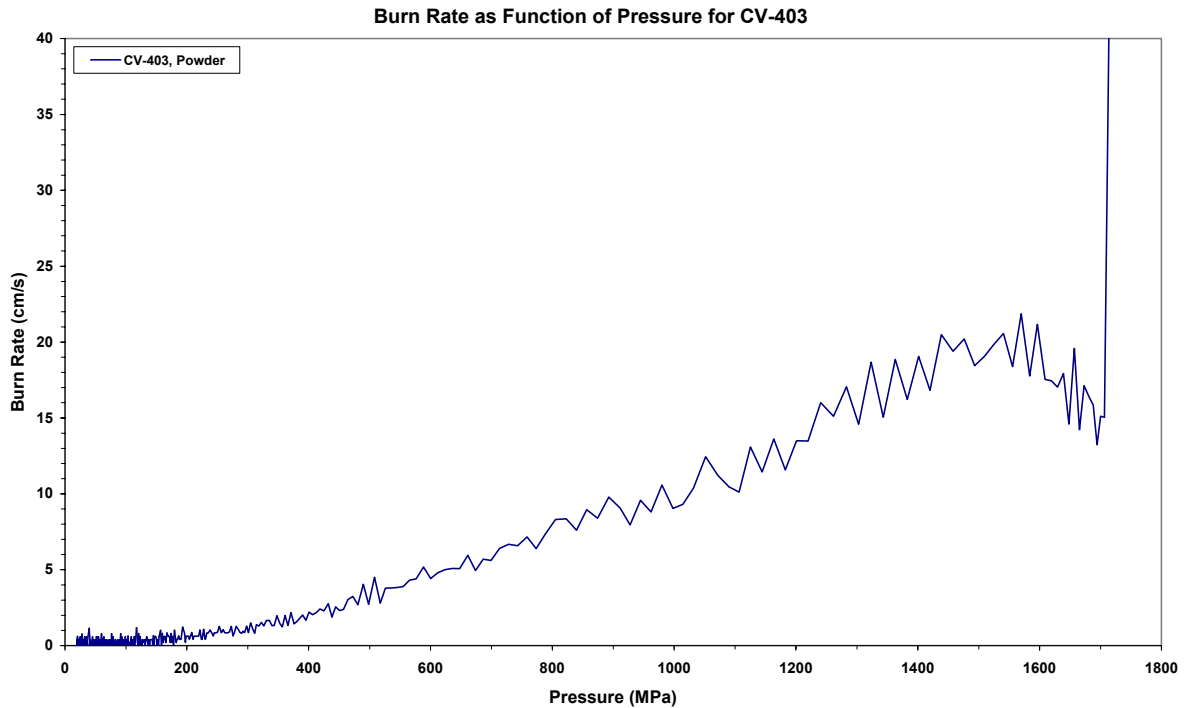


Figure 3.53 Burn rate as function of pressure for CV-403 with powder PBXN-5.

Figure 3.53 to 3.67 gives the burn rate curves as function of the pressure for the firings corresponding to conditions given in table 3.14 and 3.15. In figure 3.53 is the burn rate for powder PBXN-5 given for firing CV-403, when we use the crystal distribution and form factors given in table 3.16. This gives more or less a perfect adjustment. However, the burn rate at pressures up to 200 bars is too low, which indicates that the burning surface area used in the calculations is too high. By reducing the number of small crystals slightly we will obtain some additional larger crystals that will increase the surface area in the high-pressure region and thereby reduce the burn rate slightly in this part of the curve. Another reason for the low burn rate in the start may be due too lower burn rate for coated crystal. For PBXN-5 the binder constitutes 5 wt.% of the mass.

In figure 3.54 the burn rate curve for pellets pressed to a density of  $1.587 \text{ g/cm}^3$  has been calculated by using the dimension for the pellets given in table 3.14. As the figure shows this gives a very high burn rate, clearly indicating that the surface area that is burning is much

higher than what we obtain by using the surface area of pellets. Therefore, these pellets burn inside the pellets more or less as single crystals. The same situation is observed for the firing of pellets with density  $1.71 \text{ g/cm}^3$ , for which the burn rate curve is given in figure 3.55.

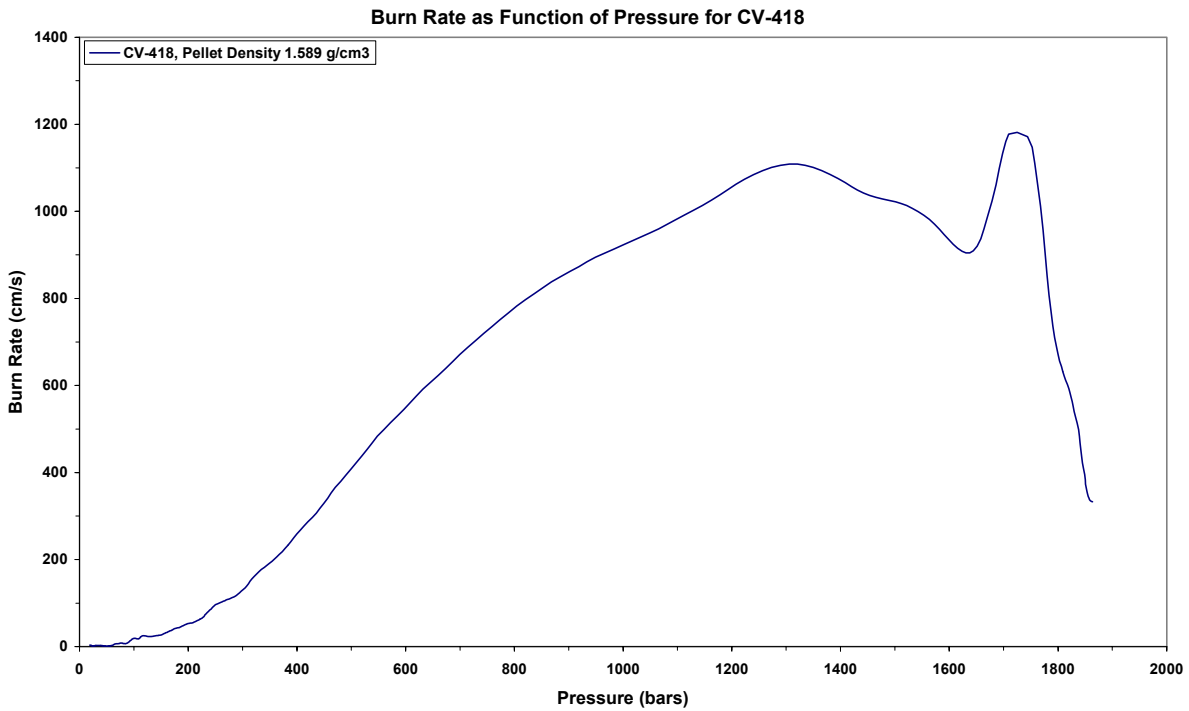


Figure 3.54 Burn rate as function of pressure for CV-418, PBXN-5 pellets, density  $1.59 \text{ g/cm}^3$ .

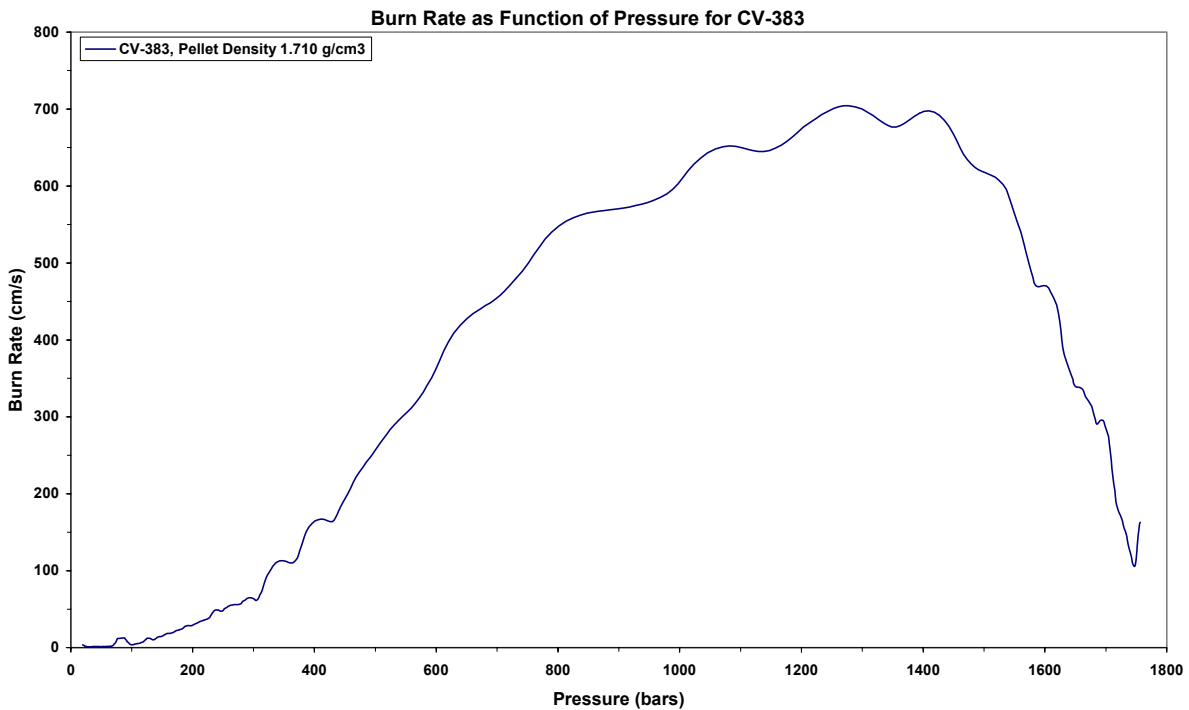


Figure 3.55 Burn rate as function of pressure for CV-383, PBXN-5 density of pellets  $1.710 \text{ g/cm}^3$ .



For the next pellet density  $1.79 \text{ g/cm}^3$  things start to change. The obtained burn rate up to approximately 500 bars for firing CV-398 in figure 3.56 seems to be correct by calculating the surface area from the dimensions of the pellets. However, at higher pressures the burn rate increases significantly, indicating, as for the pellets of lower density, that they also burn inside.

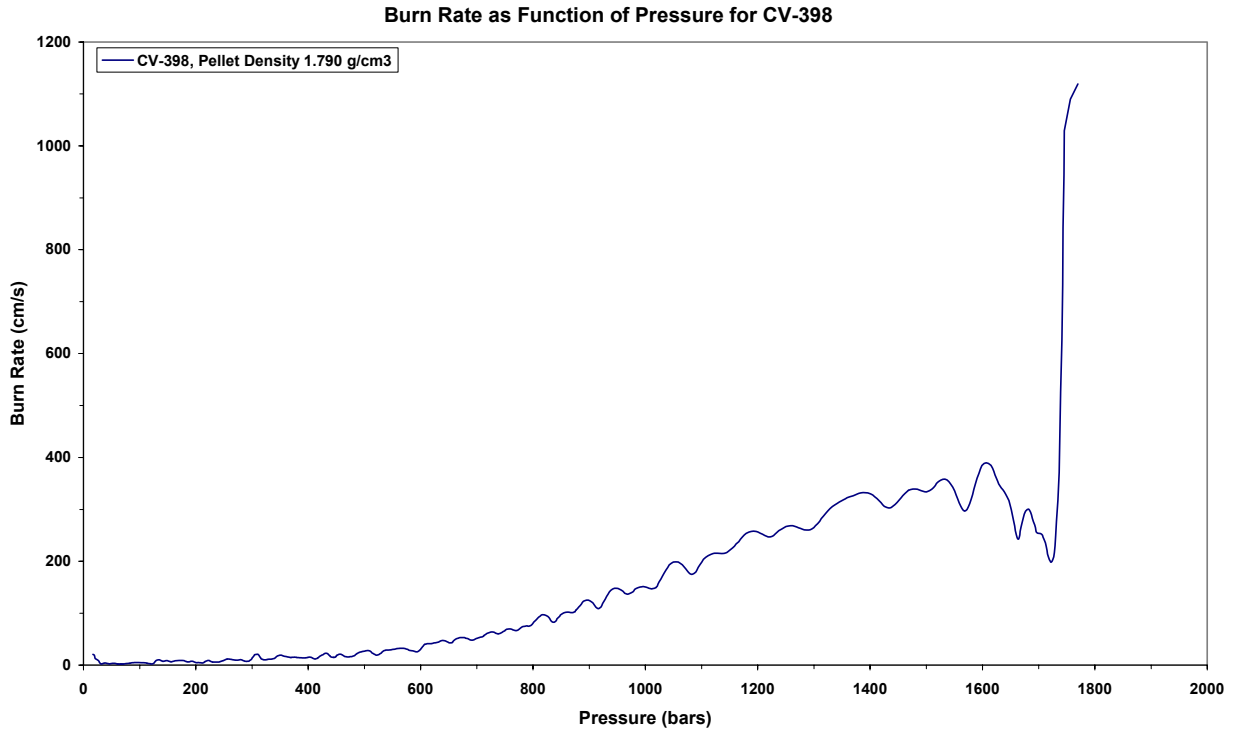


Figure 3.56 Burn rate as function of pressure for CV-398, PBXN-5 pellets, density  $1.790 \text{ g/cm}^3$ .

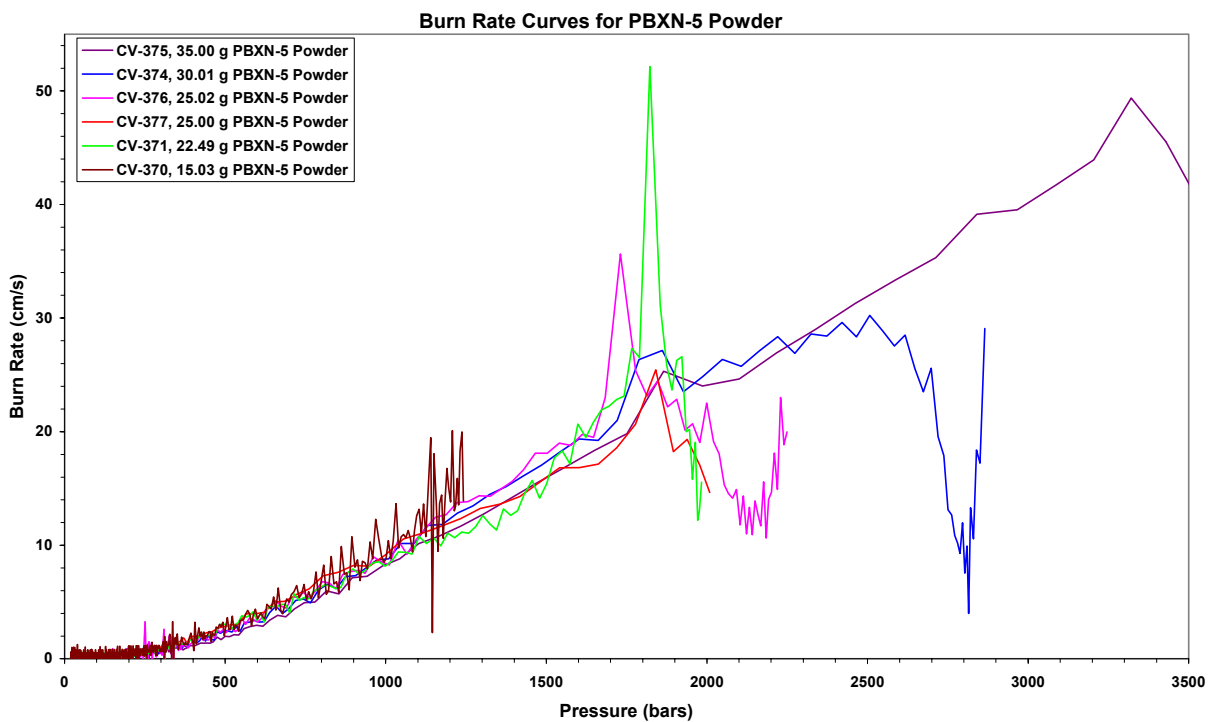


Figure 3.57 Burn rate curves for firings of PBXN-5 powder at different loading densities.

Figure 3.57 gives burn rate curves for PBXN-5 powder firings of five different loading densities showing that the burn rate is independent of the loading density. In figure 3.58 burn rate curves is given for two firings with pellets having density of  $1.8215 \text{ g/cm}^3$ . Both firing gives approximately straight burn rate curves, indicating that the geometry used for the

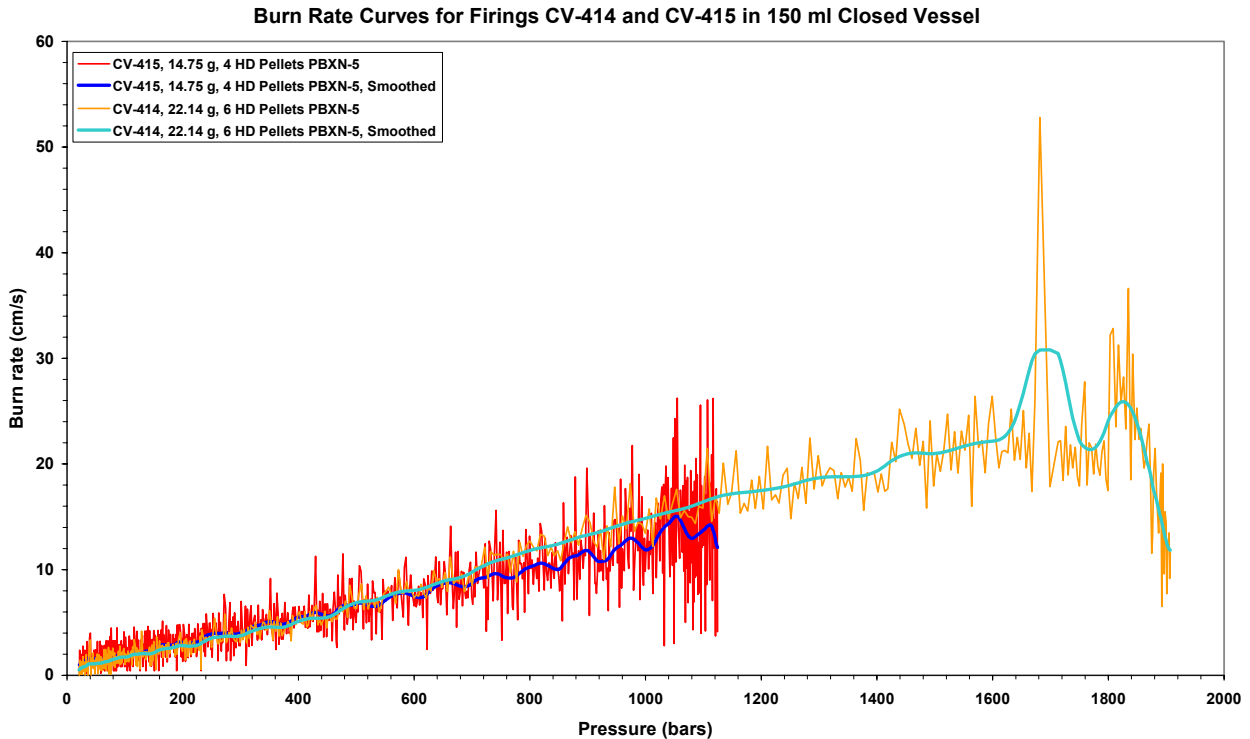


Figure 3.58 Burn rate curves for firings of pellets, density  $1.8215 \text{ g/cm}^3$  at different loading densities.

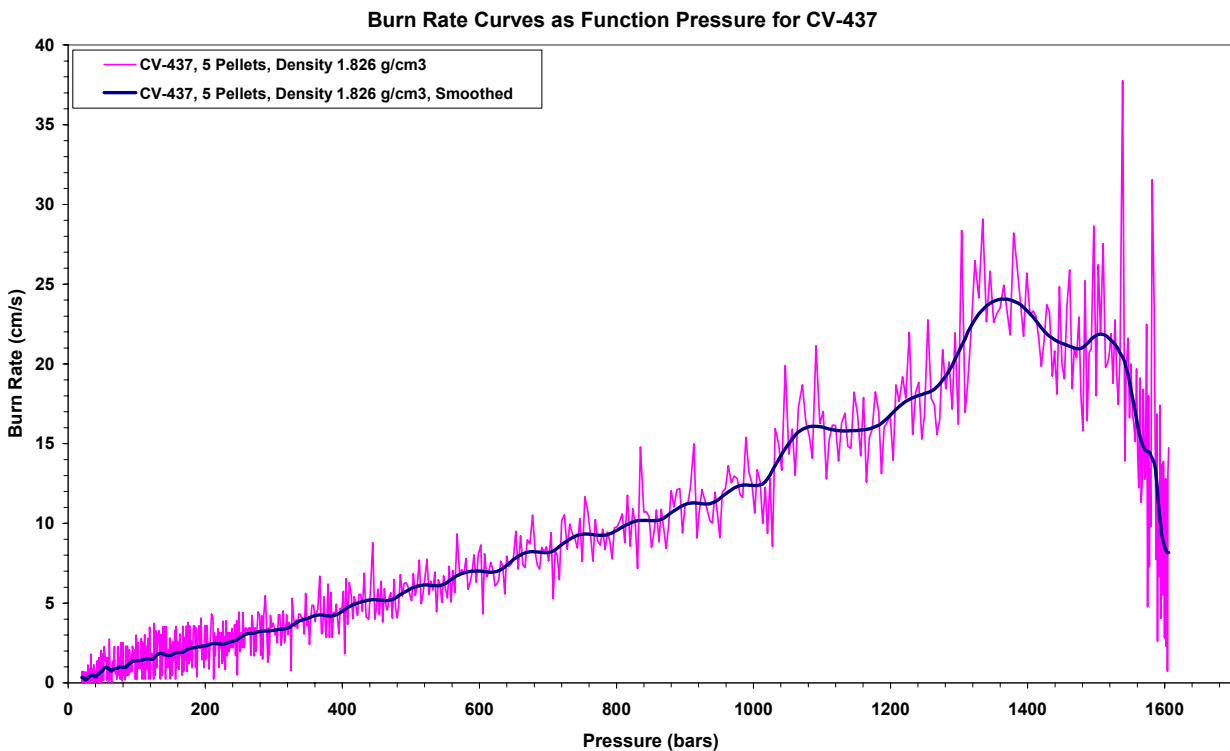


Figure 3.59 Burn rate curves for firing CV-437 with PBXN-5 pellets, density  $1.826 \text{ g/cm}^3$ .

calculation of surface for burning, is correct, and that the pellets only burn at the surface. The same results have been found for the second series of firings with pellets of density of  $1.826 \text{ g/cm}^3$ . The burn rate curves for these firings are given in figure 3.59 to 3.62.

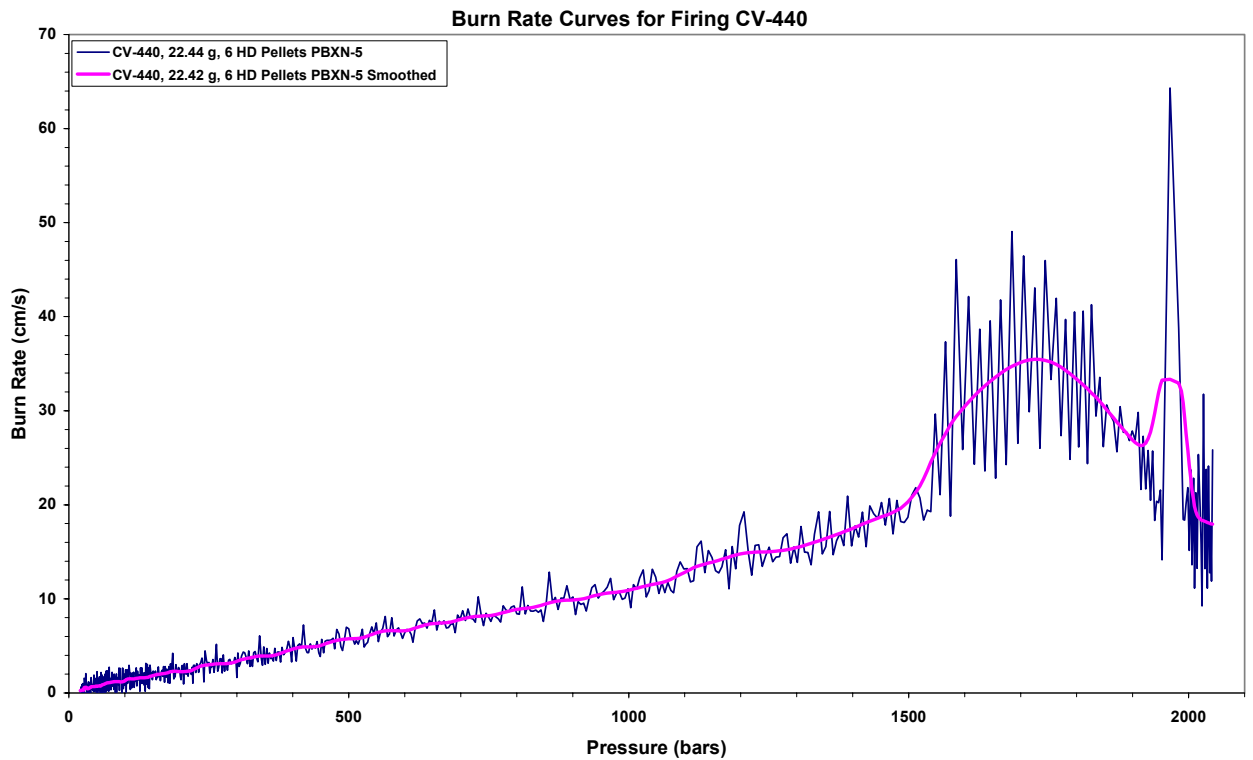


Figure 3.60 Burn rate curves for firing CV-438 with PBXN-5 pellets density  $1.826 \text{ g/cm}^3$ .

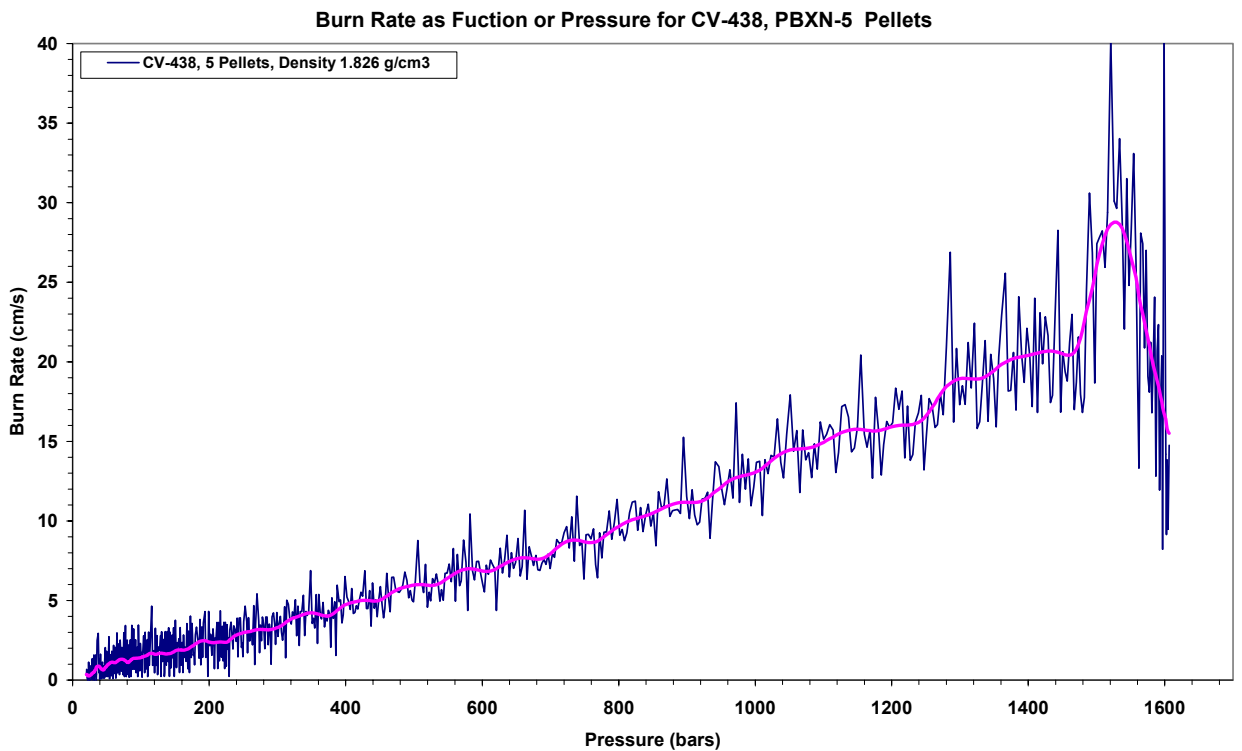


Figure 3.61 Burn rate curves for CV-440 with PBXN-5 pellets density  $1.826 \text{ g/cm}^3$ .

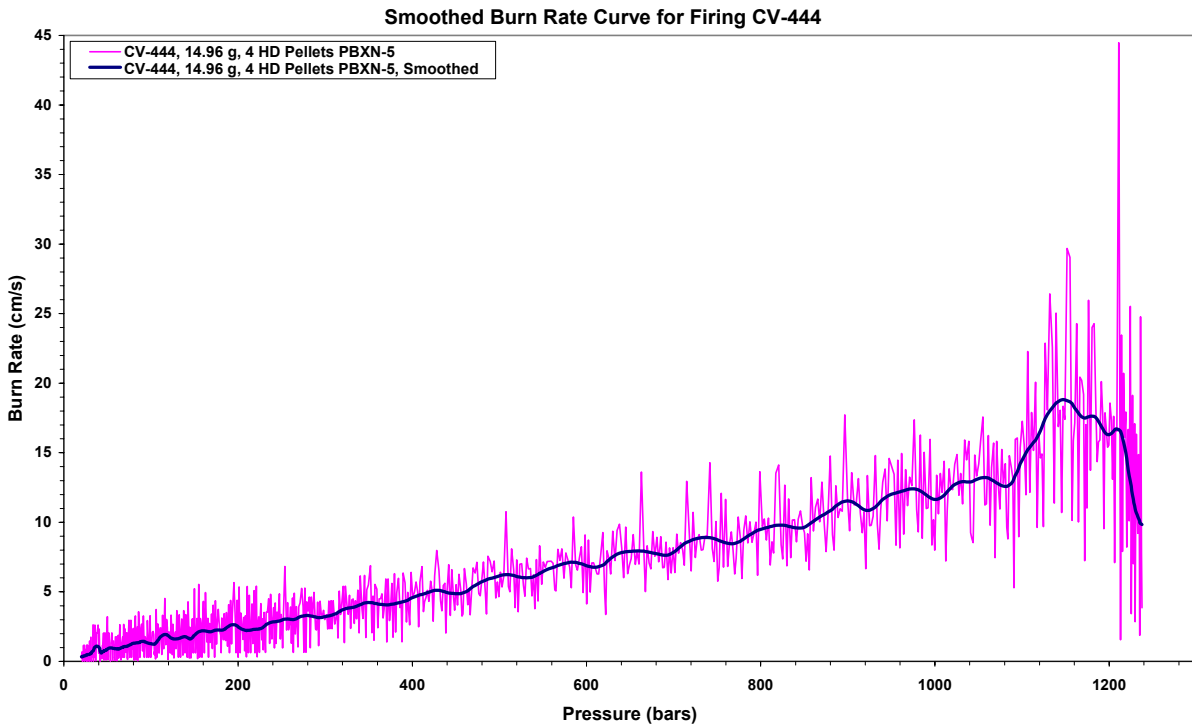


Figure 3.62 Burn rate curves for CV-444 with PBXN-5 pellets density  $1.826 \text{ g/cm}^3$ .

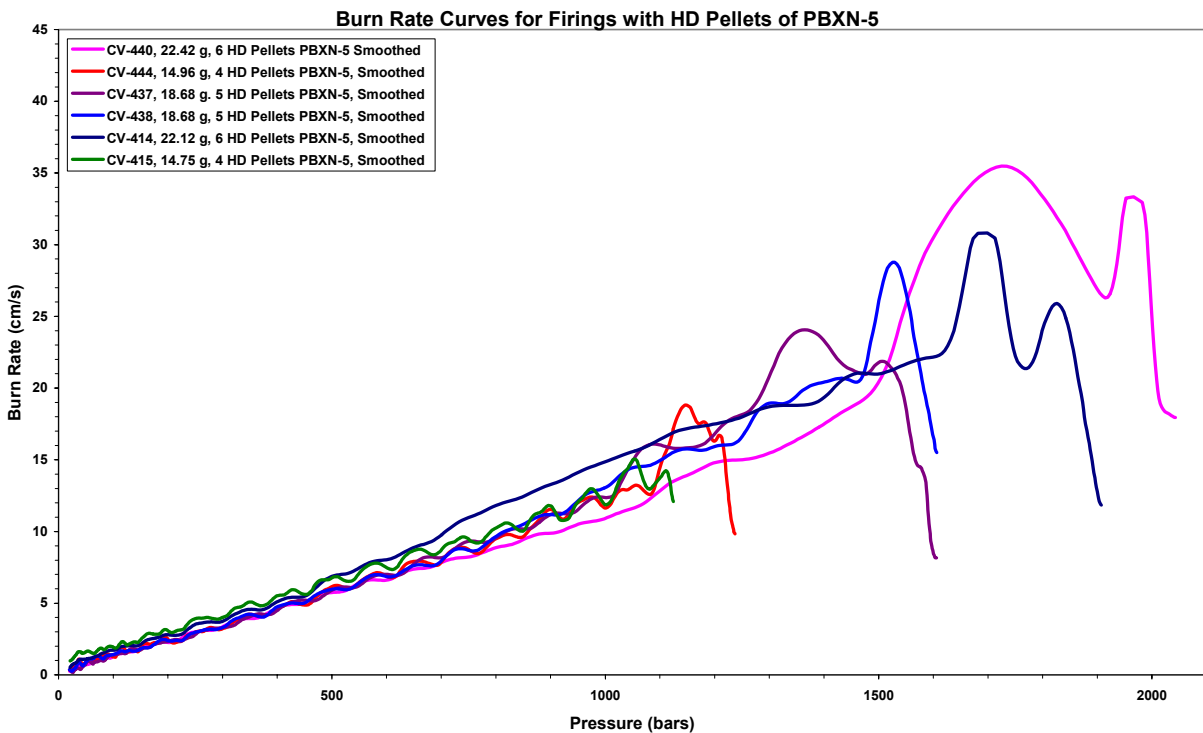


Figure 3.63 Smoothed burn rate curves for HD pellets of PBXN-5.

Figure 3.63 gives smoothed burn rate curves for all firings of pellets pressed with a pressure of 1 GPa. In figure 3.64 burn rate curves for all five tested conditions are been given. From this figure we see that the burn rate for pellets of high density and powder is very close, and that the pellets of lowest density do not burn as pellets but more or less as a powder. By using the

properties of powder to calculate the burn rate for pellets with density of  $1.59 \text{ g/cm}^3$  as performed for firing CV-418 in figure 3.65, we obtain more or less the same burn rate curve as for the firings of powder. Figure 3.66 gives burn rate curves for powder, pellets of high density and pellets of low density treated as powder and shows that there are only small differences in the burn rate.

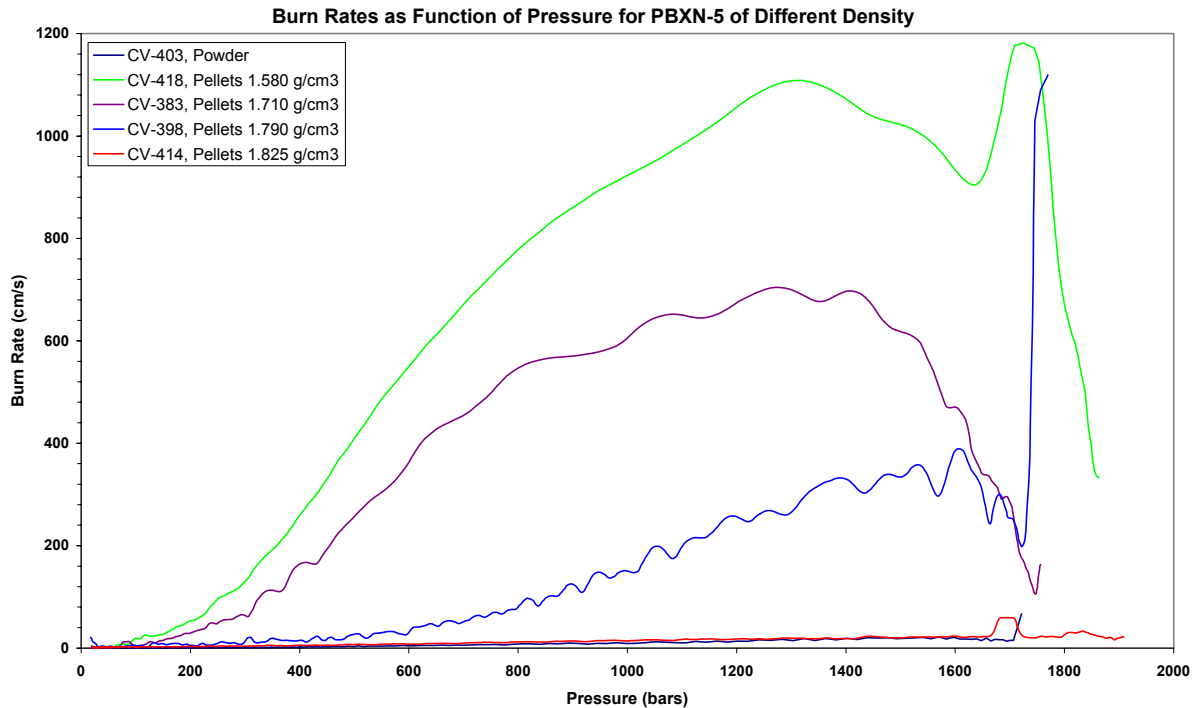


Figure 3.64 Burn rate curves for different pellet and powder firings of PBXN-5.

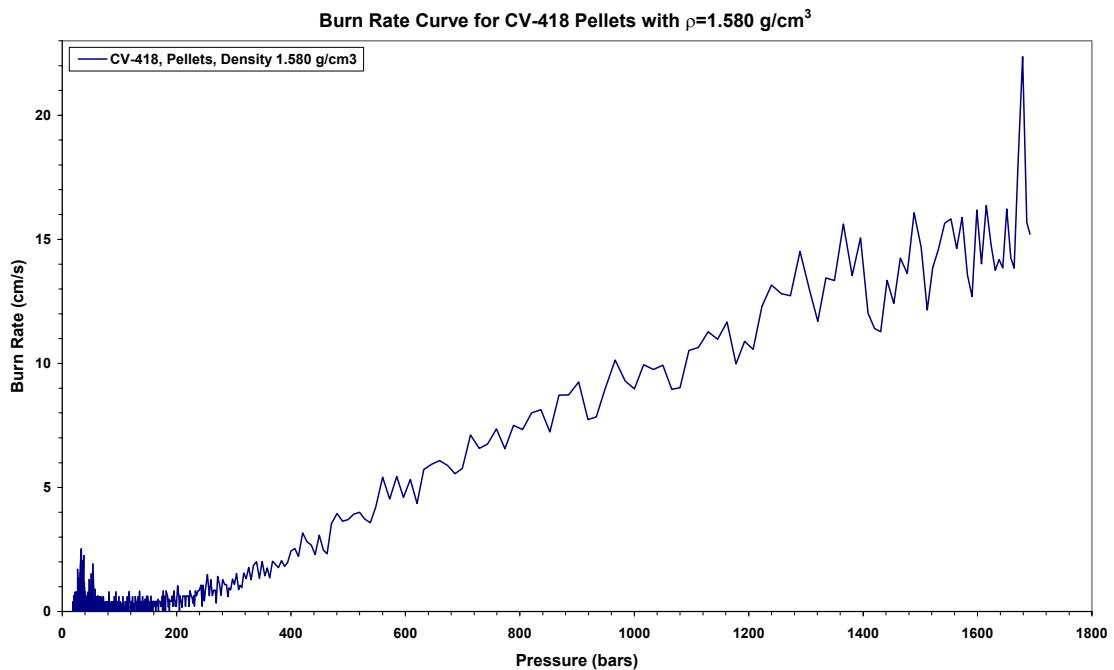


Figure 3.65 Burn rate curve for firing CV-418 of pellets with a density of  $1.580 \text{ g/cm}^3$ , but treated as powder in calculations.

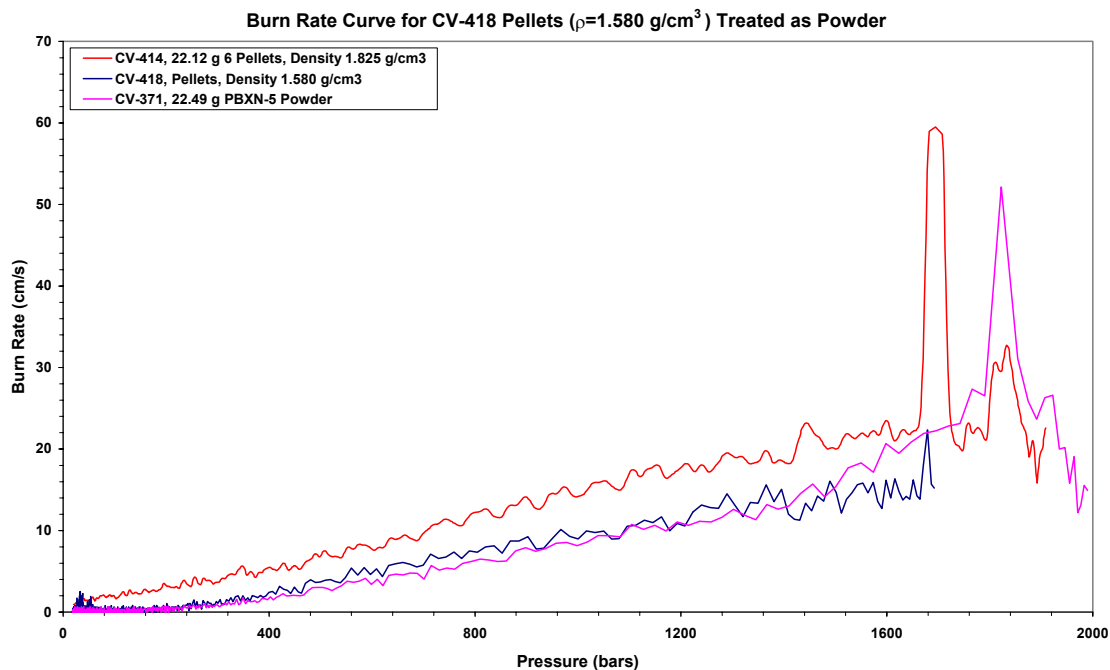


Figure 3.66 Burn rate curve for firing CV-418 treated as powder in calculations compared with CV-371-powder and CV-414 pellets of high density.

#### 4 SUMMARY

Pellets of four different densities have been pressed with different presses and tools. They have in addition to powder been tested at different loading densities in a 150 cm<sup>3</sup> Closed Vessel at room temperature. One of the purposes with the testing was to identify if and when the burning changes from grain or crystals to involve pellets only. In the last case the burn time of a given amount of explosive would increase significantly. A second purpose with the CV-testing was to determine the burn rate, impetus and co-volume of PBXN-5.

With respect to burn time we start to observe some small changes for pellets with density of 1.71 g/cm<sup>3</sup>, but first for pellets with density 1.79 g/cm<sup>3</sup> are changes in burn time significant. For firings with approximately the same amount PBXN-5, pressure-time curves for the five different conditions we have studied have been plotted in figure 4.1. For CV-444, containing pellets with density of 1.826 g/cm<sup>3</sup>, we can see that the burn time has increased by a very large factor compared with the burn time for powder and loosely pressed pellets. This result gives, that the burning of PBXN-5 fillings with a certain density, change from burning as grains or crystals to burn as one body.

The burn rate of PBXN-5 has been determined for both powder and pellets at different loading densities. The powder of PBXN-5 consists of relatively large grains with a lot of single crystals of different size in each grain. The performed calculations of burn rate have shown that the powder and loosely pressed pellets burn as single crystals and not as pellets or grains.

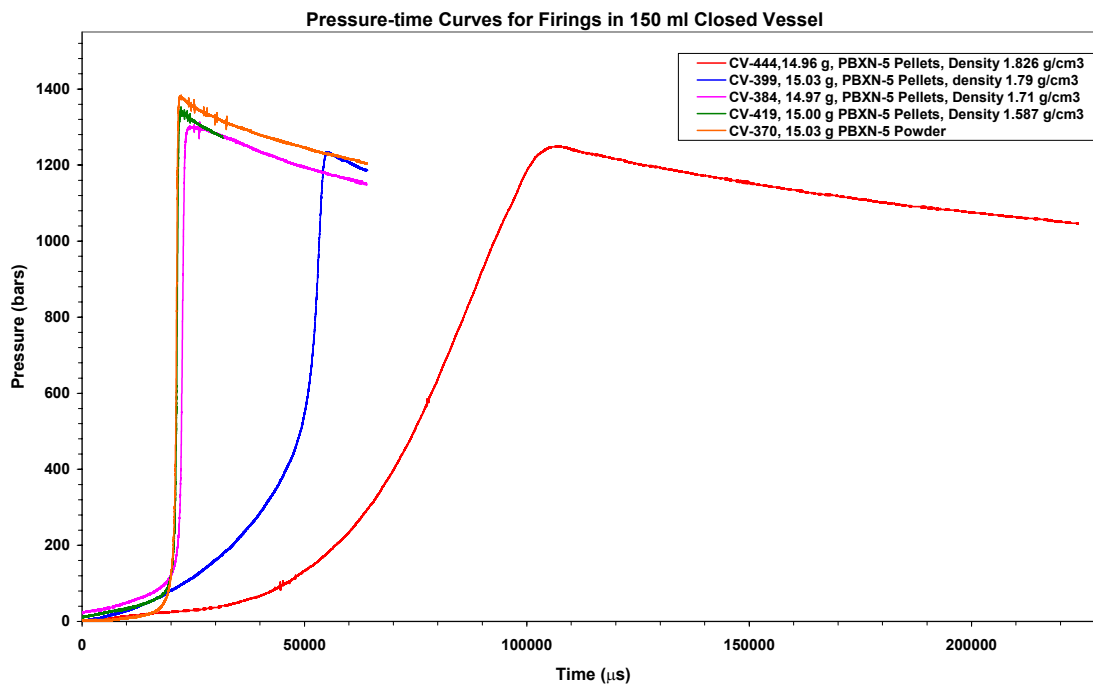


Figure 4.1 Pressure-time curves for different firings of PBXN-5.

For PBXN-5, when treating the pellet as one body and the powder as a mixture of single crystals, we obtained the same burn rate for pellets of high density and powder. This result has influence on the reaction rate of explosive fillings in warhead. The time from ignition of the explosive to a critical pressure level able to fragmenting the warhead is reached, is a function of the density of the filling.

In (2) we did study the two explosives PETN and H-764. For H-764, also an HMX-based explosive, we found a much weaker dependence between density of pellets and burn time compared to PBXN-5. PETN pellets with high density did burn as observed for PBXN-5 pellets with high density, as one body.

The experimental impetus of PBXN-5 decreases as the density of the pellets increase. For co-volume the trend is the opposite, with an increase as pellet the density increases. Experimentally measured impetus is lower than the theoretically calculated for all tested conditions.

## Appendix

## A CONTROL REPORT FOR PBXN-5, TYPE II, CLASS 2

**DYNO**  
Forsvarsprodukter

**KONTROLLRAPPORT B**  
I henhold til EN 10204 - 3.1 B



Kjøper/ Mottaker Forsvarets Forskningsinstitutt Avd. for våpen og matriell Postboks 25, 2007 Kjeller		Bestillingsnummer Etter avtale Bestillingsdato 05.04.02		Rapport nummer 160 Kontroll dato 09.04.02		
Produsent Dyno Nobel ASA N-3476 Sætre NORWAY		Produksjonsdato 12.10.01		Offentlig oppdragsnummer		
Lot nummer		Mengde 2 kg				
Sprengstofftype <b>PBXN-5, Type II, klasse 2</b>		Leveringsbetingelser/ Teknisk underlag MIL-E-81111B				
Analyseresultater						
Spesifikasjon	Sammensetning		Fuktighet	Volum vekt	Vacum. stab	Auto-ignition
	HMX	Viton				
Krav	95,0 ± 0,5 %	5,0 ± 0,5 %	≤ 0,15 %	≥ 0,7 g/ml	≤ 0,5 ml/g	≥ 225 °C
Charge nr. 11/01	95,1	4,9	0,05	0,85	0,06	257
Spesifikasjon	Kornfordeling, % gjennom USSS Nr.			Density	Impact sensitivity, BAM	Forurensning
	4	20	40			
Krav	≥ 98 %	50 - 100 %	≤ 5 %	17 av 20 pellets ≥ 96,5 % TMD	Joule	Ingen
Charge nr. 11/01	100	25	0	-	3	ingen
 Kvalitetssjef						
						

Figure A. 1 Control report for used PBXN-5, type II, class 2.



**B CHEETAH CALCULATIONS FOR PBXN-5**

Product library title: the blake product library

Executing library command: gas eos, virial

Reactant library title:# Version 2.0 by P. Clark Souers

Name	% wt.	% mol	% vol.	The Composition			Mol. wt.	Formula
				Heat of formation (cal/mol)	Standard volume (cc/mol)	Standard entropy (cal/K/mol)		
viton	5.00	4.00	5.14	-665392	202.24	0.000	374.14	c10h7f13
hmx	95.00	96.00	94.86	17866	155.46	0.000	296.16	c4h8n8o8

Heat of formation = -31.614 cal/gm  
 Standard volume = 0.526 cc/gm  
 Standard entropy = 0.000 cal/k/gm  
 Standard energy = -31.627 cal/gm

The elements and percent by mole

c 15.100  
 h 28.348  
 f 1.852  
 n 27.351  
 o 27.351

The average mol. wt. = 299.275 g/mol

Input&gt;composition, viton, 5, hmx, 95, weight

Name	% wt.	% mol	% vol.	The Composition			Mol. wt.	Formula
				Heat of formation (cal/mol)	Standard volume (cc/mol)	Standard entropy (cal/K/mol)		
viton	5.00	4.00	5.14	-665392	202.24	0.000	374.14	c10h7f13
hmx	95.00	96.00	94.86	17866	155.46	0.000	296.16	c4h8n8o8

Heat of formation = -31.614 cal/gm  
 Standard volume = 0.526 cc/gm  
 Standard entropy = 0.000 cal/k/gm  
 Standard energy = -31.627 cal/gm

The elements and percent by mole

c 15.100  
 h 28.348  
 f 1.852  
 n 27.351  
 o 27.351

The average mol. wt. = 299.275 g/mol

Input&gt;gun, 0.100000, 0.100000, 2.000000

GUN calculation:

	Rho	Temp	Pressure	Impetus	Mol Wt.	Covol	Frozen	Phi
	g/cc	K	MPa	J/g	Gas	cc/g	Cp/Cv	
1.)	0.1000	3880.0	151.1	1345.79	23.972	1.094	1.237	1.123
2.)	0.2000	3935.3	343.6	1358.63	24.084	1.046	1.237	1.264
3.)	0.3000	3964.0	583.2	1364.31	24.159	0.994	1.240	1.425
4.)	0.4000	3982.0	876.8	1366.55	24.228	0.941	1.247	1.604
5.)	0.5000	3993.6	1229.9	1366.06	24.308	0.889	1.256	1.801
6.)	0.6000	4000.5	1646.0	1362.63	24.411	0.839	1.267	2.013
7.)	0.7000	4003.4	2124.5	1355.57	24.555	0.791	1.279	2.239
8.)	0.8000	4002.4	2659.9	1344.10	24.759	0.745	1.291	2.474
9.)	0.9000	3997.6	3240.7	1327.63	25.036	0.701	1.303	2.712
10.)	1.0000	3989.3	3852.1	1306.21	25.394	0.661	1.314	2.949
11.)	1.1000	3977.5	4479.0	1280.51	25.827	0.623	1.322	3.180
12.)	1.2000	3962.6	5108.9	1251.64	26.324	0.588	1.329	3.402
13.)	1.3000	3945.1	5733.4	1220.82	26.869	0.556	1.334	3.613

14.)	1.4000	3925.3	6347.7	1189.14	27.447	0.527	1.337	3.813
15.)	1.5000	3903.9	6950.5	1157.52	28.043	0.500	1.340	4.003
16.)	1.6000	3881.4	7542.5	1126.65	28.645	0.476	1.341	4.184
17.)	1.7000	3858.2	8126.3	1096.99	29.243	0.453	1.342	4.358
18.)	1.8000	3834.7	8705.5	1068.86	29.830	0.433	1.343	4.525
19.)	1.9000	3811.1	9284.1	1042.42	30.399	0.414	1.344	4.688

## Product concentrations (mol/kg)

Name		1.)	2.)	3.)	4.)	5.)	6.)
n2	Gas	1.275e+001	1.276e+001	1.276e+001	1.275e+001	1.272e+001	1.268e+001
co	Gas	1.146e+001	1.144e+001	1.144e+001	1.143e+001	1.139e+001	1.131e+001
h2o	Gas	8.097e+000	8.300e+000	8.439e+000	8.555e+000	8.654e+000	8.737e+000
h2	Gas	3.874e+000	3.776e+000	3.676e+000	3.559e+000	3.416e+000	3.235e+000
co2	Gas	2.698e+000	2.697e+000	2.674e+000	2.643e+000	2.611e+000	2.587e+000
hf	Gas	1.737e+000	1.737e+000	1.737e+000	1.737e+000	1.737e+000	1.737e+000
oh	Gas	4.788e-001	3.497e-001	2.732e-001	2.186e-001	1.767e-001	1.436e-001
h	Gas	4.028e-001	2.743e-001	2.036e-001	1.552e-001	1.191e-001	9.104e-002
no	Gas	1.473e-001	1.117e-001	8.970e-002	7.364e-002	6.118e-002	5.135e-002
o	Gas	2.850e-002	1.478e-002	8.962e-003	5.758e-003	3.800e-003	2.549e-003
o2	Gas	2.176e-002	1.122e-002	6.692e-003	4.219e-003	2.739e-003	1.820e-003
cho	Gas	7.285e-003	1.306e-002	1.992e-002	2.866e-002	4.002e-002	5.470e-002
nh3	Gas	4.973e-003	1.221e-002	2.308e-002	3.953e-002	6.422e-002	1.004e-001
hcn	Gas	2.958e-003	7.633e-003	1.522e-002	2.758e-002	4.755e-002	7.898e-002
nh2	Gas	1.877e-003	3.237e-003	4.692e-003	6.360e-003	8.304e-003	1.053e-002
formac	Gas	1.474e-003	4.035e-003	8.392e-003	1.584e-002	2.861e-002	5.041e-002
hnco	Gas	1.153e-003	3.243e-003	6.998e-003	1.378e-002	2.601e-002	4.788e-002
ch2o	Gas	1.006e-003	2.617e-003	5.222e-003	9.446e-003	1.626e-002	2.702e-002
hno	Gas	9.231e-004	1.151e-003	1.328e-003	1.493e-003	1.659e-003	1.835e-003
nh	Gas	6.935e-004	8.366e-004	9.342e-004	1.012e-003	1.076e-003	1.124e-003
n	Gas	6.745e-004	5.488e-004	4.636e-004	3.969e-004	3.409e-004	2.923e-004
ho2	Gas	6.239e-004	5.276e-004	4.512e-004	3.882e-004	3.357e-004	2.925e-004
h2o2	Gas	3.236e-004	3.971e-004	4.439e-004	4.800e-004	5.114e-004	5.418e-004
n2o	Gas	2.142e-004	2.859e-004	3.551e-004	4.330e-004	5.269e-004	6.447e-004
no2	Gas	9.633e-005	8.792e-005	8.127e-005	7.606e-005	7.212e-005	6.961e-005
nco	Gas	8.756e-005	1.780e-004	3.012e-004	4.789e-004	7.409e-004	1.128e-003
cn	Gas	7.334e-005	1.434e-004	2.341e-004	3.581e-004	5.293e-004	7.614e-004
hno2	Gas	4.982e-005	6.761e-005	8.273e-005	9.807e-005	1.151e-004	1.355e-004
ch3	Gas	2.100e-005	8.137e-005	2.117e-004	4.726e-004	9.699e-004	1.866e-003
ch4	Gas	8.968e-006	4.492e-005	1.366e-004	3.414e-004	7.643e-004	1.574e-003
ch2	Gas	5.209e-006	1.442e-005	2.922e-005	5.249e-005	8.808e-005	1.399e-004
ch2oh	Gas	2.670e-006	1.126e-005	3.109e-005	7.321e-005	1.588e-004	3.251e-004
ketene	Gas	1.378e-006	9.100e-006	3.607e-005	1.186e-004	3.551e-004	9.968e-004
ch4o	Gas	9.430e-007	5.712e-006	2.050e-005	6.048e-005	1.613e-004	4.010e-004
c2h2	Gas	8.240e-007	5.276e-006	2.026e-005	6.426e-005	1.841e-004	4.886e-004
c	Gas	5.463e-007	7.278e-007	8.687e-007	9.918e-007	1.099e-006	1.183e-006
c2h4	Gas	3.063e-009	3.756e-008	2.136e-007	8.992e-007	3.202e-006	1.006e-005
ch3cn	Gas	2.516e-009	3.913e-008	2.874e-007	1.600e-006	7.734e-006	3.388e-005
c(s)	solid	0.000e+000	0.000e+000	0.000e+000	0.000e+000	0.000e+000	0.000e+000
Total	Gas	4.172e+001	4.152e+001	4.139e+001	4.127e+001	4.114e+001	4.096e+001
Total	Cond.	0.000e+000	0.000e+000	0.000e+000	0.000e+000	0.000e+000	0.000e+000

## Product concentrations (mol/kg)

Name		7.)	8.)	9.)	10.)	11.)	12.)
n2	Gas	1.262e+001	1.252e+001	1.239e+001	1.224e+001	1.206e+001	1.187e+001
co	Gas	1.116e+001	1.089e+001	1.049e+001	9.944e+000	9.273e+000	8.511e+000
h2o	Gas	8.799e+000	8.829e+000	8.813e+000	8.734e+000	8.583e+000	8.358e+000
h2	Gas	3.005e+000	2.719e+000	2.384e+000	2.022e+000	1.664e+000	1.337e+000
co2	Gas	2.577e+000	2.592e+000	2.635e+000	2.707e+000	2.797e+000	2.892e+000
hf	Gas	1.737e+000	1.737e+000	1.737e+000	1.737e+000	1.737e+000	1.737e+000
nh3	Gas	1.510e-001	2.164e-001	2.925e-001	3.702e-001	4.394e-001	4.922e-001
hcn	Gas	1.260e-001	1.906e-001	2.699e-001	3.544e-001	4.317e-001	4.913e-001

oh	Gas	1.172e-001	9.627e-002	7.976e-002	6.673e-002	5.633e-002	4.790e-002
formac	Gas	8.710e-002	1.470e-001	2.403e-001	3.769e-001	5.641e-001	8.036e-001
hnco	Gas	8.612e-002	1.502e-001	2.511e-001	3.988e-001	5.986e-001	8.503e-001
cho	Gas	7.307e-002	9.471e-002	1.181e-001	1.408e-001	1.600e-001	1.737e-001
h	Gas	6.895e-002	5.150e-002	3.789e-002	2.749e-002	1.973e-002	1.408e-002
no	Gas	4.363e-002	3.771e-002	3.331e-002	3.015e-002	2.788e-002	2.623e-002
ch2o	Gas	4.334e-002	6.649e-002	9.636e-002	1.307e-001	1.657e-001	1.971e-001
nh2	Gas	1.297e-002	1.539e-002	1.750e-002	1.896e-002	1.962e-002	1.950e-002
ch3	Gas	3.350e-003	5.521e-003	8.193e-003	1.082e-002	1.276e-002	1.360e-002
ch4	Gas	2.973e-003	5.069e-003	7.640e-003	1.007e-002	1.166e-002	1.205e-002
ketene	Gas	2.621e-003	6.340e-003	1.379e-002	2.652e-002	4.495e-002	6.769e-002
hno	Gas	2.025e-003	2.235e-003	2.466e-003	2.715e-003	2.976e-003	3.237e-003
o	Gas	1.735e-003	1.204e-003	8.560e-004	6.263e-004	4.711e-004	3.629e-004
nco	Gas	1.694e-003	2.494e-003	3.574e-003	4.950e-003	6.595e-003	8.447e-003
o2	Gas	1.243e-003	8.830e-004	6.591e-004	5.194e-004	4.306e-004	3.719e-004
c2h2	Gas	1.194e-003	2.625e-003	5.054e-003	8.381e-003	1.198e-002	1.498e-002
nh	Gas	1.153e-003	1.156e-003	1.130e-003	1.073e-003	9.924e-004	8.971e-004
cn	Gas	1.062e-003	1.421e-003	1.804e-003	2.157e-003	2.428e-003	2.588e-003
ch4o	Gas	9.325e-004	2.000e-003	3.883e-003	6.731e-003	1.040e-002	1.445e-002
n2o	Gas	7.974e-004	1.000e-003	1.275e-003	1.645e-003	2.139e-003	2.786e-003
ch2oh	Gas	6.297e-004	1.141e-003	1.904e-003	2.895e-003	4.002e-003	5.064e-003
h2o2	Gas	5.748e-004	6.137e-004	6.613e-004	7.184e-004	7.833e-004	8.522e-004
ho2	Gas	2.584e-004	2.331e-004	2.161e-004	2.062e-004	2.015e-004	2.002e-004
n	Gas	2.494e-004	2.114e-004	1.780e-004	1.489e-004	1.240e-004	1.029e-004
ch2	Gas	2.096e-004	2.917e-004	3.714e-004	4.287e-004	4.498e-004	4.336e-004
hno2	Gas	1.614e-004	1.958e-004	2.430e-004	3.079e-004	3.957e-004	5.109e-004
ch3cn	Gas	1.343e-004	4.695e-004	1.401e-003	3.493e-003	7.260e-003	1.279e-002
no2	Gas	6.893e-005	7.070e-005	7.564e-005	8.449e-005	9.781e-005	1.161e-004
c2h4	Gas	2.787e-005	6.652e-005	1.329e-004	2.189e-004	2.983e-004	3.440e-004
c	Gas	1.229e-006	1.221e-006	1.150e-006	1.022e-006	8.592e-007	6.883e-007
c(s)	solid	0.000e+000	0.000e+000	0.000e+000	0.000e+000	0.000e+000	0.000e+000
Total Gas		4.072e+001	4.039e+001	3.994e+001	3.938e+001	3.872e+001	3.799e+001
Total Cond.		0.000e+000	0.000e+000	0.000e+000	0.000e+000	0.000e+000	0.000e+000

## Product concentrations (mol/kg)

Name		13.)	14.)	15.)	16.)	17.)	18.)
n2	Gas	1.169e+001	1.150e+001	1.132e+001	1.114e+001	1.098e+001	1.082e+001
h2o	Gas	8.068e+000	7.726e+000	7.350e+000	6.956e+000	6.555e+000	6.159e+000
co	Gas	7.699e+000	6.875e+000	6.070e+000	5.304e+000	4.591e+000	3.937e+000
co2	Gas	2.978e+000	3.045e+000	3.085e+000	3.096e+000	3.079e+000	3.036e+000
hf	Gas	1.737e+000	1.737e+000	1.737e+000	1.737e+000	1.737e+000	1.737e+000
hnco	Gas	1.148e+000	1.483e+000	1.844e+000	2.222e+000	2.607e+000	2.991e+000
formac	Gas	1.092e+000	1.420e+000	1.778e+000	2.156e+000	2.543e+000	2.932e+000
h2	Gas	1.057e+000	8.261e-001	6.413e-001	4.956e-001	3.819e-001	2.933e-001
hcn	Gas	5.279e-001	5.414e-001	5.346e-001	5.117e-001	4.772e-001	4.349e-001
nh3	Gas	5.256e-001	5.403e-001	5.391e-001	5.255e-001	5.026e-001	4.733e-001
ch2o	Gas	2.217e-001	2.379e-001	2.456e-001	2.455e-001	2.388e-001	2.269e-001
cho	Gas	1.812e-001	1.827e-001	1.789e-001	1.710e-001	1.601e-001	1.474e-001
ketene	Gas	9.196e-002	1.146e-001	1.329e-001	1.451e-001	1.506e-001	1.495e-001
oh	Gas	4.093e-002	3.511e-002	3.021e-002	2.606e-002	2.254e-002	1.957e-002
no	Gas	2.499e-002	2.399e-002	2.316e-002	2.246e-002	2.188e-002	2.141e-002
ch3cn	Gas	1.956e-002	2.663e-002	3.301e-002	3.785e-002	4.066e-002	4.125e-002
nh2	Gas	1.875e-002	1.756e-002	1.613e-002	1.459e-002	1.305e-002	1.156e-002
ch4o	Gas	1.833e-002	2.154e-002	2.379e-002	2.497e-002	2.511e-002	2.434e-002
c2h2	Gas	1.675e-002	1.710e-002	1.622e-002	1.449e-002	1.230e-002	9.974e-003
ch3	Gas	1.334e-002	1.225e-002	1.067e-002	8.914e-003	7.189e-003	5.621e-003
ch4	Gas	1.134e-002	9.917e-003	8.182e-003	6.441e-003	4.871e-003	3.554e-003
nco	Gas	1.042e-002	1.242e-002	1.438e-002	1.624e-002	1.797e-002	1.955e-002
h	Gas	1.002e-002	7.139e-003	5.100e-003	3.656e-003	2.630e-003	1.897e-003
ch2oh	Gas	5.935e-003	6.525e-003	6.806e-003	6.799e-003	6.552e-003	6.123e-003
n2o	Gas	3.614e-003	4.657e-003	5.957e-003	7.572e-003	9.586e-003	1.212e-002

hno	Gas	3.488e-003	3.722e-003	3.937e-003	4.135e-003	4.322e-003	4.506e-003
cn	Gas	2.633e-003	2.579e-003	2.450e-003	2.271e-003	2.061e-003	1.838e-003
h2o2	Gas	9.208e-004	9.860e-004	1.046e-003	1.101e-003	1.152e-003	1.201e-003
nh	Gas	7.960e-004	6.965e-004	6.032e-004	5.186e-004	4.437e-004	3.783e-004
hno2	Gas	6.580e-004	8.410e-004	1.065e-003	1.339e-003	1.672e-003	2.085e-003
ch2	Gas	3.900e-004	3.319e-004	2.704e-004	2.127e-004	1.626e-004	1.212e-004
c2h4	Gas	3.452e-004	3.098e-004	2.541e-004	1.935e-004	1.383e-004	9.337e-005
o2	Gas	3.310e-004	3.009e-004	2.777e-004	2.592e-004	2.444e-004	2.328e-004
o	Gas	2.849e-004	2.271e-004	1.832e-004	1.492e-004	1.227e-004	1.018e-004
ho2	Gas	2.005e-004	2.016e-004	2.028e-004	2.040e-004	2.054e-004	2.074e-004
no2	Gas	1.396e-004	1.690e-004	2.050e-004	2.487e-004	3.022e-004	3.686e-004
n	Gas	8.526e-005	7.057e-005	5.844e-005	4.846e-005	4.028e-005	3.357e-005
c	Gas	5.300e-007	3.957e-007	2.884e-007	2.063e-007	1.453e-007	1.009e-007
c(s)	solid	0.000e+000	0.000e+000	0.000e+000	0.000e+000	0.000e+000	0.000e+000
Total Gas		3.722e+001	3.643e+001	3.566e+001	3.491e+001	3.420e+001	3.352e+001
Total Cond.		0.000e+000	0.000e+000	0.000e+000	0.000e+000	0.000e+000	0.000e+000

## Product concentrations

Name	(mol/kg)	(mol gas/mol explosive)
n2	Gas	1.067e+001
h2o	Gas	5.775e+000
hnco	Gas	3.367e+000
co	Gas	3.344e+000
formac	Gas	3.316e+000
co2	Gas	2.970e+000
hf	Gas	1.737e+000
nh3	Gas	4.396e-001
hcn	Gas	3.879e-001
h2	Gas	2.245e-001
ch2o	Gas	2.111e-001
ketene	Gas	1.425e-001
cho	Gas	1.335e-001
ch3cn	Gas	3.973e-002
ch4o	Gas	2.285e-002
no	Gas	2.107e-002
nco	Gas	2.097e-002
oh	Gas	1.705e-002
n2o	Gas	1.535e-002
nh2	Gas	1.017e-002
c2h2	Gas	7.751e-003
ch2oh	Gas	5.569e-003
hno	Gas	4.696e-003
ch3	Gas	4.269e-003
hno2	Gas	2.603e-003
ch4	Gas	2.505e-003
cn	Gas	1.613e-003
h	Gas	1.371e-003
h2o2	Gas	1.252e-003
no2	Gas	4.530e-004
nh	Gas	3.218e-004
o2	Gas	2.243e-004
ho2	Gas	2.106e-004
ch2	Gas	8.818e-005
o	Gas	8.524e-005
c2h4	Gas	5.965e-005
n	Gas	2.807e-005
c	Gas	6.923e-008
c(s)	solid	0.000e+000
Total Gas		3.290e+001
Total Cond.		0.000e+000

**References**

- (1) Laurence E Fried, W Michael Howard, P Clark Souers (1998): Cheetah 2.0 User's Manual, UCRL-MA-117541 Rev. 5, Lawrence Livermore National Laboratory.
- (2) Nevstad Gunnar Ove (2002): Burning Properties of H-764 and PETN. Closed Vessel Testing, FFI/RAPPORT-2002/03622.

## DISTRIBUTION LIST

**FFIBM**
**Dato:** 25 october 2002

RAPPORTTYPE (KRYSS AV)			RAPPORT NR.	REFERANSE	RAPPORTENS DATO			
<input checked="" type="checkbox"/>	RAPP	<input type="checkbox"/>	NOTAT	<input type="checkbox"/>	RR	2002/04195	FFIBM/860/130	25 october 2002
RAPPORTENS BESKYTTELSESGRAD				ANTALL EKS UTSTEDT	ANTALL SIDER			
Unclassified				37	60			
RAPPORTENS TITTEL				FORFATTER(E)				
BURNING PROPERTIES OF PBXN-5 - Closed Vessel Testing				NEVSTAD Gunnar Ove, ERIKSEN Svein Walter				
FORDELING GODKJENT AV FORSKNINGSSJEF				FORDELING GODKJENT AV AVDELINGSSJEF:				
Bjarne Haugstad				Jan Ivar Botnan				

**EKSTERN FORDELING**
**INTERN FORDELING**

ANTALL	EKS NR	TIL	ANTALL	EKS NR	TIL
1		Nammo Raufoss AS	14		FFI-Bibl
1		Eva Friis	1		Adm direktør/stabssjef
1		Gard Ødegårdstuen	1		FFIE
1		Quoc Bao Diep	1		FFISYS
		Postboks 162	1		FFIBM
		NO-2831 Raufoss	1		FFIN
			2		Forfattereksemplar(er)
1		HFK-AMK	5		Restopplag til FFI-Bibl
1		Alf Øversveen			ELEKTRONISK FORDELING:
					FFI-veven
1		Naval Air Warfare Center Weapons Division			B Haugstad, FFIBM, (BjH)
1		Alice I. Atwood			S W Eriksen, FFIBM, (SWE)
1		Allen Lindfors			J F Moxnes, FFIBM, (JFM)
		Code 4T4310D, 1 Administration Circle China Lake, CA 93555-6100			G O Nevstad, FFIBM, (GON)
2		Dave Holt 300 Huy 361 Bldg 2540, Code 4022 NSWC Crane IN 47522  www.ffi.no			

FFI-K1

Retningslinjer for fordeling og forsendelse er gitt i Oraklet, Bind I, Bestemmelser om publikasjoner for Forsvarets forskningsinstitutt, pkt 2 og 5. Benytt ny side om nødvendig.